Stable Ion Studies of Protonation and Oxidation of Polycyclic Arenes†,‡

Kenneth K. Laali*

Department of Chemistry, Kent State University, Kent, Ohio 44242

Received July 25, 1995 (Revised Manuscript Received March 27, 1996)

Contents

Background, Rationale, and an Overview of Coverage

As distinct intermediates of electrophilic aromatic substitution, arenium ions are an important class of delocalized carbocations.[1−3] Arene radical cations and dications are also important in this juncture, since in recent years an increasing number of aromatic substitution reactions involving reactive arenes have been shown to go through radical cations (RCs).[2−4] Furthermore, with reactive fused polycyclic aromatic hydrocarbons (PAHs), there is increasing evidence that carcinogenic/mutagenic activity which ultimately leads to PAH−DNA adduct formation is initiated by electrophilic and/or oxidative chemistry involving their carbocations (via diol epoxide ring opening) or radical cations (formed by biological oxidation; for example with cytochrome P-450 or peroxidases).[5−8]

Arenium ions of protonation of PAHs can serve as models of PAH activation by positive oxygen derived from hydroxylases. Thus a more in-depth understanding of structural/dynamic features and charge distribution patterns in the reactive intermediates (carbocations, radical cations, and dications) should ultimately help with predictability, by defining common links between certain structural/electronic features and carcinogenic properties.

The most comprehensive early review of persistent arenium ions was that of Brouwer in 1970[9] with the work being almost exclusively concerned with the benzene series. In 1973, in a broader review concerned with all classes of fluorinated carbocations,

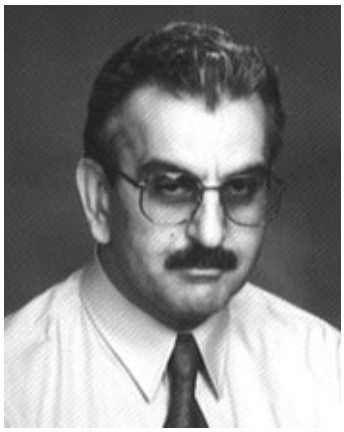

Kenneth K. Laali did his undergraduate studies at University of Tehran (B.Sc. with honors 1973) and his graduate work at University of Manchester (UMIST; Ph.D. 1977 with Robert Haszeldine and Brian Booth). After postdoctoral work with the late Victor Gold at King's College, he spent a few more years in Europe at the Universities of Strasbourg (with Jean Sommer), Amsterdam (with Hans Cerfontain), and at ETH-Zurich (with Heinrich Zollinger) before moving to George Olah's laboratory at University of Southern California in mid-1982. In 1985 he moved to Kent State where he is now full Professor. Whereas his research continues to emphasize carbocations (especially arenium ions of PAHs and cyclophanes), onium ions, and superacid chemistry, in recent years projects in organophosphorus chemistry (using phosphalkynes as building blocks for novel cations and molecules), and host–guest interactions in the gas phase and in solution, have become additional areas of activity in his laboratory.

† Dedicated to Professor George Olah, for his seminal contributions to the arenium ions area.

‡ Key to compound numbering: $\boldsymbol{n}\mathbf{H}^+$ monoprotonated arenium ion; $\boldsymbol{n}\mathbf{H_2}^{2+}$ diprotonated arenium dication; $\boldsymbol{n}^+$ monoarenium ion other than those of protonation; $\boldsymbol{n}^{2+}$ oxidation dication or iminium-pyrenium (or oxoiminium) dication.

S0009-2665(94)01175-1 CCC: $25.00 © 1996 American Chemical Society

Olah and Mo[10] reviewed what was known at that time about long-lived fluoroarenium ions. In 1984, as part of a review of stable carbodications,[11] Olah et al. included sections on diprotonation of arenes and oxidation to stable dications.

In 1984, in a review dealing with multiply charged carbocations in a broad sense, Pagni[12] briefly summarized the recent advances in arene oxidation dications and diprotonation of arenes and annulenes. In 1985, Hansen[13] in a review article entitled "NMR of Polycyclic Aromatics" included a brief discussion of the NMR characteristics of carbocations of PAHs. Finally, in their monograph on superacids Olah et al.[14] provided brief summaries of arenium ions and aromatic dications.

To our knowledge no other, more recent, review of the field has appeared in the literature.

Since the early 1980s, the availability of high field multinuclear and 2D NMR, adapted for low-temperature stable ion studies has greatly extended the boundaries in terms of system complexity that can be tackled.

Since the topic was last reviewed, a large body of experimental and theoretical data have become available on persistent arenium ions, oxidation dications and the radical cations of various classes of PAHs and their derivatives, including some of the methano-bridged analogues.

Although the close parallel between ^{13}C NMR chemical shifts and charge had already been established and tested for a number of classes of carbocations and carbanions, recent work based on dications (two-electron oxidation) and dianions (two-electron reduction) has emphasized the importance of ring current anisotropy.

In this review emphasis is being placed on multinuclear NMR studies of arenium ions as a means to delineate their charge distribution mode. Possible relationship between charge distribution and carcinogenicity, and its modulation via strategically positioned substituents are addressed.

Buttressed nitro-PAHs are NO_2 diprotonated in superacids to give iminium-arenium dications (see Figure 5), a process not observed with nitrobenzenes and which apparently requires steric inhibition to delocalization as a driving force. In view of the presence of nitro-PAHs as environmental pollutants formed by exhaust fumes and in cigarette smoke in the atmosphere and their mutagenic behavior, their oxidation and protonation chemistry and how these processes might influence carcinogenic behavior are challenging arguments.

AM1, DEWAR-PI, and HMO π calculations have been carried out on a large number of PAHs. Comparisons between the predicted arenium ion energies and those observed under persistent ion conditions are instructive.

The electrophilic and oxidative chemistry of some PAHs has been examined by mass spectrometry (CI/MS−MS and EI/MS−MS). The decomposition pathways of the resulting protonated, acetylated, and trimethylsilylated adducts were examined by collisional decomposition experiments in a tandem mass spectrometer. These studies (see gas-phase studies) extend our understanding concerning the electrophilic and oxidative chemistry of larger fused PAHs for which solution data are scarce.

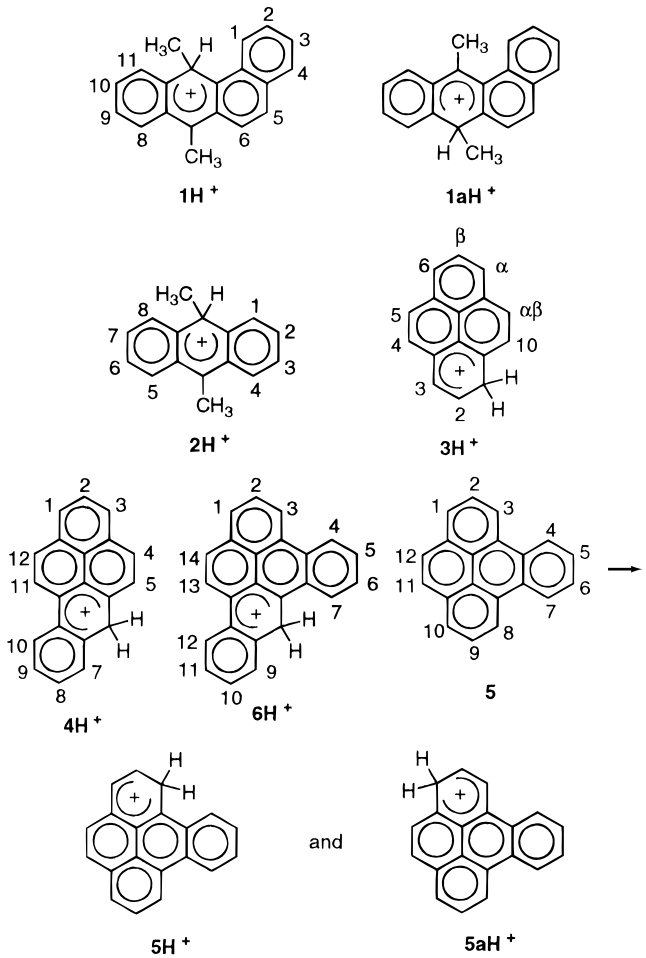

Figure 1. The first series of persistent PAH arenium ions (definitive site of protonation not determined by early NMR data).

A number of oxidation dications have been studied under stable ion conditions in superacid media (see Figure 6); many have also been probed by theory. The ^{13}C NMR studies provide insight into the mode of charge distribution in the oxidation dications and a comparison with the monoarenium ions. Furthermore, ^{1}H NMR chemical shifts in the dications can provide a measure of paramagnetic ring current.

We also review persistent radical cations of PAHs (RCs) which have been studied by EPR. Relationship between the hyperfine coupling and the calculated spin densities (HMO) are examined and the coexistence of the RCs with the arenium ions in superacids are emphasized.

Seminal Earlier Studies (How Did It All Begin?)

In a historically significant paper dealing with the UV spectra of conjugate acids of hydrocarbons published in 1951, Gold and Tye[15] suggested the arenium ion structure for parent anthracene in sulfuric acid. In the late 1950s the Dutch group[16] published the first examples of persistent arenium ions of PAHs in $TFAH/H_2O{\cdot}BF_3$ or $HF{\cdot}BF_3$ (Figure 1). The first 40 MHz proton NMR spectra of protonated 7,12-dimethylbenzo[*a*]anthracene (**1**), 9,10-dimethylanthracene (**2**), parent pyrene (**3**), and benzo[*a*]pyrene

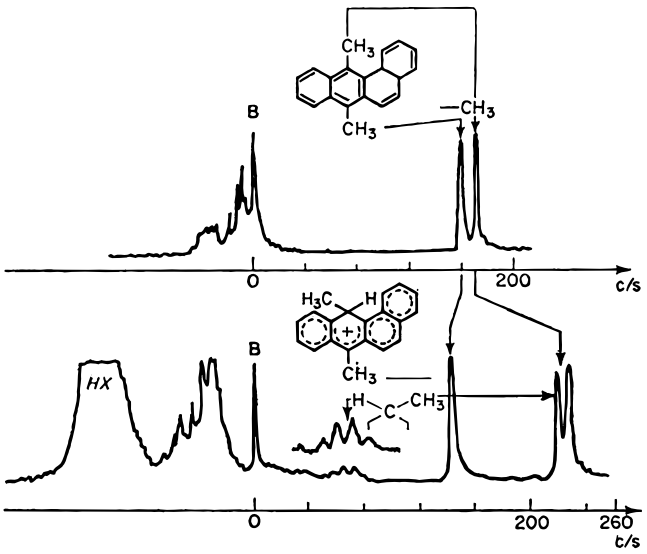

Figure 2. ^{1}H NMR (40 MHz) spectrum of protonated **1H**$^+$ (spectrum of **1** is also shown). B = benzene. (Reprinted from ref 18. Copyright 1966 Academic Press.)

(**4**) cations were reported along with protonated pentamethyl- and hexamethylbenzene cations (actual spectrum for protonated **1** is shown in Figure 2).

The significant feature of these early spectra was the distinct appearance of the methylene or methine proton(s) of the sp^2-hybridized carbon as a separate signal. For **1**, *ipso* protonation was readily apparent by the doublet appearance of one methyl group.[16,18] The absorption spectra of a series of arenium ions formed in HF and HF·BF_3 were also reported;[17] SCF-MO calculations were used to predict the site of protonation.[17] For example C-6 was predicted as the preferred protonation site for **4**, and a mixture of two arenium ions (C-1 and C-3 protonation) was predicted for benzo[*e*]pyrene (**5**).[17] These predictions have been fully confirmed in recent stable ion studies (see later).

The early progress in probing stable arenium ions by spectroscopic methods of the time was gathered in a substantial review on basicity of hydrocarbons by Perkampus[18] in the late 1960s.

The last two decades witnessed an explosive growth in stable ion chemistry which included many persistent benzenium ions (and also cyclophanes) generated in various superacid media.[10,14,19] The following issues were the focal points: charge distribution in the arenium ion (NMR), influence of substituents on the charge distribution mode and the site of attack, intramolecular hydride and alkyl shifts (VT-DNMR work), the *ipso*-protonated/alkylated analogues, including heptaalkylbenzenium cations and their dynamic features (solution and solid-state NMR); transannular shielding of the arenium ion by a cofacial phenyl ring in protonated cyclophanes.

In a landmark paper published over two decades ago using early NMR, Olah et al.[20] reported direct NMR observation of parent naphthalenium ion (**7H**$^+$) in HF·SbF_5/SO_2ClF and examined a series of substituted naphthalenium cations. The paper included the first report of a ^{13}C NMR spectrum (25.1 MHz) of a representative example namely C-4 protonated 1,5-dimethylnaphthalenium cation (Figures 3 and 4);

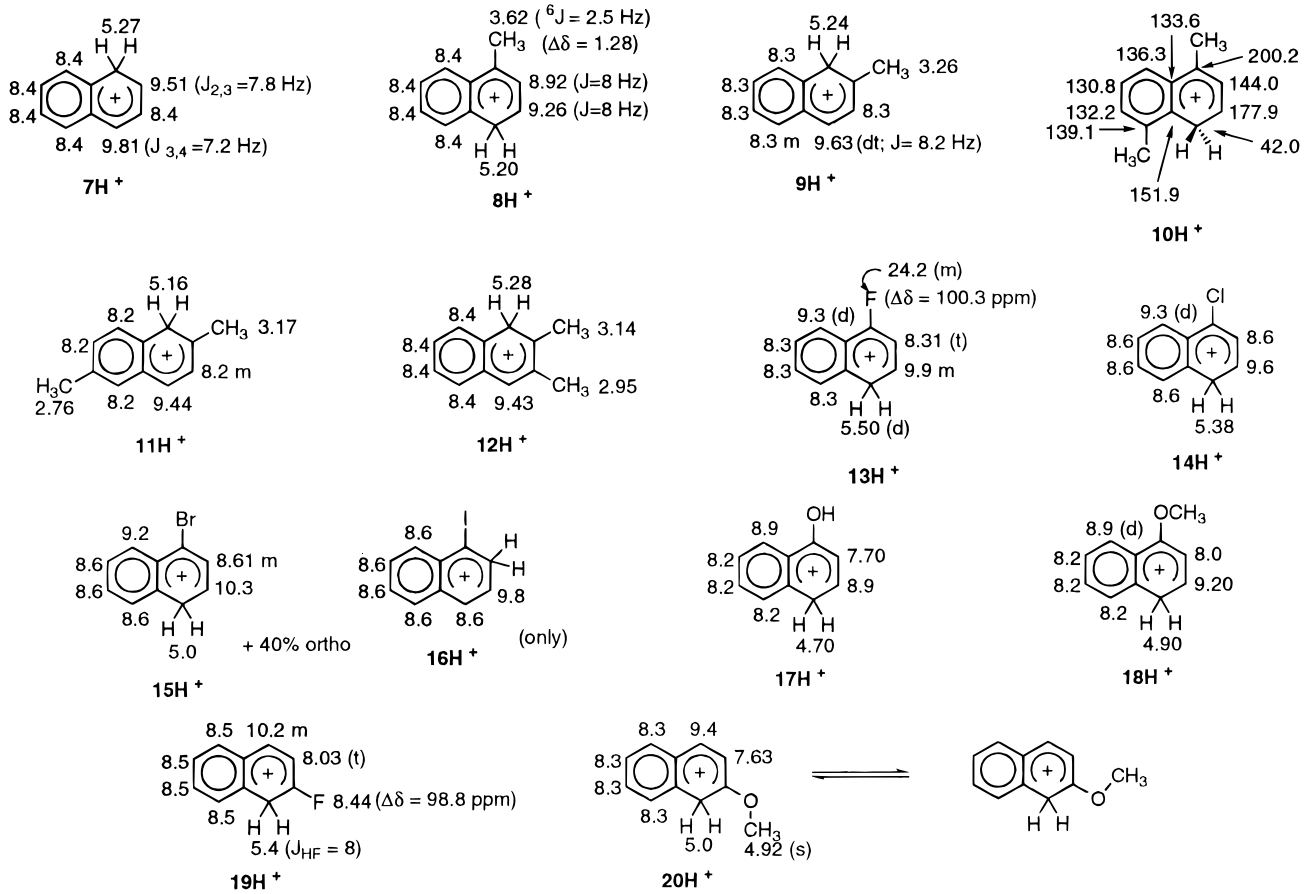

Figure 3. Compilation of ^{1}H (and ^{19}F) NMR data for naphthalenium ions; ^{13}C NMR data for **10H**$^+$ are also shown.

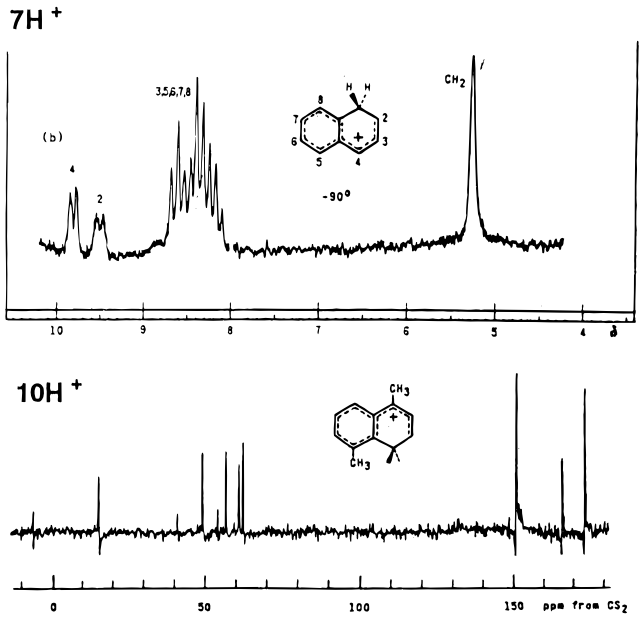

Figure 4. Actual ^{1}H and ^{13}C NMR spectra of **7H**$^+$ and **10H**$^+$. (Reprinted from ref 20. Copyright 1973 American Chemical Society.)

two actual NMR spectra are illustrated (Figure 4).

With **7H**$^+$, there is a rapid equilibrium between 1-protonated and 2-protonated cations. The positive charge is predominantly located *para* and *ortho* in the protonated ring.

1-Methylnaphthalene is protonated at C-4 (**8H**$^+$); 2-methylnaphthalene, at C-1 (**9H**$^+$). A six-bond proton−proton coupling ($^6J_{H-H}$) was observed in **8H**$^+$ between the methyl and the sp^3 (CH_2). There is substantial fluoronium ion character in the C-4-protonated 1-fluoro-naphthalenium ion (**13H**$^+$) ($\Delta\delta^{19}$F = 100.3 ppm) which is the exclusive ion formed. Competing formation of the *ortho*-protonated cation is observed in the series I > Br > Cl. For iodonaphthalene the latter becomes exclusive. This was attributed to an increased tendency for rapid initial kinetic protonation at halogen followed by intramolecular 1,2-shift to give the observed cations.

With 1-halo-, 1-hydroxy-, and 1-methoxynaphthalenium (**13H**$^+$−**16H**$^+$, **18H**$^+$ and **17H**$^+$) cations it was found that *peri*-H was noticeably more deshielded (a *peri* effect).

The 2-methoxynaphthalene is protonated at C-1 (**20H**$^+$). There is also a rapid equilibrium between the two rotational isomers, a process which is slow on the NMR time scale at −50 °C. In view of the current activity on dications,[21] it is highly probable that under suitable conditions at sufficiently high acidities (H_o) an arenium−oxonium dication may be produced.

The ^{13}C NMR spectrum of **10H**$^+$ (Figure 4) provided the first analogy between the ^{1}H and ^{13}C charge delocalization trends. The *para* carbon is at 200.2 ppm; the ring junction *ortho* carbon is less deshielded (151.9 ppm) than the other *ortho* carbon (177.9 ppm). Limited charge delocalization into the nonprotonated ring was noted.

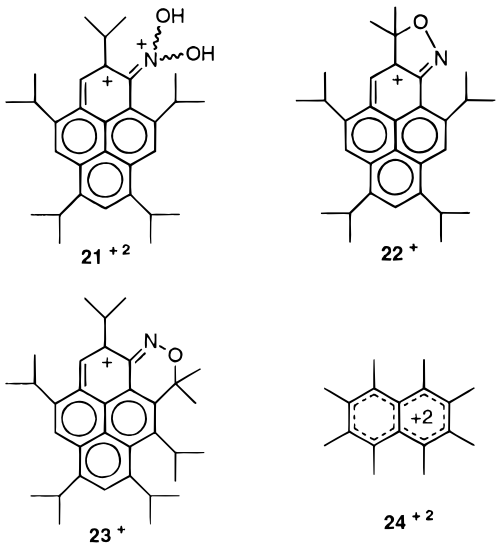

Figure 5. Iminium-pyrenium dication, their cyclized versions, and octamethylnaphthalene oxidation dication.

Correlation of NMR Chemical Shift with Charge and Theoretical Studies of Arenium Ions and Oxidation Dications

The proportionality between ^{13}C NMR chemical shifts and π-charge density in persistent carbocations and carbanions has over the years been tested for a large variety of singly and doubly charged models and discussed in several important reviews.[11,22−24] For naphthalenium ions the proportionality constant is typically ∼151 ppm/e,[25,26] and for diarenium ions like diprotonated hexahydropyrene ∼183 ppm/e.[26] For monoarenium ions of benzo[*a*]pyrene **4H**$^+$, benzo[*e*]-pyrene **5H**$^+$ and **5aH**$^+$, and dibenzo[*a*,*e*]pyrene **6H**$^+$ total deshieldings of about 180 ppm were found,[27] and for a series of iminium-pyrenium dications (NO_2-diprotonated) like **21**$^{2+}$ and their *ortho*- (or *peri*-) cyclized monoarenium ion analogues e.g. **22**$^+$ and **23**$^+$ (Figure 5) values above 200 ppm were obtained.[28]

The oxidation dications of PAHs show typically ∼220 ppm/e total deshielding.[29] Sterically crowded dications like **24**$^+$ may exhibit even larger values (∼244 ppm/e).[29] In a series of alkylpyrenium dications (**27**$^{2+}$−**30**$^{2+}$) (Figure 6) total deshieldings were typically 207−216 ppm/e.[30] The observed deshielding for octamethylbiphenylene dication **31**$^{2+}$ is ∼185 ppm/e.[31]

For a number of substituted anthracence dications Olah and Singh[32] found total deshieldings of 208−212 ppm/e.

The importance of paramagnetic contribution in the ^{13}C vs charge relationship (K_c) has recently been emphasized by Edlund et al.[33] An additivity model is suggested (eq 1), where K_c (total chemical shift change per electron) depends on both F_c (the charge term) and X_c [the variable paramagnetic contribution; where $X_c = a[X_H$ (proton anisotropy)]:

$$K_c = F_c + (n_c/\rho_\pi)X_c \qquad (1)$$

n_c is the number of conjugated carbons; ρ_π is the total change in π charge.

Thus for oxidation dications or dianions of annulenes, the measured K_c values can be empirically

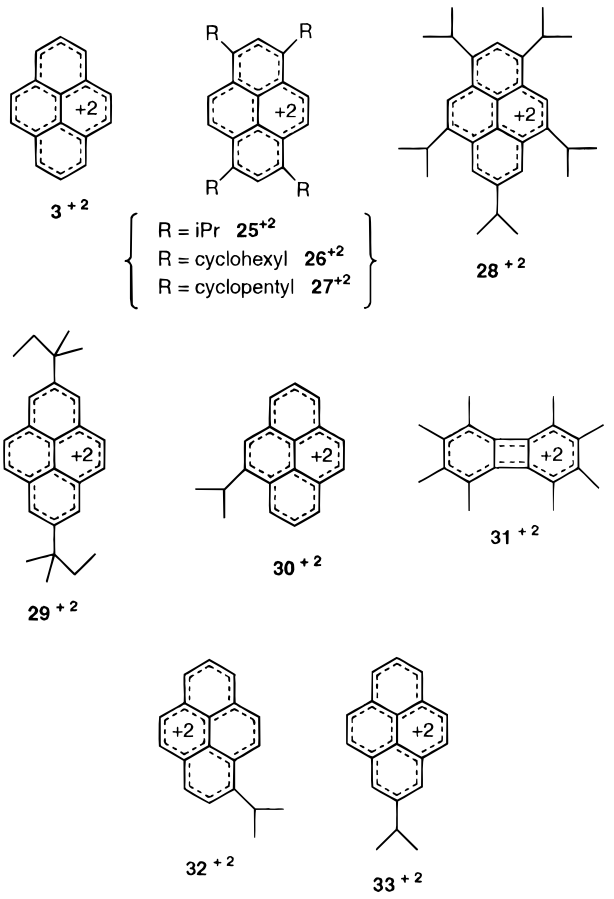

Figure 6. Examples of PAH oxidation dications.

divided into the charge term and the ring current anisotropy term. The most paratropic dications (such a $\mathbf{3}^{2+}$) give the largest total low field shifts (ppm/e values), because their ring current anisotropy term is most significant. This is seen for instance from the ^{1}H NMR spectrum of $\mathbf{3}^{2+}$,[30,34] which shows proton shielding due to paramagnetic ring current "PRC" in the 12π perimeter.

For crowded alkyl(cycloalkyl)-substituted pyrene dications,[30] a large degree of variation in the ^{1}H NMR shifts were observed. Depending on the substituents, large upfield or large downfield shifts were seen. It was suggested that since HOMO orbitals are involved in PRC, substitution at these positions leads to decreased PRC, hence a low field shift of proton resonances. Only limited examples are so far available and additional studies are needed to more fully examine these substituent-induced perturbations of the paramagnetic contribution in oxidation dications of PAHs.

The correlation between Hückel charges and NMR chemical shifts are approximate because the electron repulsions are neglected. Nevertheless reasonable correlations have been found for oxidation dications of PAHs[25] and for dimethylnaphthalenium ions (see appropriate sections below).

The DEWAR-PI calculations predict the relative arenium ion energies.[35] Good correlations between theory and typical electrophilic aromatic substitution experiments (bromination, acylation, nitration) have been found for a series of alternant and nonalternant (fluoranthene type) PAHs.[35] Sites within 5 kcal/mol of the site of the lowest energy cation are considered to be possible candidates for electrophilic substitution.

Rabinovitz et al.[36] have emphasized the generality of charge alternation concept in PAH dianions and dications. It has been discussed that such charge alternation and donor−acceptor interactions stabilize these systems. The Δq_π (difference between calculated charge density for a given carbon in the neutral and in the doubly charged system) and $\Delta\delta^{13}$C shifts were both used to underscore this phenomenon.

For a series of PAHs the vertical ionization potentials (IP) and $\Delta\Delta H°_f$s (difference between the heat of formation of the dication and its neutral precursor) were calculated by Mills[37] by the AM1, MNDO, and MINDO/3 methods. The IP values are reasonable predictors of dication formation provided there is no geometrical change upon oxidation. AM1 predicts that dication formation is favorable when $\Delta\Delta H°_f \leq 463 \pm 3$ kcal/mol.

The AM1 energies, charges, and geometries for $\mathbf{3}^{2+}$, $\mathbf{30}^{2+}$, $\mathbf{32}^{2+}$, and $\mathbf{33}^{2+}$ have been calculated (Table 1).[30] The calculated order of carbon charges are $C_\alpha > C_{\alpha\beta} > C_\beta$ regardless of substitution. In the optimized structures, the methine CH is coplanar with the aromatic ring. For the α and $\alpha\beta$ isomers there are two coplanar rotamers which are both minima and differ by 2 kcal/mol.

For the monoarenium ions of benzo[*a*]pyrene **4**, benzo[*e*]pyrene **5**, and dibenzo[*a*,*e*]pyrene **6** ($\mathbf{4H}^+$, $\mathbf{5H}^+$, $\mathbf{5aH}^+$, $\mathbf{6H}^+$) it was found that patterns of AM1 calculated changes in carbon charges ΔQ [q_c (ion) − q_c (neutral)] (illustrated in Figures 7−9) and $\Delta\delta^{13}$C values are similar.[27] A plot of $\Delta\delta^{13}$C vs ΔQ_c (Figure 10) is roughly linear, but there is considerable scatter. Ring carbons close to protonation site fall to high $\Delta\delta^{13}$C values.

Protonation of benzo[*a*]pyrene (a potent carcinogen; see Table 2 and later section on relationship to carcinogenicity) is most favored at C-6 (→ $\mathbf{4H}^+\mathbf{A}$);[27] the persistent arenium ion observed in superacid is

Table 1. AM1 Charges in Pyrenium Dications

pyrene dication (iPr position)	$\Delta H°_f$ neutral	$\Delta H°_f$ dication	$\Delta\Delta H°_f$	calculated charges at ring carbons in the dication[a] C_1 (α)	C_2 (β)	C_3 (α)	C_4 (αβ)	C_5 (αβ)	C_6 (α)	C_7 (β)	C_8 (α)	C_9 (αβ)	C_{10} (αβ)
$\mathbf{3}^{2+}$	67.3	515.7	448.4	+0.162	−0.209	+0.162	+0.011	+0.010	+0.162	−0.208	+0.162	+0.009	+0.010
$\mathbf{32}^{2+}$ (α)[b]	54.5	493.5	439.1	+0.265	−0.222	+0.123	−0.025	+0.030	+0.162	−0.205	+0.143	+0.005	−0.011
$\mathbf{32}^{2+}$ (α)[c]	52.7	491.7	439.0	+0.268	−0.219	+0.118	−0.028	+0.032	+0.161	−0.205	+0.143	+0.006	−0.009
$\mathbf{33}^{2+}$ (β)	50.2	494.2	444.0	+0.156	−0.125	+0.143	−0.001	+0.015	+0.160	−0.208	+0.159	+0.011	+0.003
$\mathbf{30}^{2+}$ (αβ)[d]	53.2	494.1	440.9	+0.156	−0.204	+0.134	−0.014	−0.000	+0.171	−0.209	+0.150	+0.005	+0.126
$\mathbf{30}^{2+}$ (αβ)[e]	54.6	495.8	441.2	+0.157	−0.208	+0.134	−0.013	+0.004	+0.171	−0.210	+0.151	+0.000	+0.119

[a] Excluding ring junctions and the iPr substituent. [b] Methine C−H bond syn to C1−C2 bond. [c] Methine C−H bond anti to C1−C2 bond. [d] Methine C−H bond anti to C9−C10 bond. [e] Methine C−H bond syn to C9−C10 bond.

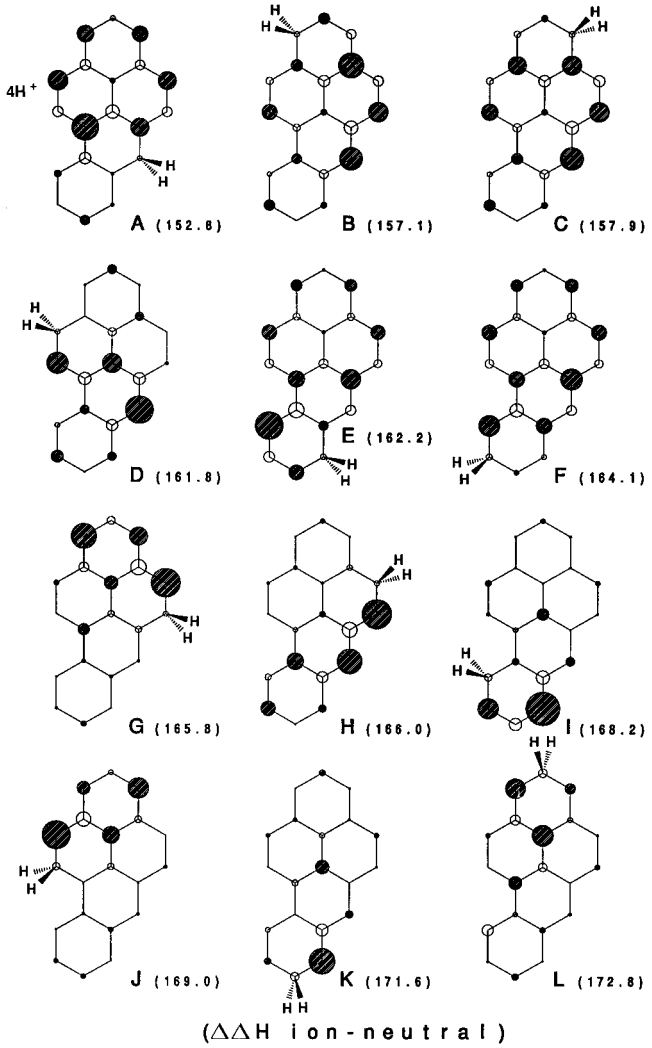

Figure 7. AM1 energies and ΔQ profiles for **4H**$^+$ (size of circles is proportional to changes in AM1 carbon charges). (Reprinted from ref 27. Copyright 1995 Royal Society of Chemistry.)

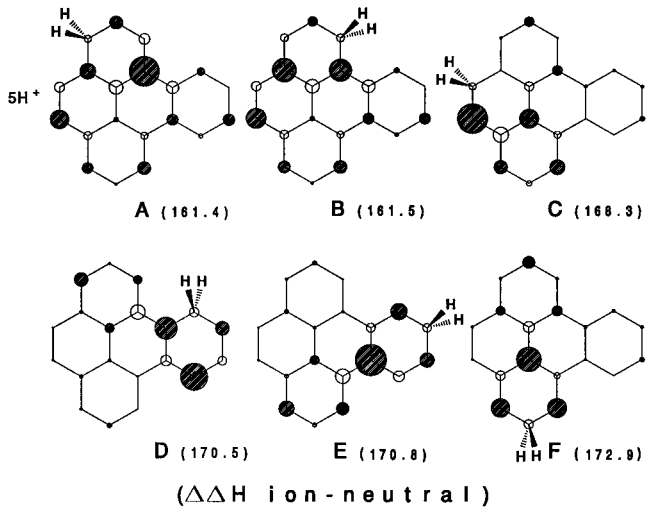

Figure 8. AM1 energies and ΔQ profiles for **5H**$^+$ (size of circles is proportional to changes in AM1 carbon charges). (Reprinted from ref 27. Copyright 1995 Royal Society of Chemistry.)

the same (see later). The ΔQ profiles (Figure 7) clearly point to the importance of phenalenium cation.

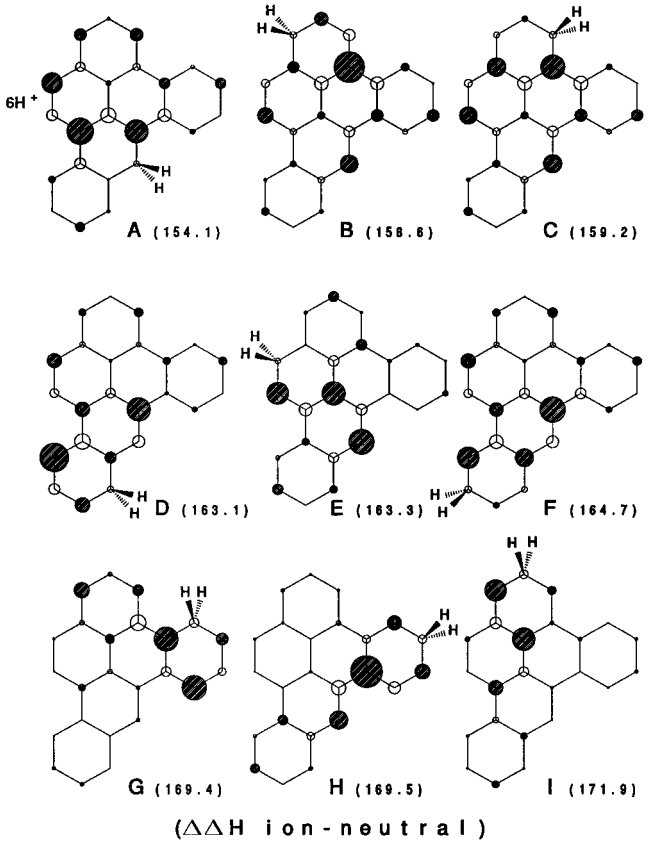

Figure 9. AM1 energies and Δq profiles for **6H**$^+$ (size of circles is proportional to changes in AM1 carbon charges). (Reprinted from ref 27. Copyright 1995 Royal Society of Chemistry.)

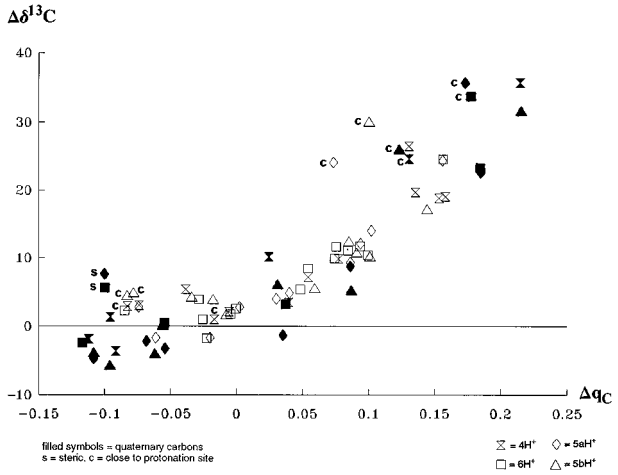

Figure 10. Plot of $\Delta\delta^{13}$C vs ΔQ_c (changes in AM1 carbon charges). (Reprinted from ref 27. Copyright 1995 Royal Society of Chemistry.)

The predicted (and observed) site of protonation is the same in **6** (a mild carcinogen); cation **6H**$^+$**A** clearly exhibits phenalenium ion character (Figure 8). For benzo[*e*]pyrene **5** (not a carcinogen) protonation at C-1 and C-3 are almost equally favored (**5H**$^+$**A** and **5H**$^+$**B**). Superacid studies concur (see below), showing a mixture of the two arenium ions.

The AM1 ΔQ/energy profiles illustrate that cations which exhibit effective charge alternation at their periphery and have extended conjugation paths are usually the most stable.

It was concluded that despite varied degrees of carcinogenic character (see Table 2), the charge

Table 2. PAH Structure vs Carcinogenic Activity (Adapted from Ref 7a)

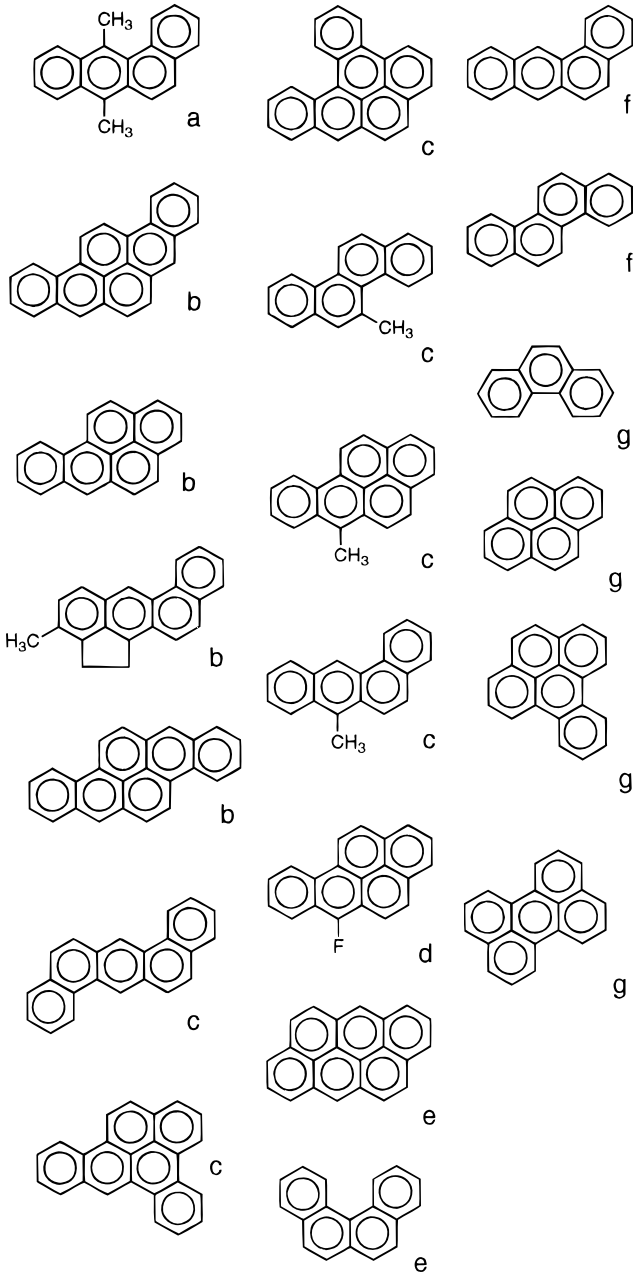

[a] Key: (a) potent carcinogen, (b) very active, (c) active, (d) moderately active, (e) weakly active, (f) very weakly active, (g) inactive.

distribution mode in the arenium ions are very similar; the importance of a robust phenalenium ion moiety has been emphasized.[27] Relevance of these model studies to the carcinogenic activity induced either by biological oxidation (→ RC) or by epoxide ring opening (→ carbocation) have been discussed.[27]

AM1 energies and charges have been reported for mono- and diprotonation of 4-methyl[6]hexahelicene **34** and [6]hexahelicene **35** (Figure 11); theoretical data for diprotonation of coronene **36** are also available.[38]

The AM1-predicted reactivity order for protonation of **35** closely parallels the positional reactivity order of Taylor et al.[2,39] for protiodetritation.

AM1 energies and charges for singlet and triplet dications of **36**,[40] and for protonation of chrysene

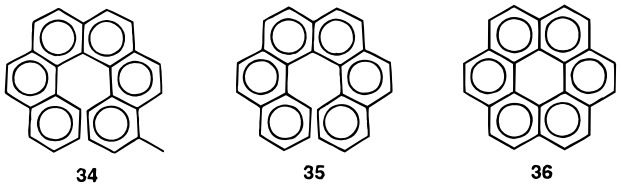

Figure 11. [6]Helicenes and coronene.

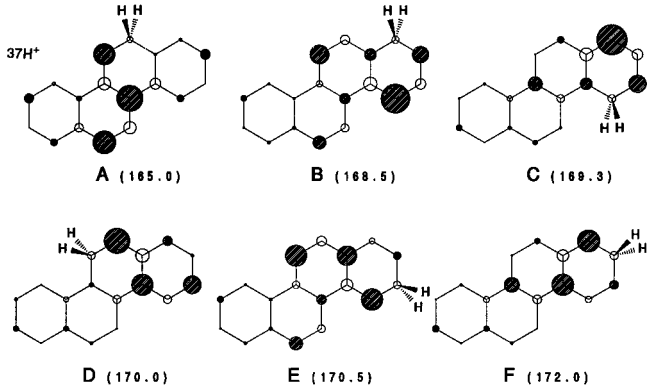

Figure 12. AM1 energies and Δ*Q* profiles for **37H**$^+$ (size of the circles is proportional to changes in AM1 carbon charges).

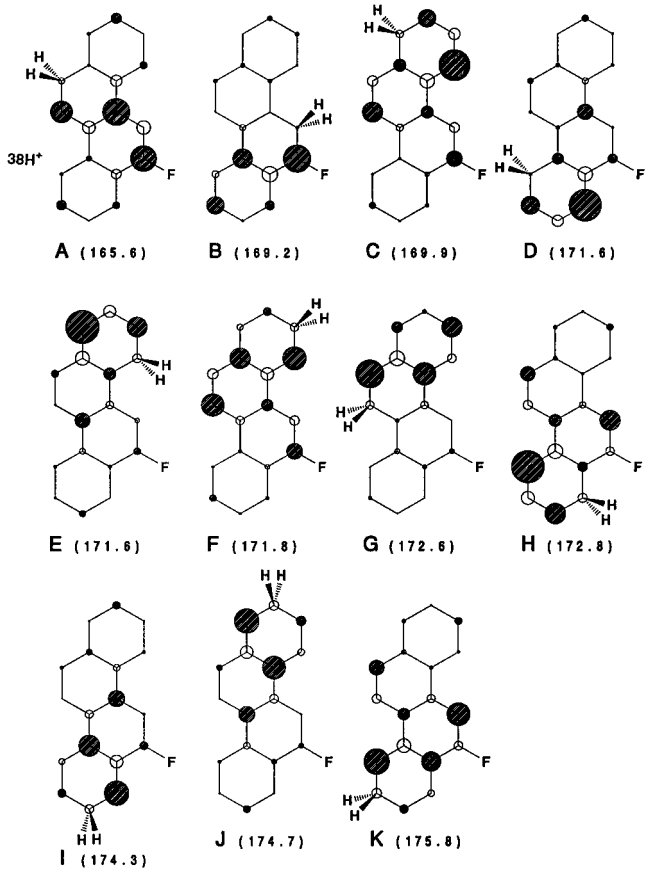

Figure 13. AM1 energies and Δ*Q* profiles for **38H**$^+$ (size of circles is proportional to changes in AM1 carbon charges).

37H$^+$ (**A** → **F**; Figure 12), 6-fluorochrysene **38H**$^+$ (**A** → **K**; Figure 13), cyclopenta[*def*]chrysene **39H**$^+$ (**A** → **J**; Figure 14), and cyclopenta[*def*]phenanthrene **40H**$^+$ (**A** → **D**; Figure 15) have been probed.[41]

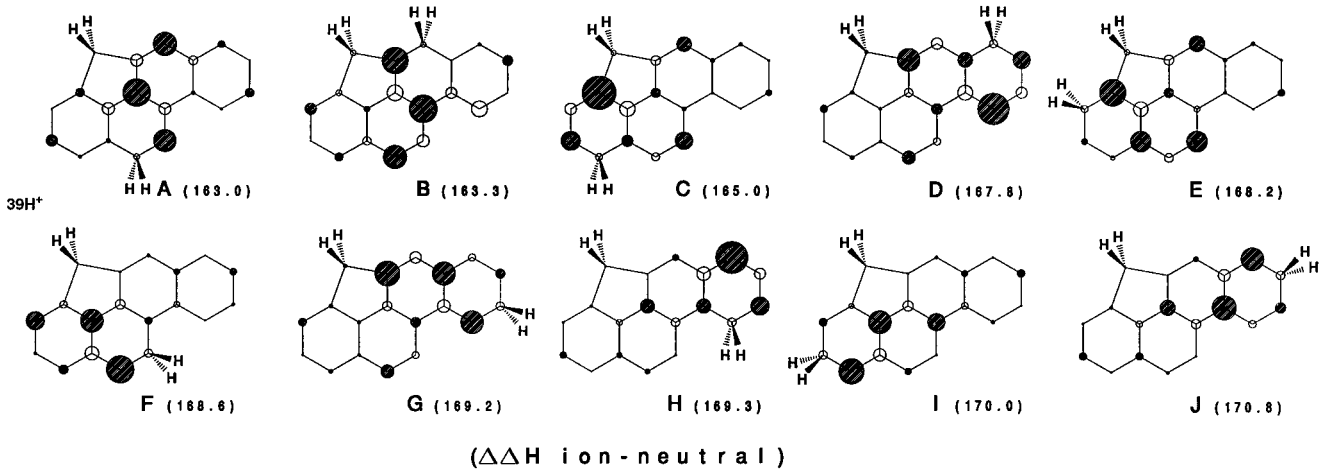

Figure 14. AM1 enegies and ΔQ profiles for **39H**$^+$ (size of circles is proportional to changes in AM1 carbon charges).

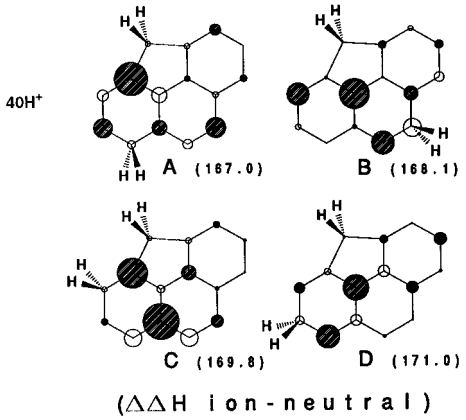

Figure 15. AM1 energies and ΔQ profiles for **40H**$^+$ (size of circles is proportional to changes in AM1 carbon charges).

AM1 predicts the reactivity order 6 > 1 > 4 > 5 > 3 > 2 for the parent chrysene,[33] this is practically the same order predicted by Hückel localization energies (6 > 1 > 5 ~4 > 3 > 2)[42] and by Dewar-PI calculations (6 > 1 > 4 ~ 10 > 5 > 3 > 8 ~ 2).[35] Taylor's protiodetritiation data gave 6 > 5 > 1 > 4 > 3 > 2.[42]

The energy/charge profiles (see figures) provide rapid visual comparisons of the charge delocalization mode vs energy in the arenium ions:

The observed persistent ion **37H**$^+$**B** (C-1 protonated; see also studies in superacids) is calculated to be 3.5 kcal/mol higher in energy than the predicted most stable C-6 protonated ion **37H**$^+$**A**.[41] Charge delocalization in chrysenium cation is not as extensive as in pyrenium ions and its benzannelated derivatives;[41] for **37H**$^+$**A** carbons having the most positive charge are C-5, C-10b, and C-12. For **38H**$^+$**A** the preferred site of protonation remains unchanged (C-12). Magnitude of ΔQ increases at the fluorine-bearing carbon indicative of fluoronium ion character.[41]

For **39H**$^+$, AM1 predicts attack at C-11 and C-5 to be almost equally the best candidates.[41] The positions of highest positive charge in the arenium ions are the "*ortho*", "*para*", and one other conjugated carbon. The unsymmetrically 1,5-diprotonated dication **39H$_2$**$^{2+}$**A** is 3.9 kcal/mol more stable than the symmetrically 3,5-diprotonated methanochrysene (B) (Figure 16).[41]

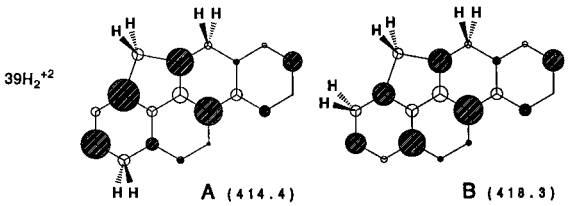

Figure 16. AM1 energies and ΔQ profiles for **39H$_2$**$^{2+}$ (size of circles is proportional to changes in AM1 carbon charges).

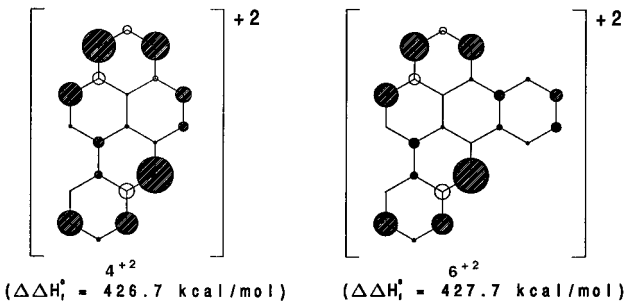

Figure 17. Charge distribution in the oxidation dications of **4** and **6**.

For **40H**$^+$ protonation at C-3 is only slightly favored over that at C-4; potonation *peri* to the bridge is 2.8 kcal/mol higher in energy and C-2 protonation is unfavorable (Figure 15).[41]

AM1 predicts that charge distribution in the oxidation dications of **4** and **6** are quite extensive and also involve the benzo[*a*] ring (Figure 17).[27]

More Recent Stable Ion Studies of Naphthalenium and Hexahydropyrenium Cations

A series of long-lived dimethylnaphthalenium DMN$^+$ compounds were generated by Lammertsma and Cerfontain.[25] The NMR data are sketched in Figure 18.

Magnitude of the $\Delta\delta^{13}$C values indicate rather uniform charge alternation at the periphery with significant delocalization taking place in the protonated ring where the *para* carbon almost always sustains the greatest positive charge.

For DMN$^+$ good agreement was found between theoretically predicted lowest energy arenium ions

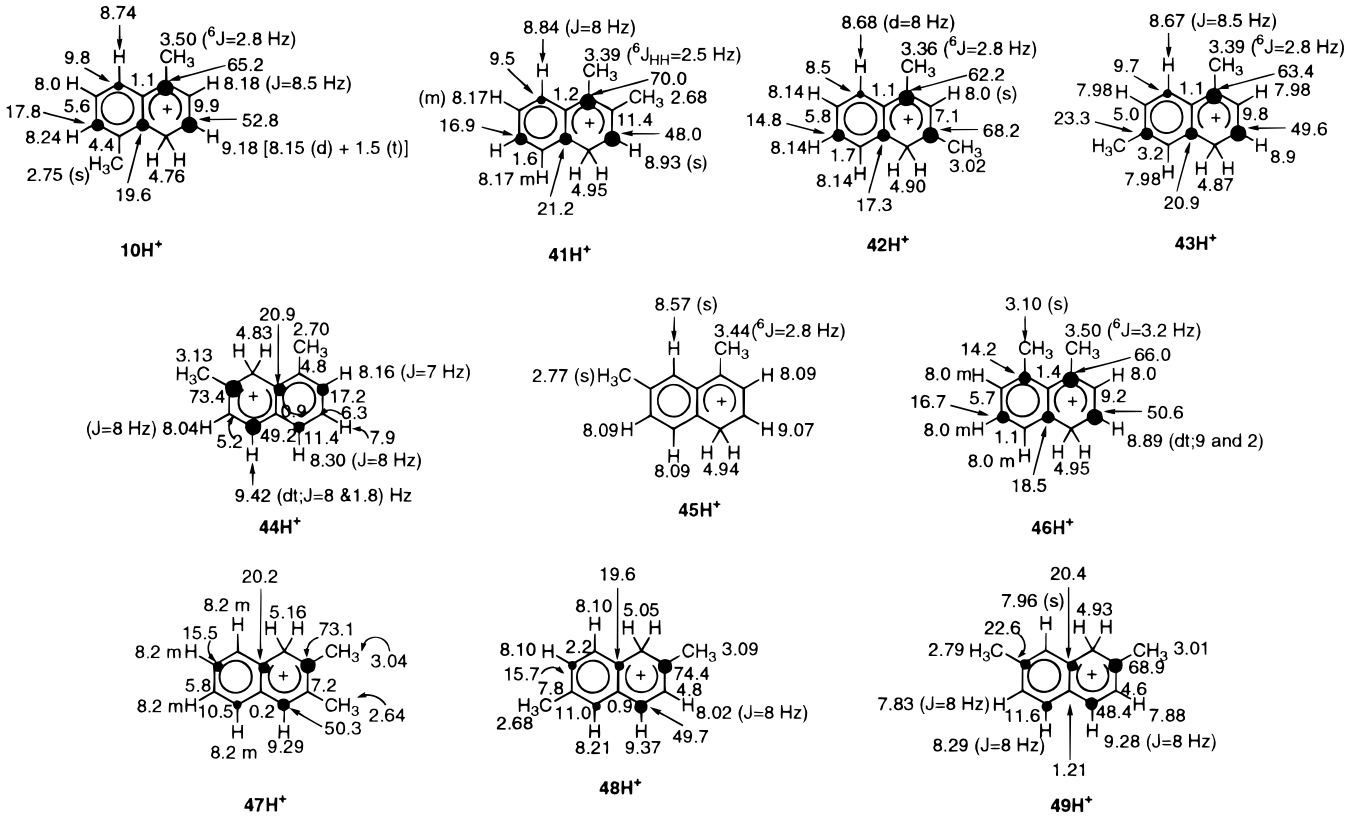

Figure 18. Compilation of ^{1}H NMR and $\Delta\delta^{13}$C values for DMNs (dark circles are roughly proportional to magnitude of carbon deshielding).

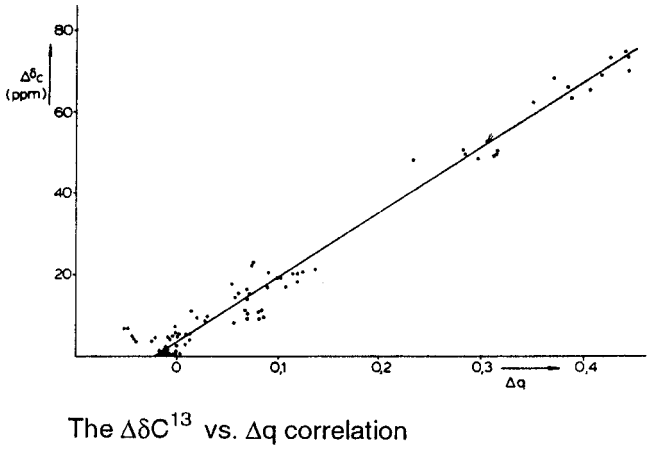

Figure 19. $\Delta\delta^{13}$C vs Δq correlation. (Reprinted from ref 25. Copyright 1979 American Chemical Society.)

(Hückel MO) and those observed under stable ion conditions. A correlation between $\Delta\delta^{13}$C and Δq (charge density) was established (see also the preceding section). A linear correlation was also found in a $\Delta\delta^{13}$C vs Δq plot (Figure 19) after adjusting the theoretical inductive parameter for methyl, taking into account the increase in methyl hyperconjugation and negative inductive effect which increase the positive charge at the Me-bearing ring carbons and push π-electron density away from that ring carbon.[25] Such an adjusted $\Delta\delta^{13}$C vs Δq plot yielded a slope of 158.1 ppm/e.

It was suggested that a more shielded *ortho* carbon at the ring junction of naphthalenium ions (C-10) may reflect hyperconjugation from the cationic center into the rigid C-10.[25]

A six-bond H−H coupling ($^6J_{p\text{-Me}-CH_2^+}$) of 2.5−3.0 Hz was observed in the ^{1}H NMR spectra for the *p*-methyl-substituted naphthalenium ions. Two independent equilibria were discovered for protonated 1,4-dimethylnaphthalene **50**, giving four arenium ions (Figure 20).[25]

Protonation of 1,8-DMN initially gives **46H**$^+$ (Figure 21). On raising of the temperature **44H**$^+$ begins to appear; complete conversion occurs quickly. Ion **46aH**$^+$ is a logical intermediate with relief of *peri* strain as the driving force for rearrangement.[16]

Lammertsma[26] showed that hexahydropyrene is monoprotonated in FSO_3H/SO_2ClF (→ **51H**$^+$), and diprotonated in "magic acid"/SO_2ClF (→ **51H$_2^{2+}$**). For **51H**$^+$, the alkylated *ortho* carbon is substantially more positive than the unsubstituted *ortho*. Positive charge retention at the *para* position is surprisingly small and the two conjugated carbons are more positive (Figure 22). The charge alternation mode in **51H$_2^{2+}$** is interesting: The alkyl-bearing *ortho* positions are dramatically more positive than the other *ortho* carbons. The C-9/C-10 ring junction carbons (formally *para*/*para*) are both positive.

Polymethylnaphthalenium Cations

The *ipso*-protonated octamethylnaphthalene **24H**$^+$ was first reported by Hart (TFAH, rt).[43] Hexamethylnaphthalenium ions **52H**$^+$ and **53H**$^+$ were similarly prepared (Figure 23). *Ipso* protonation is favored in these cases because of relief of *peri* strain.

A more detailed ^{1}H NMR study of persistent polymethylnaphthalenes was reported by Koptyug et al. (Figure 24).[44] Kinetic monoprotonation (FSO_3H/SO_2ClF below −80 °C) occurs at the unsubstituted

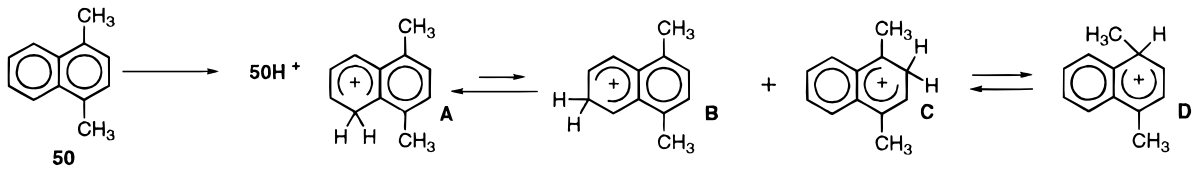

Figure 20. Skeletal rearrangements in protonated **50**.

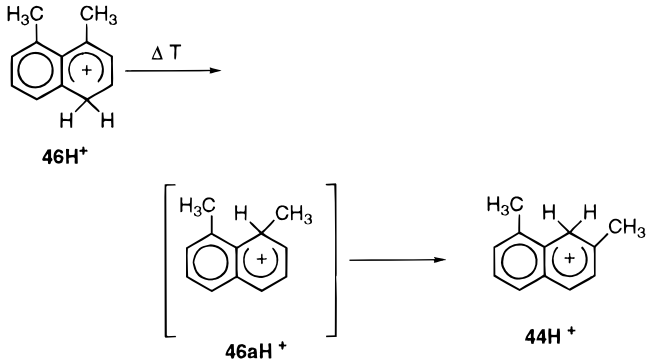

Figure 21. Skeletal rearrangement in **46H**$^+$.

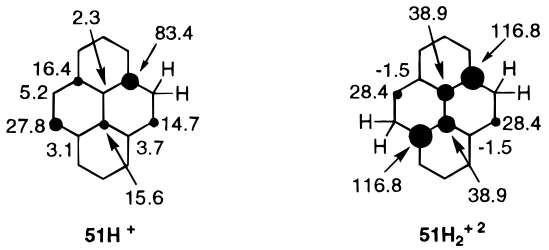

Figure 22. Mono- and diprotonation of hexahydropyrene (only $\Delta\delta^{13}$Cs are shown).

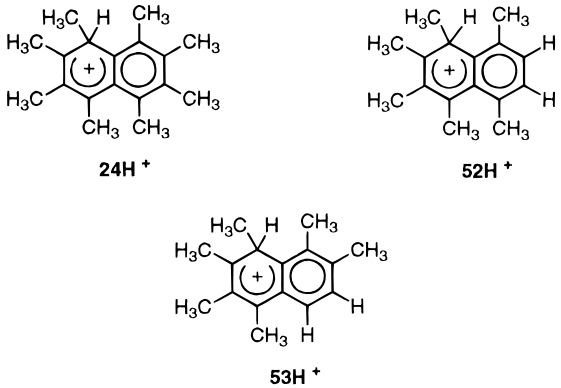

Figure 23. Hart's polymethylnaphthalenium cations.

peri position to give **58H**$^+$. Irreversible rearrangement of **59H**$^+$ occurs at higher temperatures (∼−50 °C) to give **60H**$^+$ for which *peri* strain is relieved by rehybridization.

When one arene ring is fully methylated, kinetic protonation occurs exclusively (by NMR) at the *ipso* α-position. Thus **61H**$^+$ and **62H**$^+$ are initially formed at low temperature and subsequently rearrange to **56H**$^+$ and **57H**$^+$ respectively on raising of the temperature.[36]

It was suggested that these rearrangements go through a diprotonated naphthalenium dication. Two such dications **63H$_2$**$^{2+}$ and **64H$_2$**$^{2+}$ were independently prepared in "magic acid"/SO_2ClF as models. The ^{13}C NMR data for the latter were reported.

Lammertsma[26] carried out a detailed stable ion protonation study of polymethylnaphthalenes. For-

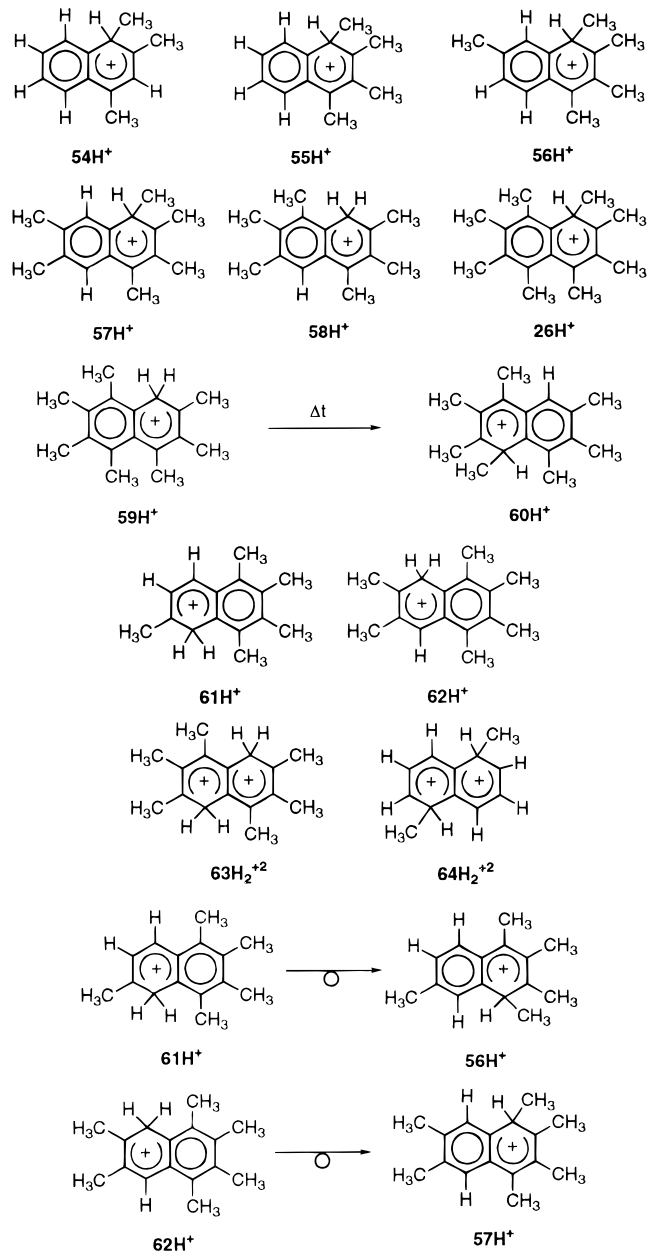

Figure 24. Koptyug's polymethylnaphthalenium mono- and dications.

mation of a single naphthalenium ion, equilibrium between two (or more) naphthalenium ions or isomerization processes were all identified, depending on the substrate structure (see Figure 25).

The following four categories of reactions have been noted for naphthalenium ions:

(1) "free" α-cation ⇌ "free" *β*-cation

(2) *ipso* α-cation ⇌ "free" *β*-cation

(3) "free" α-cation ⇝ *ipso* α-cation

(4) *ipso* α-cation ⇝ "free" α-cation

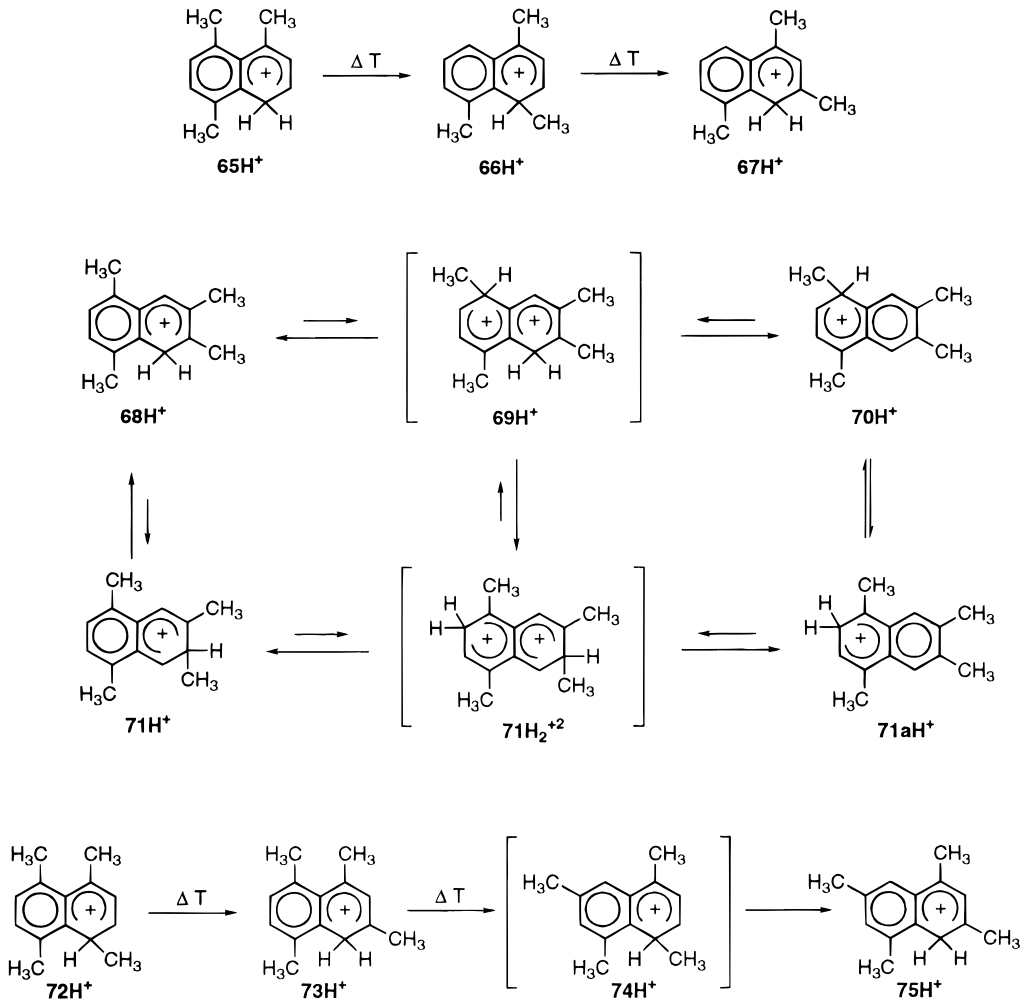

Figure 25. Skeletal rearrangements in tetramethylnaphthelenium ions.

These may occur by intra- or intermolecular H-shifts; process 3 may go through the dication (see also Koptyug). The $\Delta\delta^{13}C$ (cation-neutral) profiles are gathered in Figure 26 for comparison. Extensive positive charge resides *ortho* and *para* to the site of attack. The annelated *ortho* position is less positive than the other *ortho* position, two conjugated carbons of the nonprotonated ring consistently sustain more positive charge.

Bridged Annulenium Cations

Persistent monocation **77H**$^+$ was first reported by Winstein.[45] Lammertsma and Cerfontain[46a] showed that diprotonation occurs in "magic acid"/SO_2ClF to give **77H$_2$**$^{2+}$. The dication is best represented by structure **A**, showing a cyclopropyldicarbinyl dication moiety. When the temperature was raised, the monocation **77H**$^+$ formed in FSO_3H/SO_2ClF rearranges to **78H**$^+$ having a cyclopropylcarbinyl cation moiety (Figure 27).[46b]

Persistent monocations of 1,6:8,18-propanediylidene (**79**), 1,6:8,13-butanediylidene (**80**), and *syn*-1,6:8,13-bismethano[14]annulene (**81**) were generated by Michl and Vogel[47] by protonation with $FSO_3H{\cdot}SbF_5$ (4:1)/SO_2ClF (Figure 28). In all cases protonation occurred at C-7. The charge delocalization pattern in the annulenium cations (magnitude of $\Delta\delta^{13}Cs$) is illustrated in Figure 28. The resulting ions are slowly converted to oxidation dications (see later section). Protonation of the ethano-bridged analogue

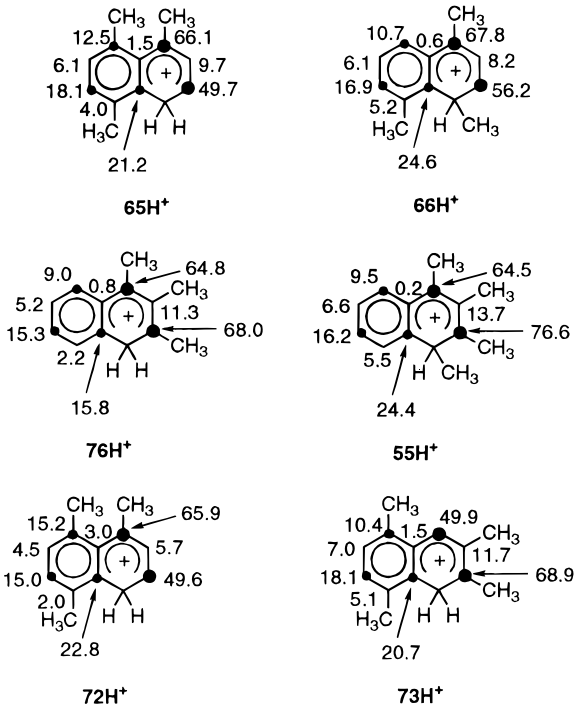

Figure 26. $\Delta\delta^{13}C$ profiles for trimethyl- and tetramethylnaphthalenium ions (size of dark circles is roughly proportional to magnitude of carbon deshielding).

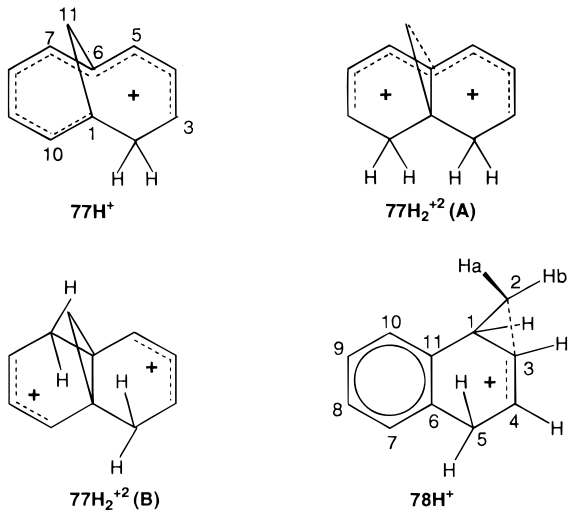

Figure 27. Mono- and diprotonation of methano[10]-annulene.

1,6:8,13-ethanediylidene[14]annulene **82** gave initially a mixture of monocations which converted to the C-4 protonated species **82H**$^+$. The varying behavior of the ethano-bridged [14]annulene was ascribed to variation in the degree of transannular interactions as a function of bridge size. Charge alternation at the periphery of these annulenes is clearly seen on the basis of ^{13}C NMR data. Ring protonation reduces the diamagnetic ring current, and this in turn reduces the anisotropic shielding of the bridgehead protons.

Anthracenium and Benzo[a]anthracenium Ions

As mentioned earlier, *ipso* protonations of **2** and **1** with TFAH/H_2O/BF_3 were shown by MacLean et al. in the early 1960s.[16] The proton NMR spectra were included and discussed in the early review of Perkampus.[18]

The low-temperature UV spectrum of benzo[*a*]-anthracene protonated with FSO_3H was reported by the Leiden group in the late 1960s[48] and interpreted as a mixture of **1H**$^+$ and **1aH**$^+$ (see Figure 1). Addition of SbF_5 to the arenium ion mixture gave the oxidation dication **1**$^{2+}$, quenching with an alkane led to hydride abstraction at C-7, selectively forming **1aH**$^+$ (on the basis of UV studies).[48]

The first detailed persistent ion study of anthracenium ions was by van de Griendt and Cerfontain,[49] who protonated a series of 9-alkylanthracenes (**83**–**88**) with FSO_3H/SO_2ClF (Figure 29).

Protonation at C-10 was observed in all cases. When Cl groups were introduced at C-1/C-8, C-9 protonation was observed as well (relief of *peri* strain). For 1-chloro-9-isopropylanthracene, the *ipso*-protonated iPr group has nonequivalent methyls; one of which is experiencing significant anisotropic shielding (at ~0.06 ppm) and the other is normal (1.57 ppm). The geminal coupling J_{A-X} is only 3 Hz (corresponding to 80° dihedral angle). The Newman projection shown (Figure 30) provides a satisfactory explanation for the NMR shifts (see isopropylpyrenium ions for additional examples of this type).

Whereas benzo[*a*]anthracene itself exhibits only weak carcinogenic activity, 7,12-dimethyl- and 7-methylbenzo[*a*]anthracenes are reactive carcinogens (Table 2).[50] Ongoing studies[51] seek to address the charge distribution issue in benzo[*a*]anthracenium cations (for comparison with anthracenium ions) and the role of substituents. Selective hydride abstraction by **1**$^{2+}$ (→ **1aH**$^+$) suggested by the Leiden[48] group based on UV work should be further examined. (The need to verify the UV-based conclusions by low-temperature NMR work has already been pointed out by Pagni in his review.)[12]

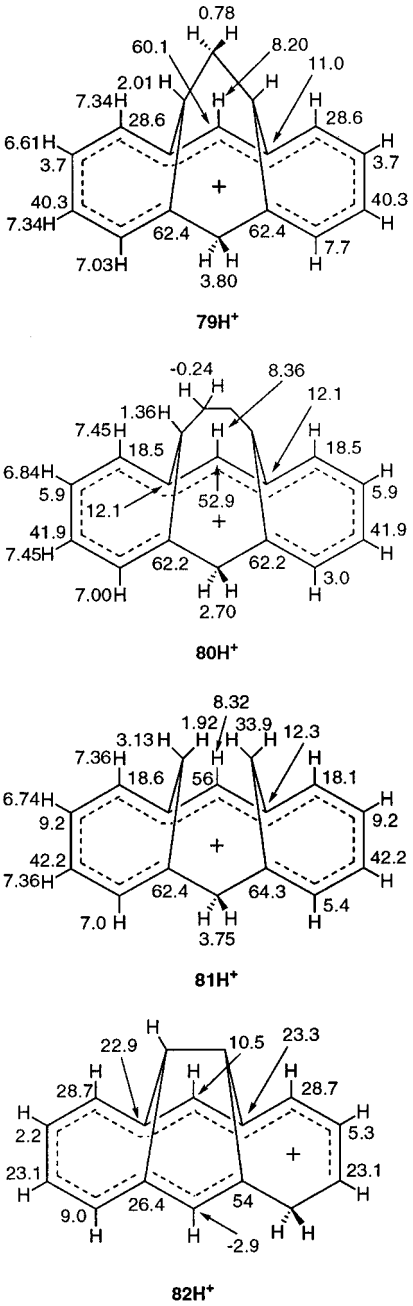

Figure 28. $\Delta\delta^{13}$C values (and ^{1}H NMR data) for Michl's [14]annulenium cations.

Phenanthrenium and 4,5-Ethanophenanthrenium (dihydropyrenium) Ions

Shubin and associates[52] generated and studied a series of 9-R substituted (R = Me,Et, CH_2Cl, and substituted Ph) 9,10-dimethylphenanthrenium ions and examined the kinetics of 1,2-migration of these

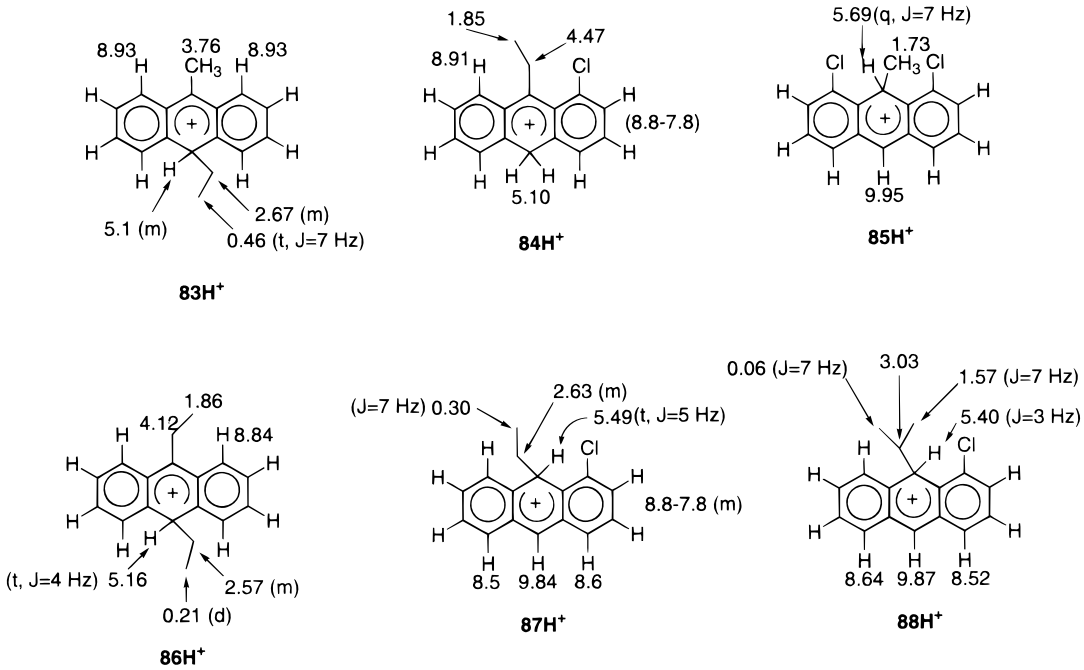

Figure 29. ^{1}H NMR data for persistent 9-alkylanthracenium ions.

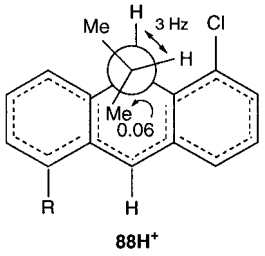

Figure 30. Newman projection for **88H**$^+$.

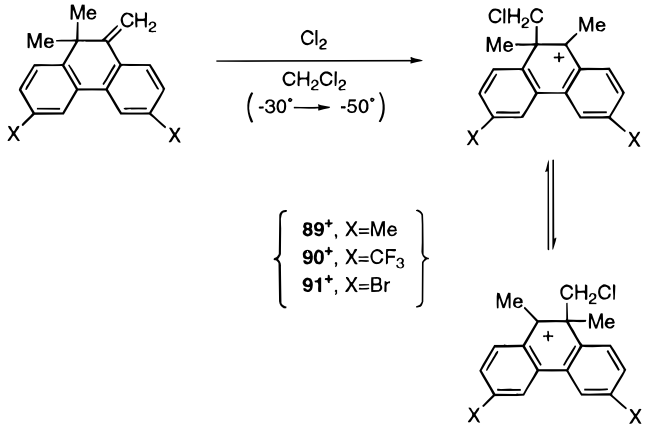

Figure 31. Degenerate rearrangements in Shubin's phenanthrenium ions.

groups by VT−^{1}H NMR (Figure 31). The NMR data for Shubin's phenanthrenium cations **89**$^+$−**91H**$^+$ undergoing degenerate rearrangement are gathered for comparison (Figure 32). These investigations allowed the migratory aptitude of various groups to be compared. The 1,2-migration of CH_2Cl group is significantly slower than methyl.[52]

In the early 1980s a series of long-lived methylphenanthrenium monocations were generated in FSO_3H/SO_2ClF for ^{1}H NMR studies.[53] Representative examples (**92H**$^+$−**96H**$^+$) are shown (Figure 33). In "magic acid"/SO_2ClF diprotonation of two tetramethyl- and several dimethylphenanthrenes was effected.[53] The observed monoprotonation sites are in accord with predictions based on localization energies calculated from simple Hückel π-calculations.

More recently,[54] it has been shown that crowded (Z)-2,2,5,5-tetramethyl-3,4-diphenylhex-3-ene is ring protonated at low temperature in $FSO_3H{\cdot}SbF_5$(1:1)/SO_2ClF or in $FSO_3H{\cdot}SbF_5$(4:1)/SO_2ClF and undergoes a rapid transannular cyclization eventually leading to **98H**$^+$ and **98H$_2$**$^{2+}$ mixture plus tBu^+ (Figure 34). The cofacial relationship of the phenyl rings in the (*Z*)-stilbene is required for cyclization to occur; the corresponding (*E*)-stilbene does not rearrange to phenanthrenium ions.

As part of the early studies of phenanthrenium ions, the mono- and dications of 4,5-ethanophenanthrene were also generated and studied by NMR.[53] On the basis of 100 MHz ^{1}H NMR spectra, the formation of dihydropyrenium ions **99H**$^+$ and **99H$_2$**$^{2+}$ was suggested (Figure 35).

More recent ^{13}C and 2D NMR studies,[55] have shown that dihydropyrene is monoprotonated in FSO_3H/SO_2ClF at C-3 (→ **99aH**$^+$; *peri* to the bridge). The 2,7-di-*tert*-butyl derivative is similarly monoprotonated at C-3 (→ **100H**$^+$). Upon standing in the superacid these monocations are converted to pyrenium cations **3H**$^+$ and **101H**$^+$ (Figure 36). Formation of 2,7-di-*tert*-butylpyrenium ion from its dihydropyrene precursor is slower than that of parent dihydropyrene to pyrenium cation.

Alkyl(cycloalkyl)pyrenium Ions

For parent pyrene, DEWAR-PI and Hückel calculations predict that α attack is most favored. The Wheland intermediates of $\alpha\beta$ and β attack are 8.8 and 20.5 kcal/mol less stable.[56] A series of crowded alkyl(cycloalkyl)pyrenes namely 1-isopropyl- (**32**), 2-isopropyl- (**33**), 4-isopropyl- (**30**), 1,3,6,8-tetraisopropyl- (**25**), 2,7-di-*tert*-butyl- (**101**), 1,3,5,7,9-pentaisopropyl- (**28**), 1,3,5,8-tetracyclohexy- (**102**), and

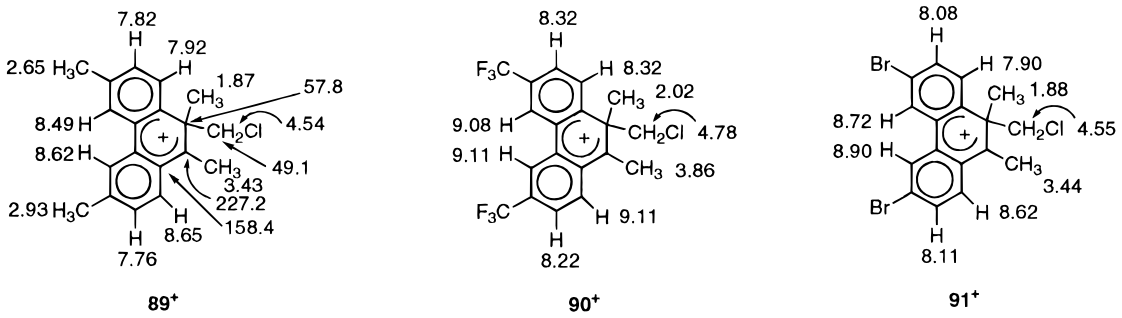

Figure 32. ^{1}H NMR data for dynamic phenanthrenium ions (some key ^{13}C values for **89**$^{+}$ are also given).

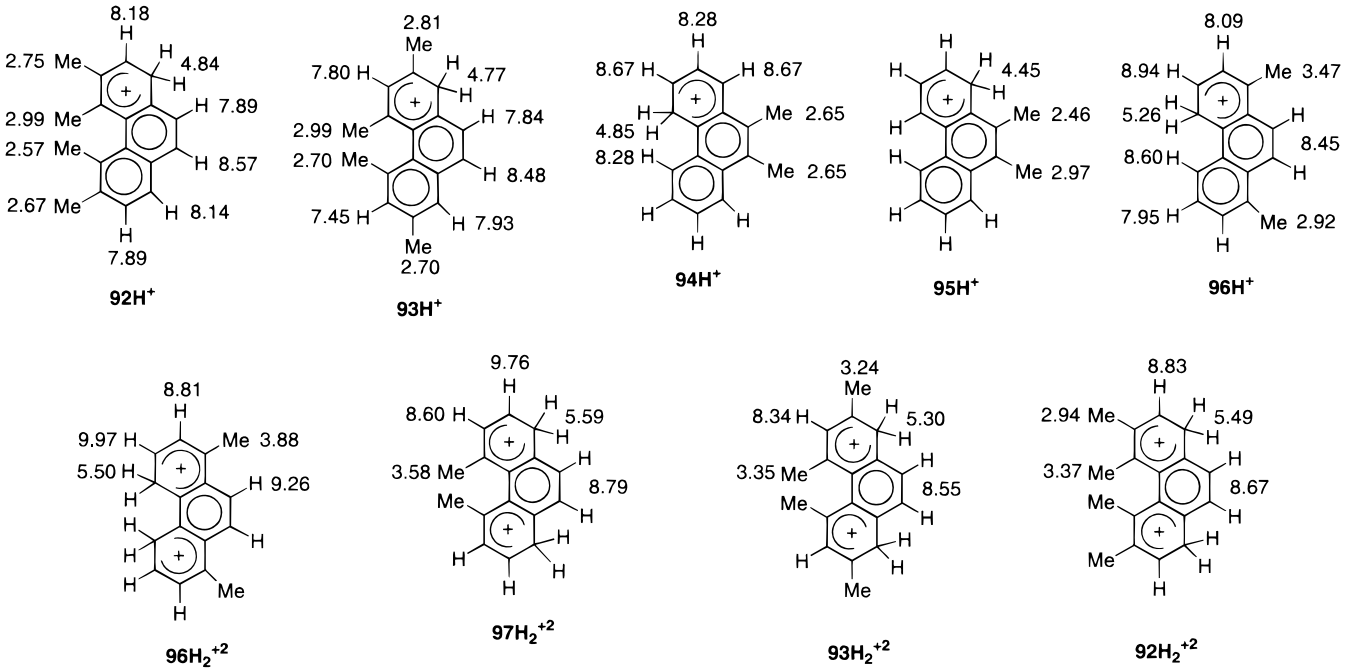

Figure 33. ^{1}H NMR data for methylphenanthrenium mono- and dications.

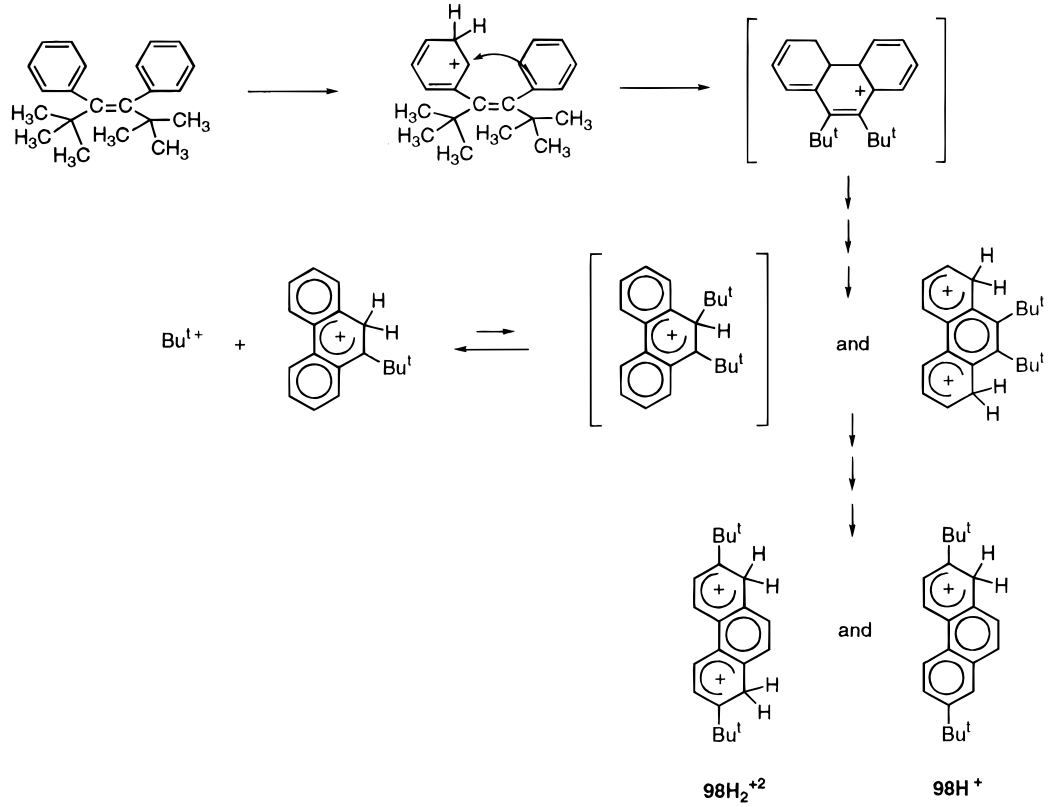

Figure 34. Formation of phenanthrenium ions from the crowded (*Z*)-stilbene by transannular cyclization.

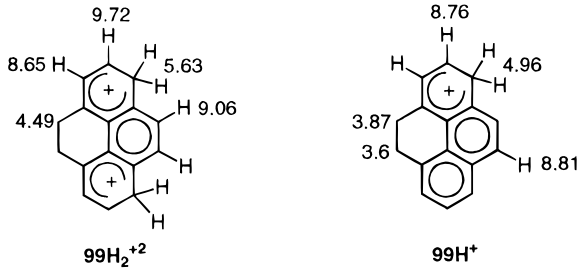

Figure 35. Protonation of ethanophenanthrene (dihydropyrene).

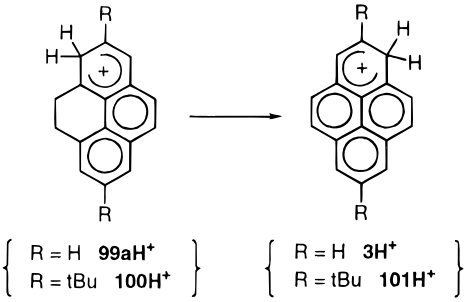

Figure 36. Formation of pyrenium ions from protonated dihydropyrenes.

2,4,7,9-tetracyclopentylpyrene (**103**) were monoprotonated in FSO_3H/SO_2ClF or $TfOH/SO_2ClF$ to give their corresponding pyrenium ions of α attack in all cases (Figure 37).[56] The inductive stabilization of alkyl(cycloalkyl) groups determines the regioselectivity of α protonation.

Stable diprotonation dications were not detected in "magic acid"/SO_2ClF due to competing oxidation. In "magic acid"/SO_2 persistent pyrenium ions of sulfinylation were obtained.[48]

^{1}H NMR studies showed that the magnitude of chemical shift changes caused by α protonation and sulfinylation of these crowded pyrenium ions are rather similar in all cases, with the remote α and two αβ positions being most deshielded; "*ortho*" (and "*meta*") protons are shielded (Figure 38).

The symmmetrical all-α-substituted **25**−**27** are monoprotonated at the *ipso* position and subsequently rearrange by R group migration to a *peri* position (Figure 39). Whereas in dilute samples **25H**$^+$ is directly observable, sterically more congested **26H**$^+$−**27H**$^+$ are not persistent, rearranging rapidly to the NMR observable **26aH**$^+$ and **27aH**$^+$. Since αβ protonation is never observed even in the presence of suitable substituents, this rearrangement provided the first examples of pyrenium ions of αβ attack.

By using ^{13}C and 2D NMR, the charge distribution mode was probed in detail for a series of crowded pyrenium ions of protonation and sulfinylation.[57] Pertinent ^{1}H NMR data (Figure 40) and the charge delocalization mode based on the $\Delta\delta^{13}$C profiles (Figure 41) are gathered for comparison.

The pyrenium ions of αβ attack exhibit phenanthrenium ion character. Thus the positive charge is located predominantly at C-1/C-3, C-4/C-10, C-5a/C-8a, and at C-7. The chemical shifts of the *ortho* carbons C-8a and C-10 show that the ring junction carbon sustains more positive charge, whereas positive charge at C-10b (*para*) carbon is quite small.

Analogous to Cerfontain's *ipso*-protonated 9-iPr anthracenium ion,[49] anisotropic shielding is observed

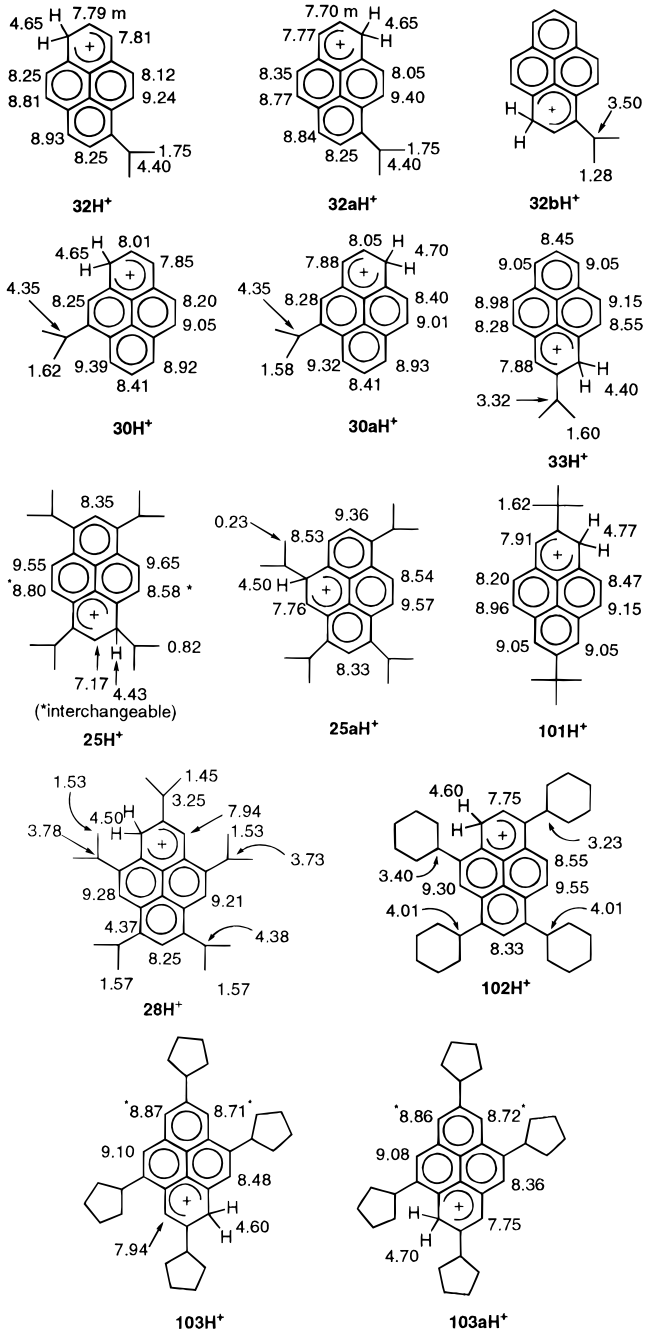

Figure 37. Persistent alkyl(cycloalkyl)pyrenium ions and their ^{1}H NMR assignments.

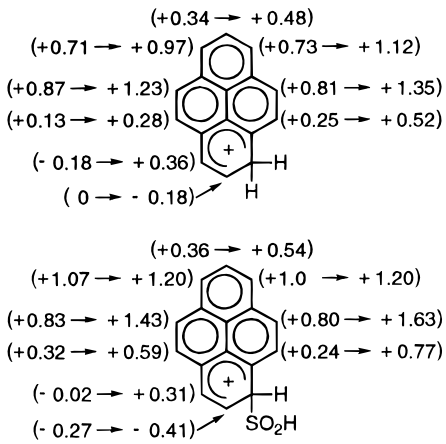

Figure 38. Comparison of magnitude of $\Delta\delta^1$Hs in pyrenium ions of protonation and sulfinylation.

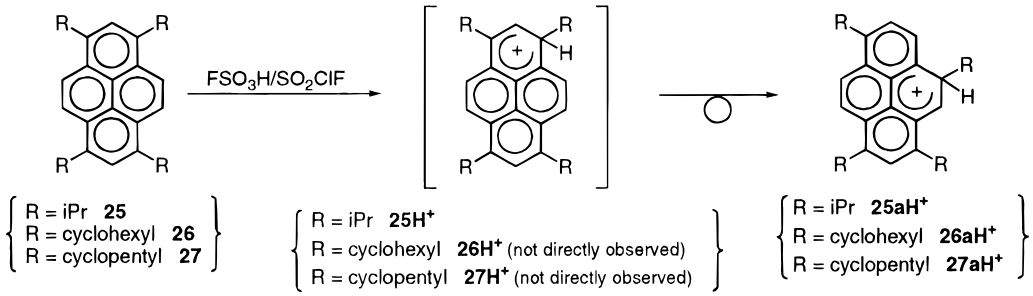

Figure 39. *Ipso* protonation and rearrangement of all α-substituted pyrenes.

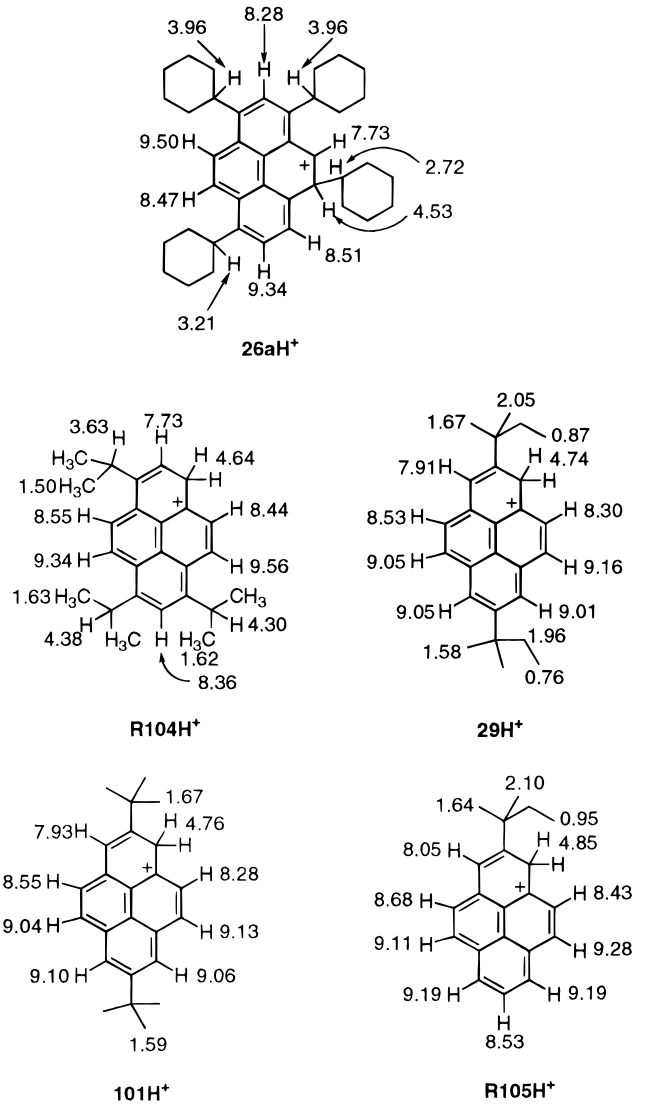

Figure 40. Compilation of ^{1}H NMR data for *ipso*-protonated pyrenium ions and their rearranged cations.

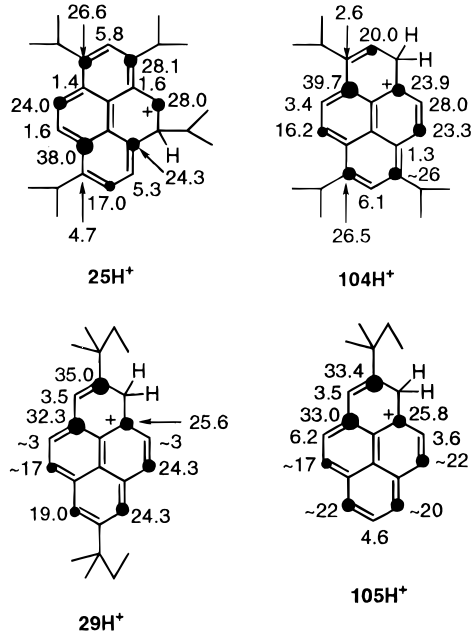

Figure 41. Charge delocalization mode in crowded pyrenium ions based on magnitude of $\Delta\delta^{13}$Cs.

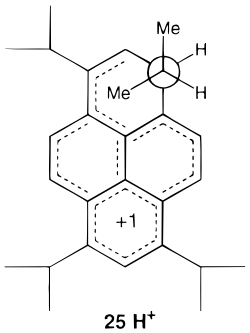

Figure 42. Newman projection for **25H**$^+$.

for one of the two iPr(Me) groups in *ipso*-protonated cation **25H**$^+$ (at 0.82 ppm) (see Newman projection; Figure 42). One of the iPr(**Me**) groups in **25aH**$^+$ is also highly shielded (at 0.23 ppm).

Fluorinated Alkyl(cycloalkyl)pyrenium Ions

A series of persistent fluorinated alkylpyrenium cations and their tetrahydro and hexahydro derivatives have been generated.[58] Multinuclear and 2D NMR were used to probe the charge distribution mode at the periphery of these arenium ions and to examine the role of fluorine in charge perturbation.

Selective fluorine introduction in the precursors was achieved by the "Berg synthesis" via $ArNO_2 \rightarrow ArNH_2 \rightarrow ArN_2^+ \rightarrow ArF$ sequence on the pyrene (α fluoro), tetrahydropyrene (β fluoro), and hexahydropyrene (αβ fluoro), respectively.[58]

Presence of a fluorine substituent in the β position increases the stability of the pyrenium ion of α protonation and leads to a single α-pyrenium ion **108H**$^+$ (Figure 43). Fluorine in the αβ (**105**) and α positions (**104**) is not stabilizing enough to alter the preferred α attack.

The charge distribution mode in the fluoropyrenium (Figures 44 and 45) and alkylpyrenium ion is rather similar, both showing very distinct phenalenium ion character. The $\Delta\delta^{13}$C, $\Delta\delta^{19}$F, and $\Delta\delta^{1}$H patterns are shown, with the most positive carbons proportionally circled.

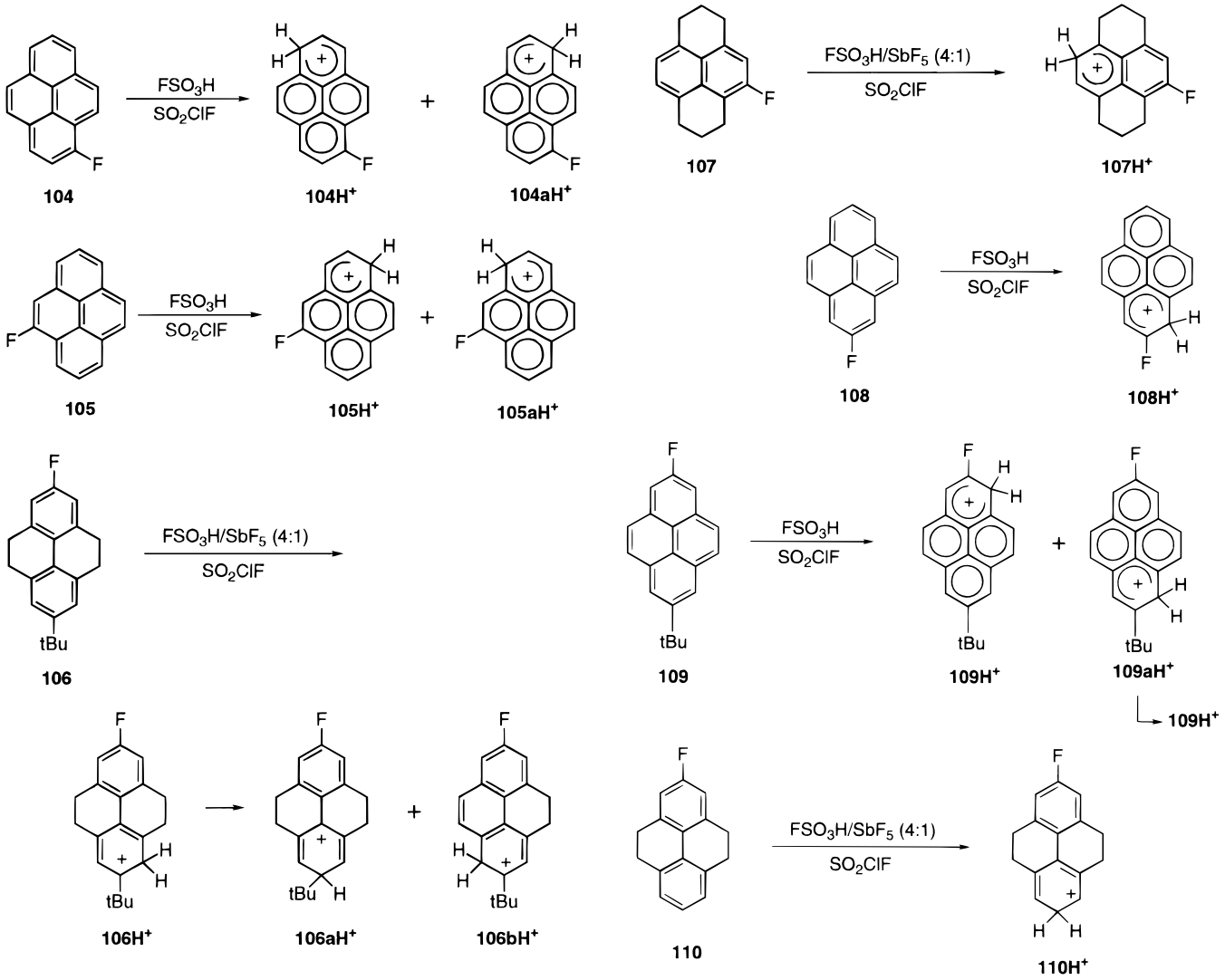

Figure 43. Fluoropyrenium ions and their tetrahydro and hexahydro derivatives.

These studies show that positive charge is extensively delocalized away from the site of attack and exists predominantly at alternating carbons of the periphery within a phenalenium ion moiety. Fluorinated pyrenium ions exhibit fluoronium ion character as deduced from increased $^1J_{C-F}$, fluorine deshielding, and reduced deshielding of fluorine-bearing carbons as compared to the position of the same carbons in nonfluorinated pyrenium cations.

A β-fluorine and a β-tBu provide almost equal kinetic stability to the pyrenium ion of α attack (**109H**$^+$ and **109aH**$^+$), but the former is thermodynamically more stable. Thus low-temperature protonation of **109** initially produced an equal mixture of **109H**$^+$ and **109aH**$^+$; cold storage led to thermodynamic equilibration and detection of almost pure **109H**$^+$.

Protonation of Isomeric Nitronaphthalenes

Earlier studies by Shudo et al.[59] suggested that isomeric nitronaphthalenes are diprotonated in triflic acid to give the corresponding iminium−naphthalenium dication (**111**$^{2+}$) which is persistent at room temperature. The oxo−iminium−naphthalenium structure (**112**$^{2+}$) was ruled out on the basis of quenching experiments with ^{18}O-labeled water and by cryoscopic measurements (Figure 46).

Nitroalkyl(cycloalkyl)pyrenium Ions

Two detailed studies on protonation of crowded nitroalkyl(cycloalkyl)pyrenes have been reported.[28,60] The first one dealt with nitration of alkyl(cycloalkyl)-pyrenes, protonation of the resulting buttressed nitroalkyl(cycloalkyl)pyrenes, cyclization to iminium−pyrenium dications, and transfer nitration reactions of protonated nitroalkylpyrenes. The subsequent study focused on the charge distribution issue in several classes of iminium−pyrenium dications, their *ortho*- and *peri*-cyclized analogues, and the generality of such nitro group cyclizations and their ring-opening chemistry.

Protonation of **113** in FSO_3H/SO_2 or FSO_3H/SO_2 gives the dihydroxyiminium−pyrenium dication **21**$^{2+}$ which when the temperature was raised rearranges to cyclic cation **22**$^+$ (Figure 47).

Reaction of **28** with $NO_2^+BF_4^-/CD_3CN$ gave two room temperature stable pyrenium ions namely the Wheland intermediate of α nitration **113H**$^+$ and the dihydroxy iminium−pyrenium dication **21**$^{2+}$. The less basic **114** is NO_2-diprotonated in "magic acid"/

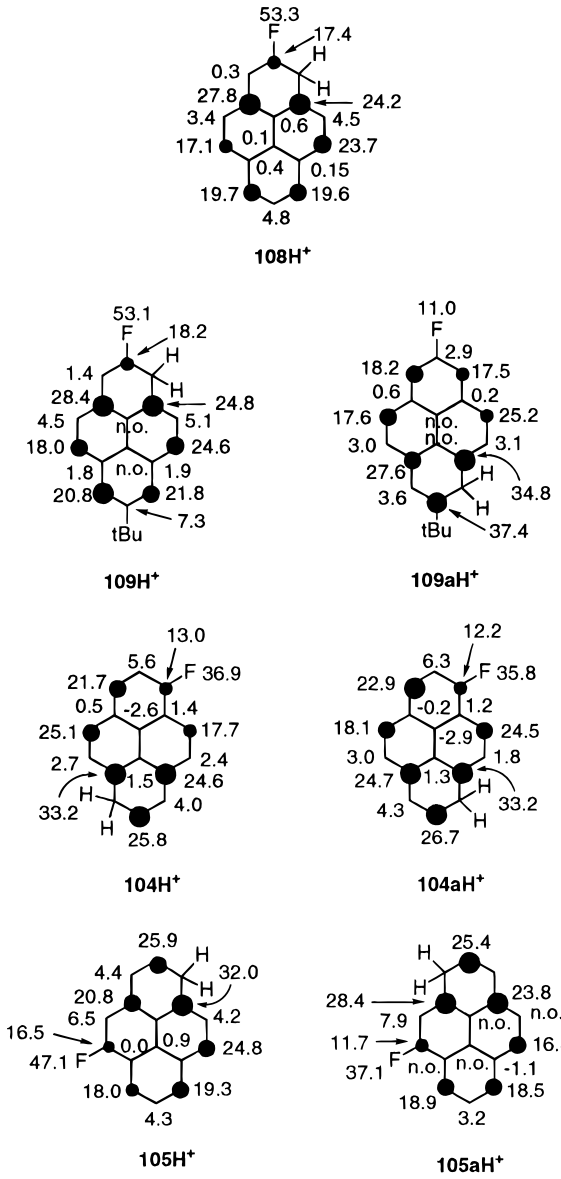

Figure 44. $\Delta\delta^{13}$C and $\Delta\delta^{19}$F profiles in fluoropyrenium cations (size of dark circles is roughly proportional to magnitude of carbon deshielding).

SO_2ClF and similarly gives a dihydroxyiminium−pyrenium dication **114**$^{2+}$, whereas 2-nitropyrene is ring protonated under these conditions.[60]

The mono- and dinitropyrene derivatives (Figure 48) were protonated in various superacid media. Nitro group diprotonation was observed in all cases, a process which appears to be general for nitro-PAH compounds with buttressed nitro group(s).[28]

Steric inhibition to delocalization is a driving force for NO_2 diprotonation; the initially twisted nitro group can undergo geometrical change on diprotonation leading to overlap between developing p orbital at nitrogen and arene π system.

The iPr- and cyclohexyl-substituted dications subsequently undergo a facile cyclization (Figure 48). When *ortho* and *peri* iPr groups are both present (**115** and **113**) 5-membered ring oxazoline formation (*ortho* cyclization) is more favored than 6-membered ring 1,2-oxazine (*peri* cyclization). Efficient *peri* cyclization was observed for **118** and **120** dications to give **119**$^{+}$ and **121**$^{+}$, respectively. When the *ortho* iPr

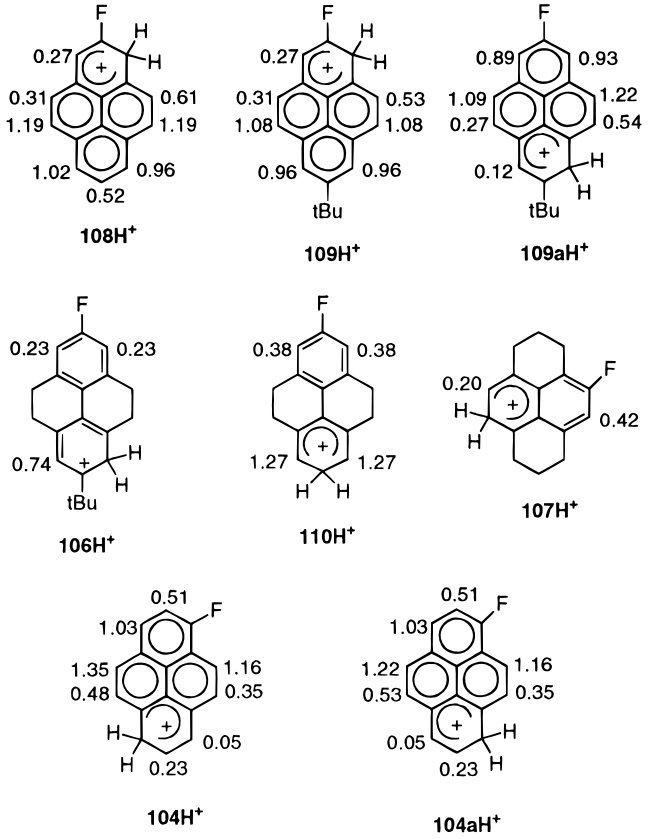

Figure 45. $\Delta\delta^{1}$H profiles for fluoropyrenium cations and their tetrahydro and hexahydro derivatives.

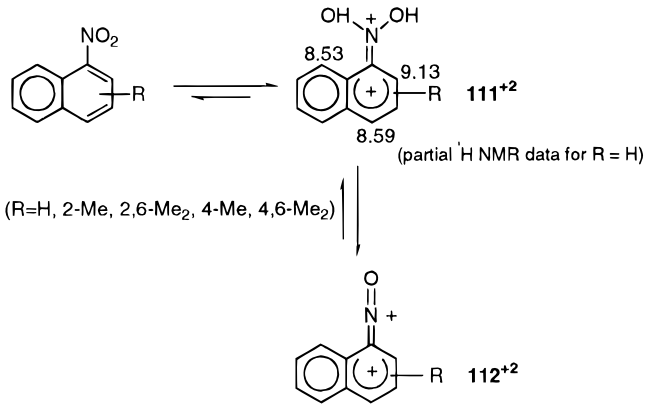

Figure 46. Protonation of nitronaphthalene in triflic acid.

group is replaced by a tBu (as in **122** and **123**) no rearrangement could be induced under the same conditions.

The resulting iminium−pyrenium dications and their cyclized derivatives show extensive delocalization away from the iminium group at alternating carbons of PAH periphery (Figure 49) and reveal significant phenalenium ion character similar to the alkylpyrenium and fluoroalkylpyrenium cations; furthermore, the remote α positions sustain more positive charge in the nitroalkylpyrenium cations which is further modulated by inductively stabilizing iPr or cyclohexyl substituents.

Upon quenching of the cyclized cations like **22**$^{+}$ (Figure 50), the corresponding nitrosoalkylpyrenium **125**$^{+}$ and their derived RC salts (EPR work) are obtained. The RCs are so stable they survive aqueous work-up conditions and are indefinitely persis-

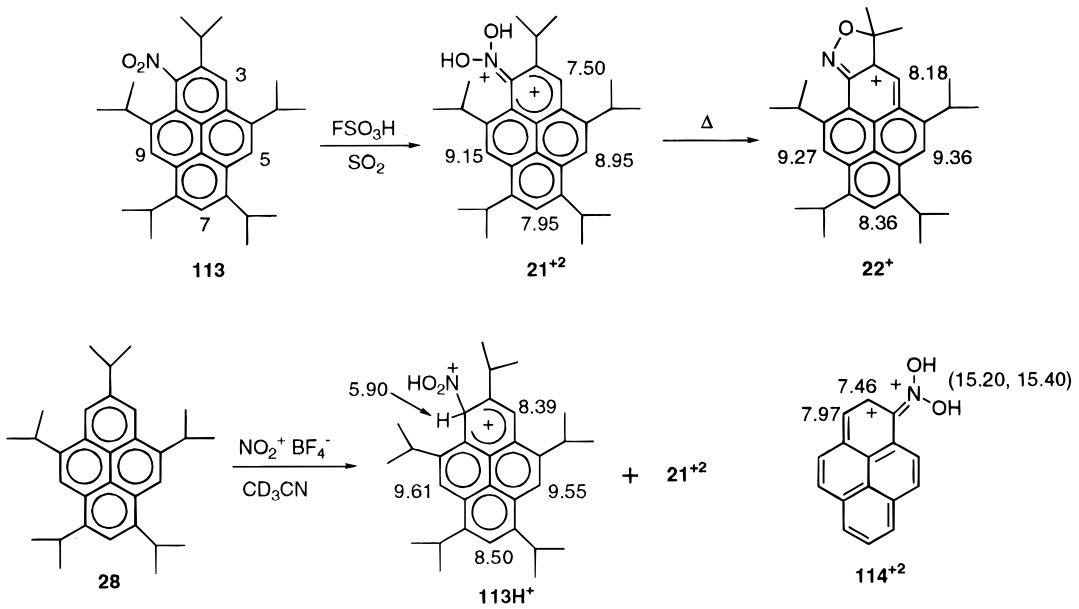

Figure 47. Protonation of **113** and **114** and reaction of **28** with $NO_2^+BF_4^-$.

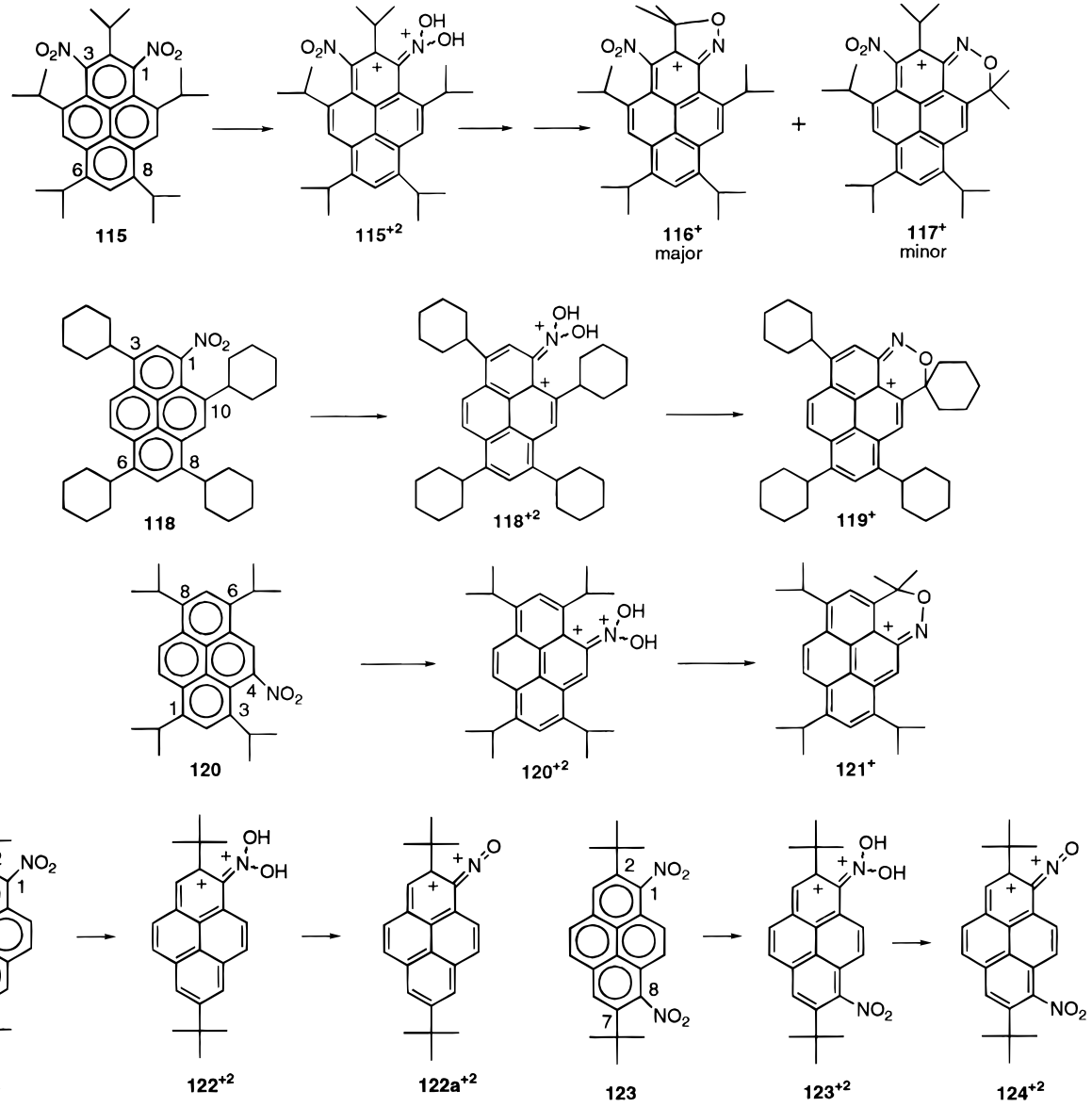

Figure 48. Diprotonation (and cyclization) of nitroalkylpyrenium cations.

tent. When they are redissolved in superacid, oxidation and cyclization return the cyclized pyrenium cations. The ring-opening reactions of cyclized cations on quenching, followed by in situ reduction and

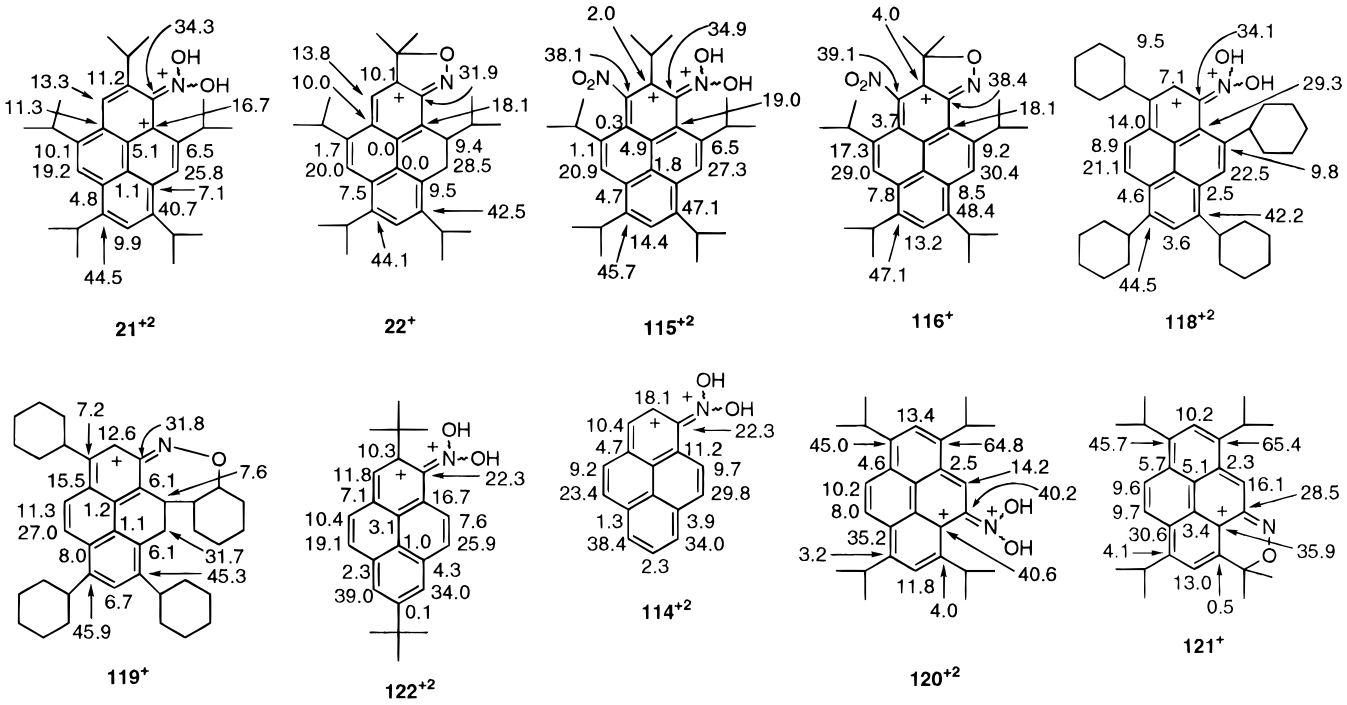

Figure 49. Charge delocalization pattern in iminium-pyrenium dications based on $\Delta\delta^{13}$C NMR data.

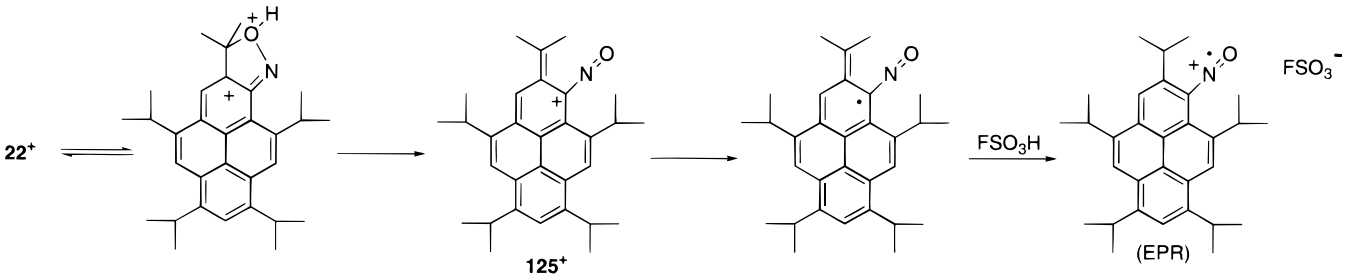

Figure 50. Quenching of **22**$^+$.

protonation events account for the observed nitrosoalkylpyrenium and the RC salt of nitrosopyrene.

Arenium Ions of Benzo[a]pyrene, Benzo[e]pyrene, and Dibenzo[a,e]pyrene

Benzo[*a*]pyrene and dibenzo[*a*,*e*]pyrene are monoprotonated with FSO_3H/SO_2ClF at C-6 and C-8, respectively, to give their persistent arenium ions **4H**$^+$ and **6H**$^+$.[27] Benzo[*e*]pyrene under a variety of conditions produced a mixture of **5H**$^+$ and **5aH**$^+$ (attack at C-3 and C-1; ~70:30 ratio). The cation ratio did not change by raising temperature or prolonged cold storage of the samples. Low-temperature NMR studies reveal significant phenalenium ion character for the three classes of PAHs (Figure 51).[27] Concomitant RC formation was also observed which is responsible for chemical shift variation in the arenium ions depending on ion concentration; protons close to protonation site shift the most.[27]

Chrysenium and 6-Halochrysenium Cations

Parent chrysene **37** and its 6-halo derivatives (F, Cl, and Br) are monoprotonated in $FSO_3H{\cdot}SbF_5$(9:1)/SO_2ClF to give persistent monoarenium ions (Figure 52).[41] Outcome of AM1 studies on the relative energies and charges for **37**H$^+$ and its 6-fluoro derivative **38H**$^+$ were discussed earlier (Figures 12 and 13).

Methanochrysenium and Methanophenanthrenium Cations

Ongoing stable ion studies[41] show that **39** and **40** are monoprotonated in FSO_3H/SO_2ClF at C-3 (*peri* to methylene bridge) or at C-1 (Figure 52). In the more concentrated ion solutions prepared for 2D NMR work, diprotonation of **40** appears to be a competing process.

Arenium Ions of [6]Helicenes

Whereas electrophlic aromatic substitution data on [6]helicenes became available mainly through the work of Laarhoven et al.,[61] no stable ion chemistry was known until recently.[38] 4-Methyl[6]helicene (**34**) is protonated at C-3 (Figure 53) in FSO_3H/SO_2 to give a persistent [6]helicenium cation (**34H**$^+$), whose sp^3-(CH_2) protons are diastereotopic appearing as two doublets with 30 Hz coupling, there is also minor oxidation (EPR) but it does not cause line broadening in the NMR spectra.

Parent [6]Helicene (**35**) is more prone to oxidation than **34**, even in a mild superacid system like CF_3SO_3H/SO_2ClF. Thus under these conditions, the

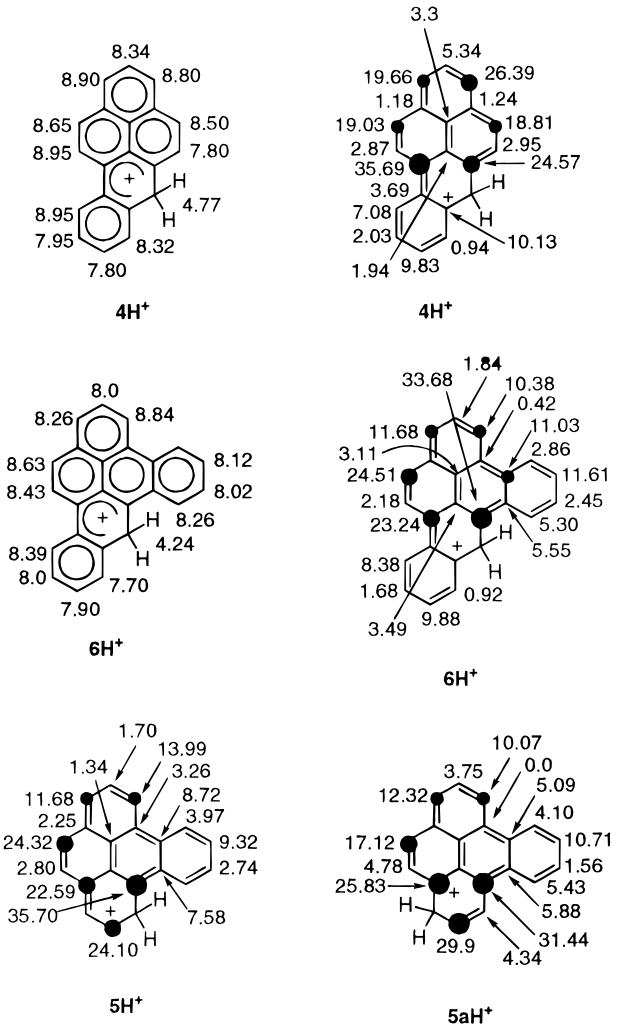

Figure 51. ^{1}H NMR data and the $\Delta\delta^{13}$C trends for **4H**$^+$, **5H**$^+$, and **6H**$^+$ cations (size of the dark circles is roughly proportional to magnitude of carbon delocalization).

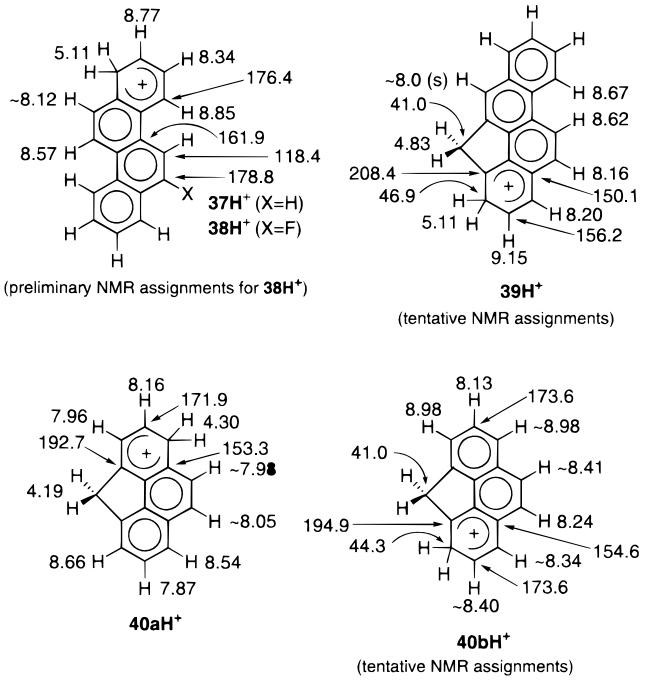

Figure 52. Protonation of chrysene, 6-halochrysenes, methanochrysene, and methanophenanthrene.

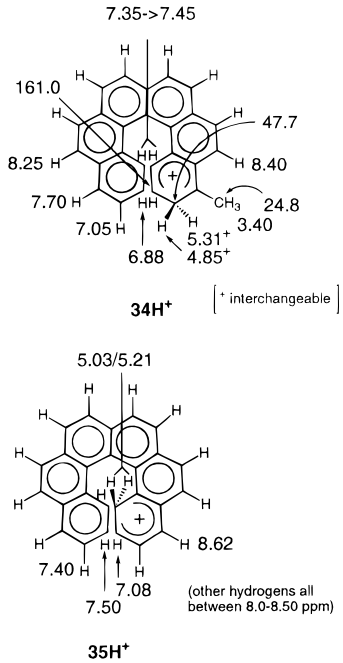

Figure 53. Protonation of [6]helicenes.

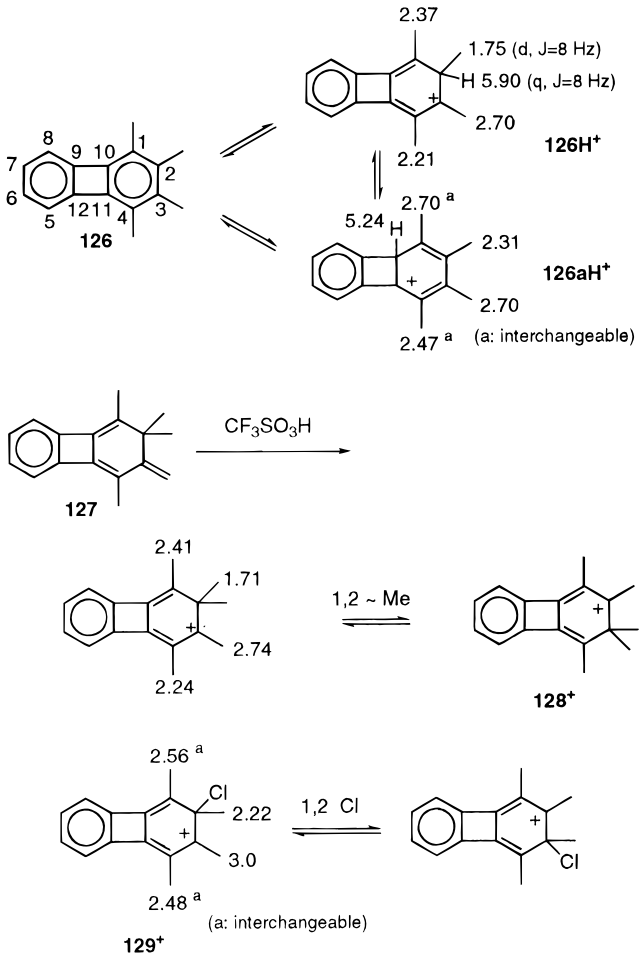

Figure 54. Degenerate rearrangements in methylbiphenylenium cations.

monoarenium ion of protonation at C-1 (**35H**$^+$) was observed by NMR but the resonances disappeared into the baseline within minutes.

With coronene (**36**) a persistent arenium ion could not be detected due to a more rapid oxidation; **36**$^{+\cdot}$ was studied (see the review of the radical cations).

Biphenylene Cation

Shubin et al.[62] showed that when 1,2,3,4-tetramethylbiphenylene (**126**) is dissolved in CF_3SO_3H/SO_2ClF at −80 °C a violet solution results whose ^1H NMR spectrum is consistent with formation of a mixture of two ions **126H**$^+$ and **126aH**$^+$. When the temperature is raised the former converts to the latter giving an equilibrium mixture of 2:3. This degenerate 1,2-H shift is intramolecular (Figure 54).

Protonation of 1,2,2,4-tetramethyl-3-methylene-2,3-dihydrobiphenylene (**127**) gives the biphenylium cation **128**$^+$, undergoing a degenerate 1,2-Me shift.[63] With $FSO_3H/SO_2ClF-Cl_2$ system the arenium ion of *ipso* chlorination (**129**$^+$) was formed,[64] again showing degenerate rearrangement.

Octamethylbiphenylene and Dodecamethylbinaphthylene

Syntheses of the fully methylated biphenylene **31** and binaphthylene **130** are conveniently accomplished via an aryne coupling reaction of their dibromides according to Hart.[65]

Facile oxidation of **31** has precluded direct observation of **31H**$^+$. When Hart et al[66] dissolved **31** in TFAH, **31**$^{\bullet+}$ was observed instead (see also the radical cation section). The sequence of events outlined in Figure 55 were suggested. Similar results were obtained later in mild superacids.[31]

Recent studies show that **130** can be monoprotonated in FSO_3H/SO_2ClF.[67] Out of three possible arenium ions, formation of **130H**$^+$ was suggested on the basis of the chemistry of benzobiphenylene derivatives.

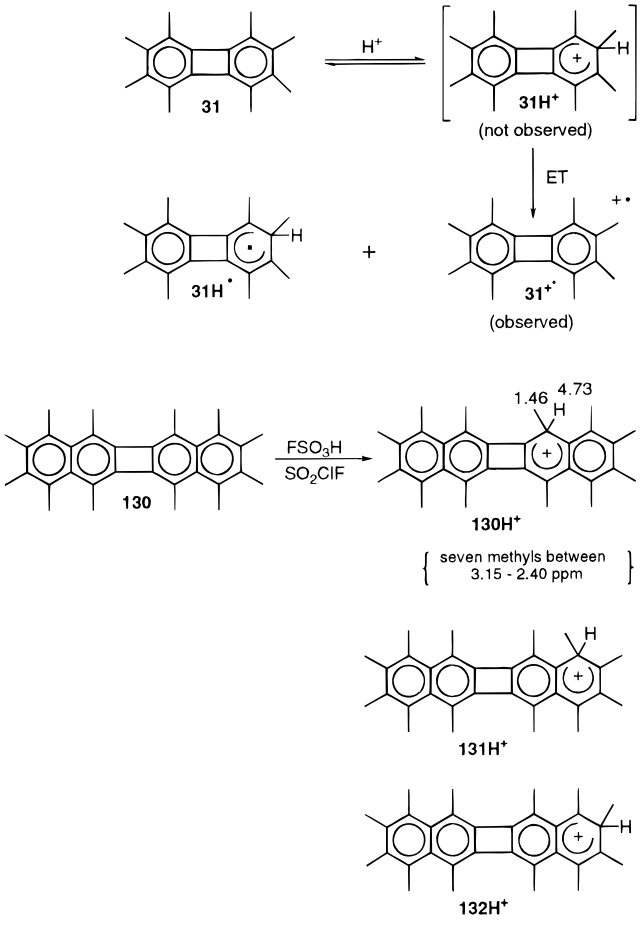

Figure 55. Protonation of **31** and **130**.

Azulenium and Homoazulenium Cations

For alkylazulenes **133**, there is a clear driving force to protonate at C-1 or C-3 in the 5-membered ring so that a very stable azulenium ion **133H**$^+$, which can be viewed as a vinyl-substituted tropylium cation, can be formed (Figure 56). Indeed the basicity of azulene is much higher than other 10π electron aromatics naphthalene and 1,6-methano[10]annulene.[68]

de Wit and Cerfontain[68] protonated a series of alkyl- and formyl-substituted azulenes with FSO_3H without a cosolvent. Protonation was observed at C-1 or C-3 depending on the substituents to give the corresponding azulenium ions. The formyl-substi-

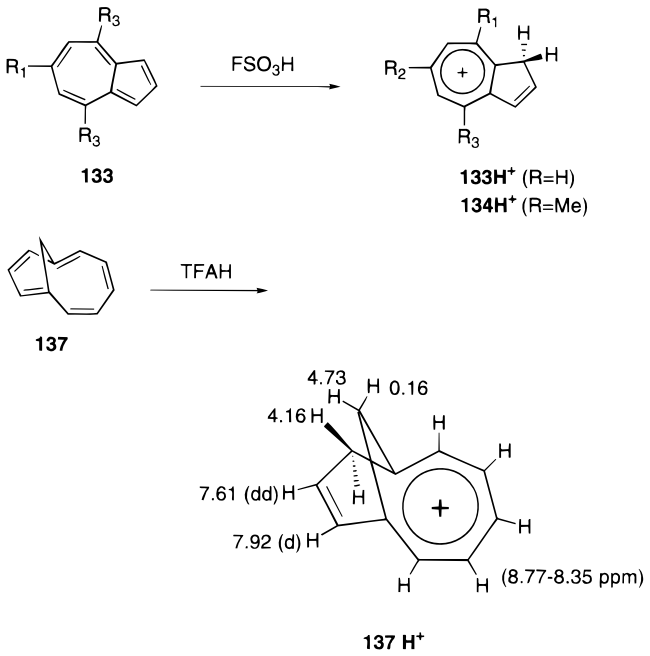

Figure 56. Protonation of azulenes and homoazulene.

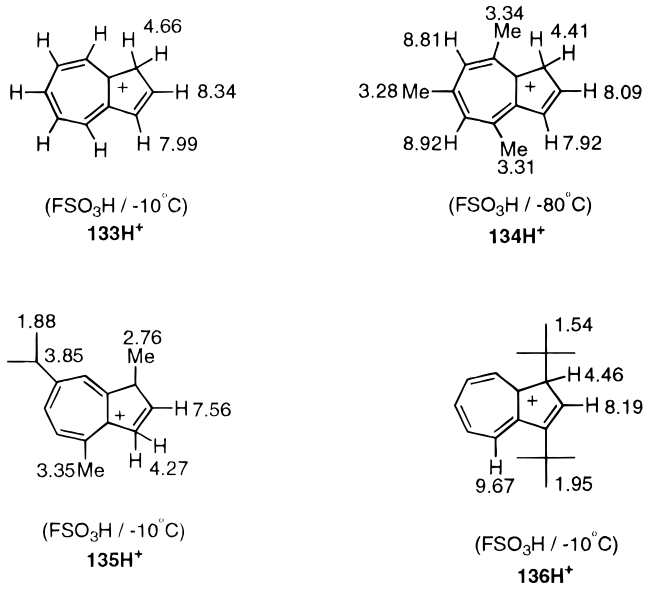

Figure 57. Partial ^1H NMR data for some azulenium ions.

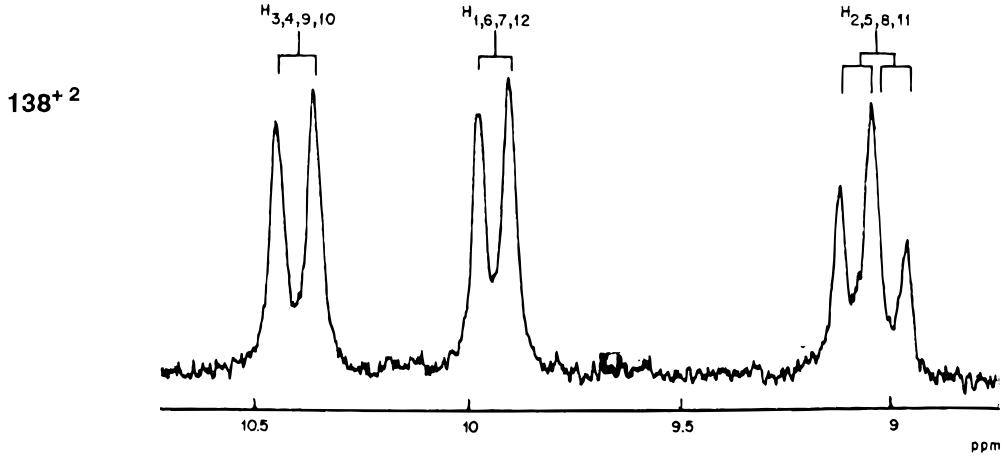

Figure 58. The first reported ^{1}H NMR spectrum of perylene dication. (Reprinted from ref 71. Copyright 1972 Royal Netherlands Chemical Society.)

tuted analogues are CO protonated. Only ^{1}H NMR data have been reported (partial data are gathered in Figure 57 on the basis of ref 68).

Homoazulene **137** has been synthesized by Masamune[69a] and by Scott.[69b] Despite significant distortion from planarity, the 10π system supports a large induced diamagnetic ring current.[69c] It is highly reactive toward electrophiles and fully protonates in TFAH to give a homoazulenium ion **137H**$^+$, for which the endo-bridge hydrogen is at 0.16 ppm, whereas the anti-bridge hydrogen is at 4.73 ppm (the coupling is 6.6 Hz).[70]

Persistent Oxidation Dications of Polycyclic Arenes and Bridged Annulenes

The SbF_5/SO_2ClF system is the most widely used medium for PAH^{2+} generation for direct low-temperature NMR (EPR) studies. In some cases, the oxidizing power of the more easily handled "magic acid"/SO_2ClF (or SO_2) is adequate for dication generation.[31,71]

$FSO_3H{\cdot}SbF_5$(1:9)/SO_2ClF and $FSO_3H{\cdot}SbF_5$(4:1)/SO_2ClF superacid systems have also been used for dication generation.[30,47]

The first examples of persistent PAH^{2+} were provided by Brouwer and van Doorn,[71] who oxidized perylene (**138**), tetracene (**139**), pentacene (**140**), and several substituted anthracenes to their dications. The 100 MHz ^{1}H NMR spectrum of **138**$^{2+}$ reported by Brouwer over two decades ago is shown (Figure 58). Whereas the total ^{1}H deshielding in **138**$^{2+}$ (18π Hückel dication) amounts to 28 ppm, values of 3.2 and 2.3 ppm were found for the 4n dications **139**$^{2+}$ and **141**$^{2+}$.

An extensive survey of PAH dications and their ^{13}C NMR characteristics was conducted by Forsyth and Olah.[29] The NMR data for the fully assigned cases are gathered (Figure 59).

With picene and 1,2,3,4-dibenzanthracene nonuniform line broadening was observed in the ^{13}C NMR spectra indicative of electron exchange between the dication and the RC.

Although naphthalene itself does not produce a dication its octamethyl derivative **24**$^{2+}$ does.[29] The persistent dication of 1,4,5,8-tetramethylnaphthalene **72**$^{2+}$ has also been generated (Figure 60).[72]

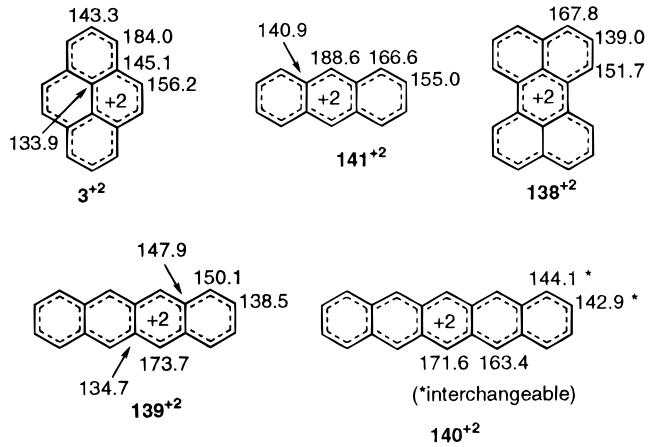

Figure 59. ^{13}C NMR data for PAH dications.

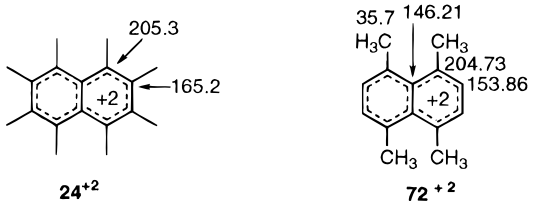

Figure 60. ^{13}C NMR data for octamethylnaphthalene dication and 1,4,5,8-tetramethylnaphthalene dication.

The isomeric 1,2,3,4-tetramethylnaphthalene gave a dication/RC equilibrium; similar results were found with hexahydropyrene.[72]

A series of persistent dications of *meso*-substituted anthracenes has been reported by Olah and Singh.[32] The observed total carbon deshielding in these systems are between 208.4 and 212.9 ppm/e. The ^{13}C NMR chemical shifts of four representative examples (**142**$^{2+}$−**145**$^{2+}$) are sketched (Figure 61).

Persistent oxidation dications of a series of crowded alkyl(cycloalkyl)pyrenes have been generated and studied by NMR.[30] The deshielding order $C_\alpha > C_{\alpha\beta} > C_\beta$ was established on the basis of ^{13}C NMR, regardless of the number and position of the alkyl substituents. The overall picture based on AM1 calculated charge densities (Table 1) and the NMR data is the same.

For alkylpyrenium dications $\Delta\delta^{13}$C for the *ipso* carbon resonances relative to parent pyrene dication

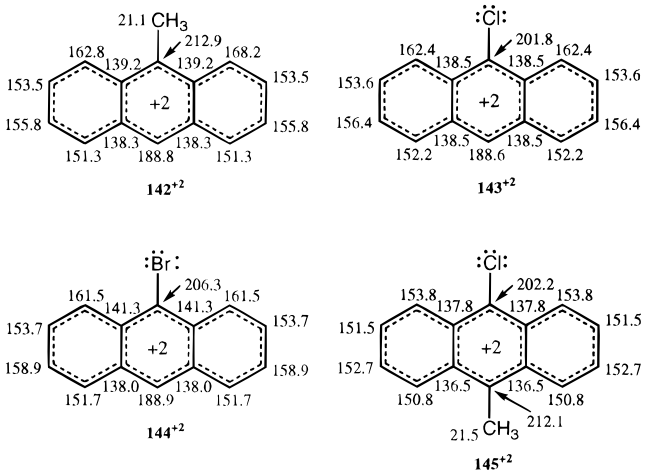

Figure 61. ^{13}C NMR data for anthracene dications.

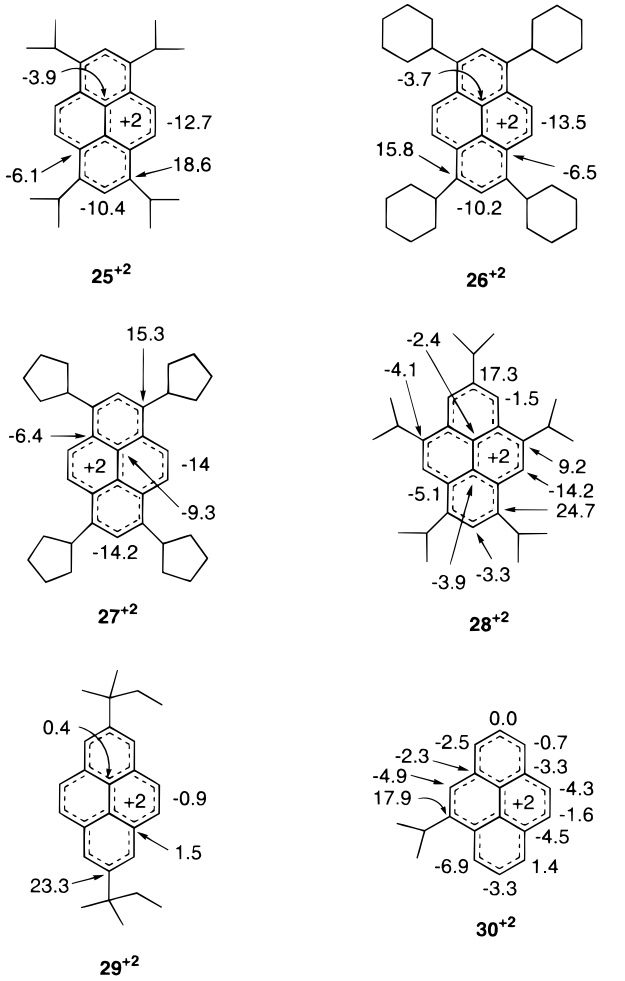

Figure 62. $\Delta\delta^{13}C$ profiles (relative to parent pyrene dication) for alkyl(cycloalkyl)pyrene oxidation dications.

were slightly larger than expected for a normal substituent effect in the precursors. The $\Delta\delta^{13}C$ (in this case relative to parent pyrene dication) were small for the unsubstituted carbons except for ring carbons in crowded positions which were noticeably more upfield (Figure 62).

Parent biphenylene dication $\mathbf{146}^{2+}$, its tetramethyl-($\mathbf{72}^{2+}$) and dimethyl-substituted analogues were generated by Olah and Liang.[73] The octamethylbiphenylene dication $\mathbf{31}^{2+}$ was independently generated in two laboratories (Figure 63).[31,74] They represent fully delocalized closed-shell 10π electron aromatic systems.

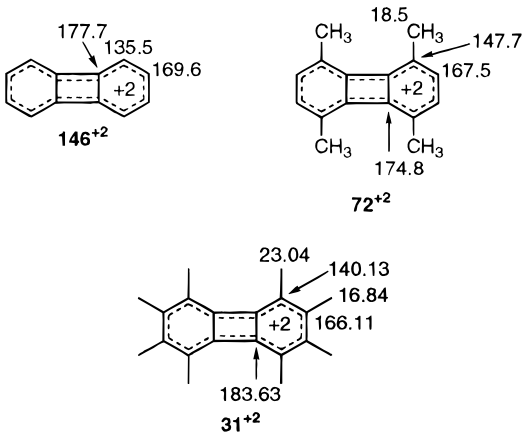

Figure 63. Biphenylene dications.

The $\mathbf{31}^{2+}$ can be generated either by two-electron oxidation with SbF_5/SO_2ClF (or magic acid/SO_2), or by stepwise oxidation to the RC (with FSO_3H) and further oxidation (with SbF_5 or NO_2^+ BF_4^-).[31]

Hexamethoxytriphenylene forms a complex with $TCNQF_4$.[75] Doping with AsF_5 gave a dication which was suggested to be a ground-state triplet on the basis of EPR measurements.[75]

When **36** is reacted with SbF_5/SO_2ClF its oxidation dication is formed. EPR studies showed that the planar dication is a thermally accessible triplet.[40]

Müllen and associates[76] carried out an extensive study of dianions and dications of bridged [4*n*+2]-annulenes where the ring size, conformation, and configuration of the perimeter were varied. These factors were shown to influence the degree of paratropism of the resulting $4n\pi$ ions. As part of this investigation, oxidation dications $\mathbf{81}^{2+}$, $\mathbf{147}^{2+}$, and $\mathbf{79}^{2+}$ were generated by two-electron oxidation with SbF_5/SO_2ClF. The same dications were prepared by Michl and Vogel indirectly via the the C-7 protonated bridged [14]annulenes in $FSO_3H{\cdot}SbF_5$(4:1)/SO_2ClF by heating or upon storage (Figure 64).[47]

The Radical Cations

The most comprehensive early study of PAH radical cations was by Lewis and Singer[77] who oxidized a series of PAHs to persistent RCs, using $SbCl_5/CH_2Cl_2$ as oxidant, and obtained well-resolved EPR spectra in a number of cases. This work extended earlier work of de Boer and Bolton on arene radical cations in H_2SO_4.[78,79]

In most cases, the magnitude of a_H in the radical cations corresponds to the calculated HMO spin densities.[77] Hence the spin densities are mainly located at the *meso* positions in $\mathbf{148}^{\bullet+}$ and $\mathbf{2}^{\bullet+}$, at the internal *meso* positions in $\mathbf{139}^{\bullet+}$ and $\mathbf{140}^{\bullet+}$, at the α positions of $\mathbf{3}^{\bullet+}$ and $\mathbf{138}^{\bullet+}$, and the β positions of $\mathbf{146}^{\bullet+}$ and $\mathbf{32}^{\bullet+}$ (Figure 65 provides a compilation).

Buchanan et al.[80] introduced molten $SbCl_3$ as a medium for PAH RC generation. The EPR spectra of $\mathbf{2}^{\bullet+}$ and $\mathbf{138}^{\bullet+}$ obtained under these conditions are shown (Figure 66).

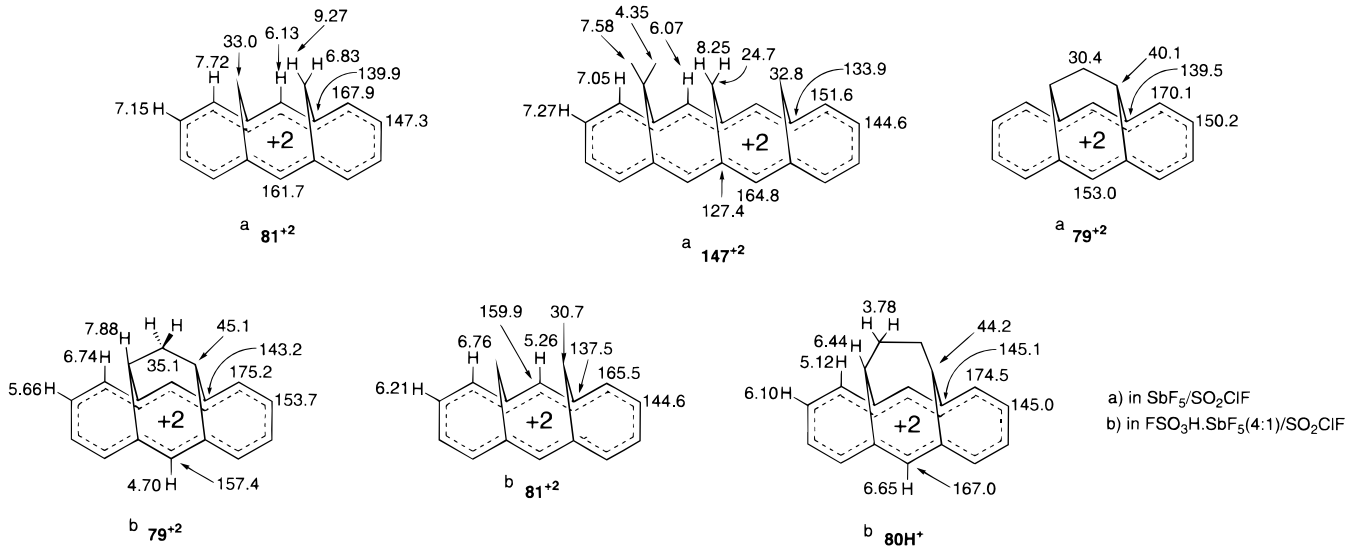

Figure 64. Persistent oxidation dications of [4*n*+2]annulenes.

Davies' group has investigated the RCs of various classes of PAHs over the years.[81−87] They showed that the biphenylene RC **146**$^{\bullet+}$ can be generated in H_2SO_4 or TFAH/Tl(TFA)$_3$.[83] In TFAH or in $AlCl_3$/CH_2Cl_2, a mixture of monomeric (**146**$^{\bullet+}$**)** and dimeric (**146**)$_2^{\bullet+}$ RCs is formed; the dimer dissociated into the monomer RC above 220 K. Under the conditions used by Lau and Kochi[88] for generation of radical cations of polymethylbenzenes namely Hg(TFA)$_2$/TFAH/UV light, Davies et al.[83,86] found that prior to irradiation, the EPR spectrum is that of biphenylene RC **146**$^{\bullet+}$, but after irradiation progressive mercuration of biphenylene RC was observed in the β position. Thus β-proton hyperfine coupling was lost and mercury satellites appeared. Mercuration was complete when tetra-β-mercurated RC was formed.

Photolysis of a solution of triphenylene in TFAH in the presence of either Hg(TFA)$_2$ or Tl(TFA)$_3$ gave an EPR spectrum consistent with the dimer radical cation.[85] The hyperfine coupling in the dimer is about half that in the monomer RC. Earlier, Lewis and Singer[77] had reported an incomplete EPR spectrum for biphenylene RC in $SbCl_3/CH_2Cl_2$.

Anodic oxidation of PAHs in the presence of suitable gegenions appears to be a general method for the synthesis of [PAH]$_2^{\bullet+}$ X^- salts which have potential as organic metals.[89] Examples include naphthalene, triphenylene, perylene, pyrene, and fluoranthene. The X-ray analysis of [fluoranthene]$2^{\bullet+}PF_6^-$ (shiny black crystals) shows that the aromatic rings are stacked within van der Waals distances (320−325 pm) and the anions are located in the channels between the stacks. The radical cations are delocalized and crystallographically identical.

Contrary to the behavior of dialkylalkynes which upon irradiation from butadiene radical cations or hexaalkylbutadiene radical cations (R = tBu), irradiation of diphenylethyne/TFAH (with pyrex-filtered UV light) containing Hg(TFA)$_2$ gave 1,2,3-triphenylazulene RC **162**$^{\bullet+}$. Upon quenching, bright blue 1,2,3-triphenylazulene was obtained in 38% yield.[84] A similar reaction of bis(4-*tert*-butylphenyl)-ethyne gave **163**$^{\bullet+}$ (Figure 67). Although there are only few examples reported so far, this one-electron oxidation followed by dimerization/rearrangement protocol to form the azulene skeleton is novel and offers a method for one-pot photochemical synthesis of substituted azulenes from alkynes.

Persistent radical cations of a series of di-, tri-, and tetraalkyl-substituted azulenes were recently generated and studied by EPR and ENDOR techniques.[90] Addition of Hg(TFA)$_2$ to a methylene chloride solution of the azulene gives the Hg^+-substituted vinyltropylium ion (blue to yellow) which homolytically cleaves upon UV irradiation to give the azulene RCs **164**$^{\bullet+}$ (Figure 68). The hyperfine couplings to H-1/H-3 are the largest for azulene$^{\bullet+}$ [a_H (1,3) > (5,7) > (2) > (6) > (4,8)].

The lifetime of the RCs depends on the position, number, and nature of the alkyl groups. Substitution at both C-1 and C-3 is most effective; presence of bulky tBu groups at C-1/C-3 enhances the stability dramatically. For the less substituted alkylazulene RCs, rapid dimerization gave 1,1′-biazulenyl RC **165**$^{\bullet+}$.[90]

The FSO_3H/SO_2 system is a convenient medium for RC generation at low temperature.[30,81] The arenium ion and the radical cation can coexist in many cases without noticeable line broadening in the NMR spectra. This was first shown by Davies and Shields[81] for **148H**$^+$/**148**$^{\bullet+}$ system (Figure 69).

Subsequently,[30] persistent RC of tetraisopropylpyrene **25**$^{\bullet+}$ was observed by EPR in a sample for which NMR shows the clean formation of the *ipso*-protonated pyrenium ion **25H**$^+$; without EPR work, concomitant formation of RCs in superacid solutions of arenium ions could not have been suspected from NMR spectra alone (Figure 70).

Minor presence of arene RCs in superacid solutions of arenium ions is rather general;[30,28,27,60] however, EPR resonances detected in the arenium ion samples are in many instances broad and featureless and their hyperfine couplings could not be determined.

More concentrated ion solutions prepared for 2D NMR work usually contain higher concentrations of RC possibly because of increased local overheating. For dibenzo[*a*,*e*]pyrene, RC formation could be inferred from the NMR spectra because of line broad-

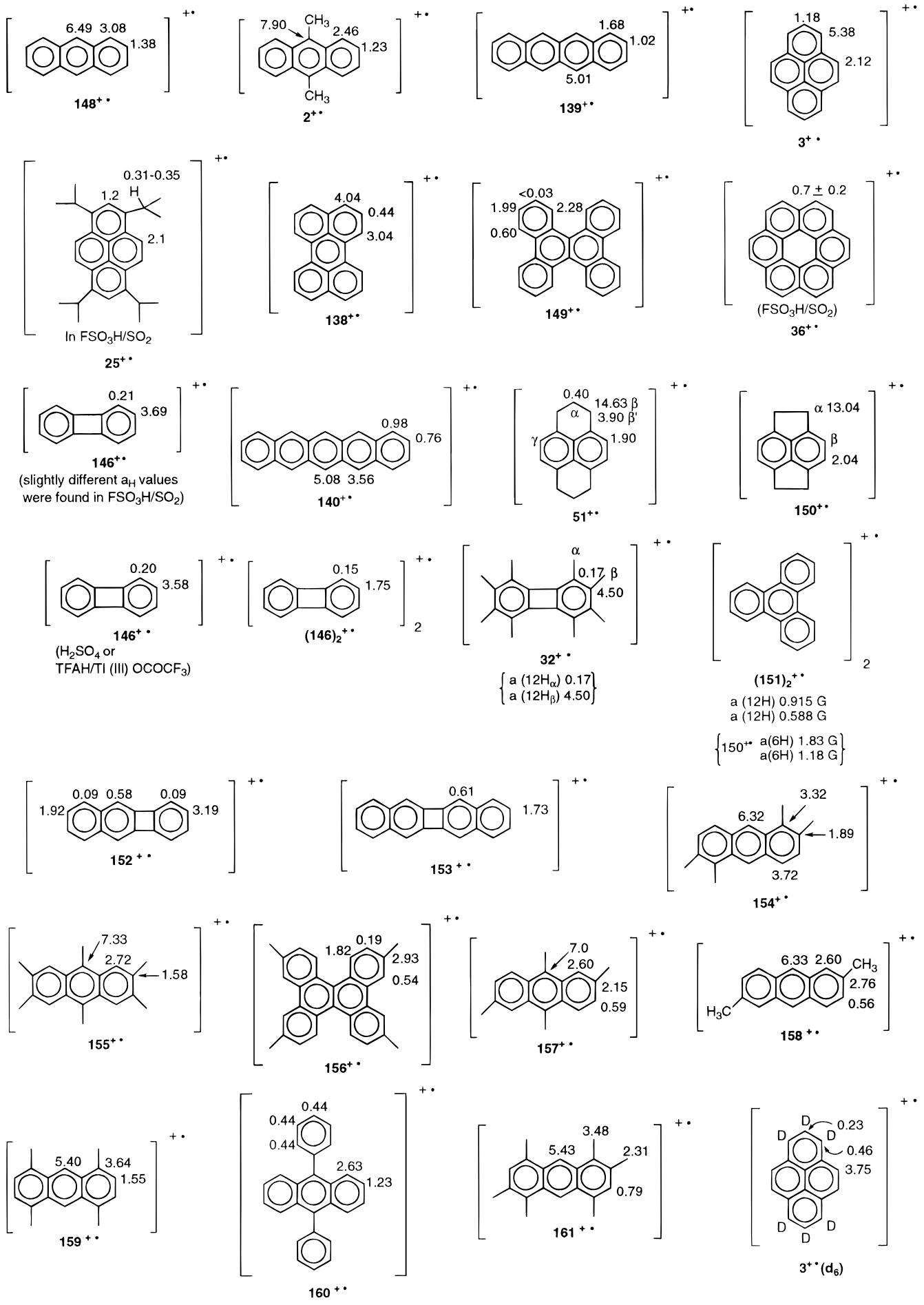

Figure 65. Compilation of PAH radical cations with a_H values given on structures.

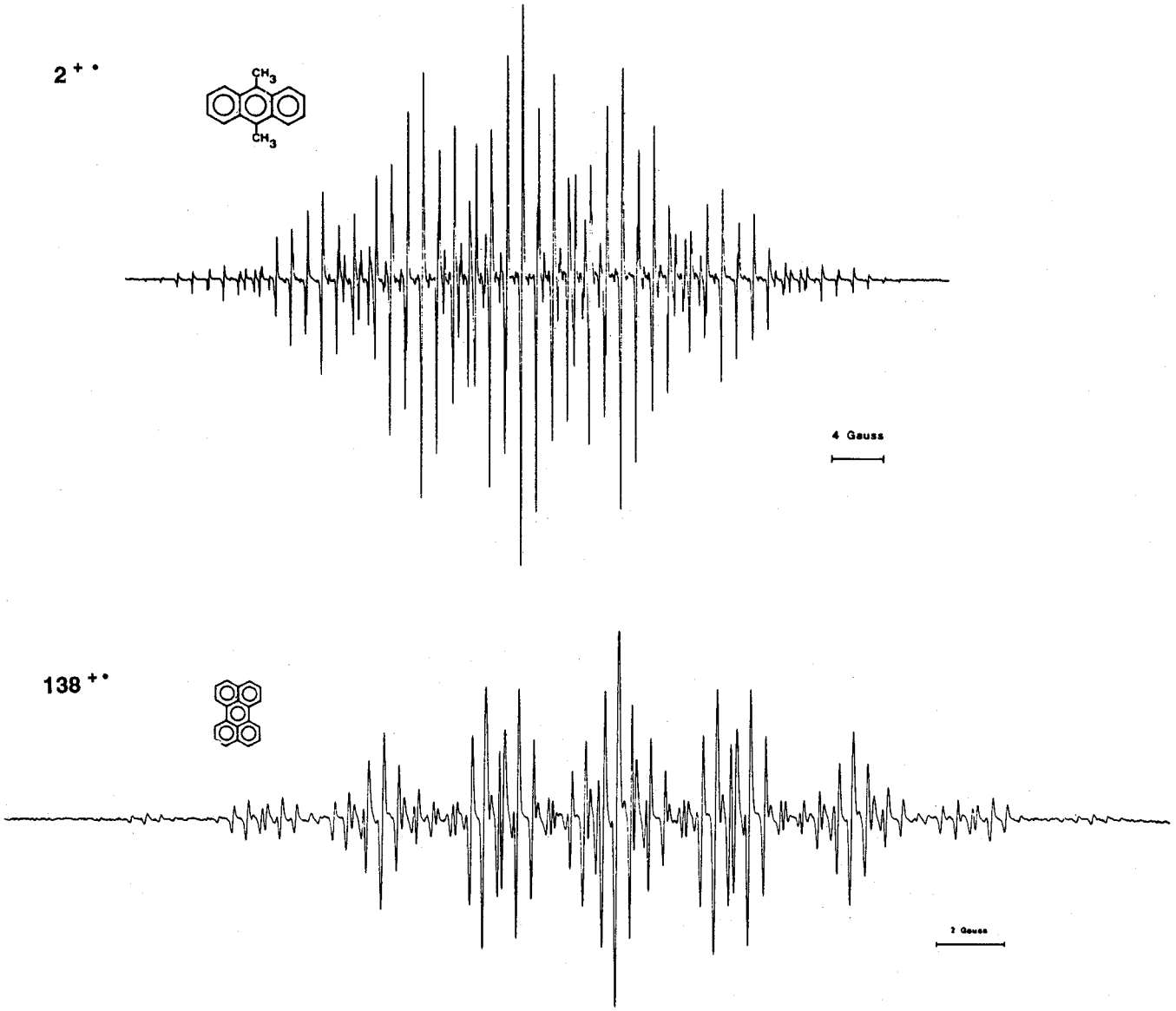

Figure 66. EPR spectra of $\mathbf{2}^{\bullet+}$ (in molten $SbCl_3$) and $\mathbf{138}^{\bullet+}$ (in $SbCl_3$-8 mol % $AlCl_3$). (Reprinted from ref 80. Copyright 1980 American Chemical Society.)

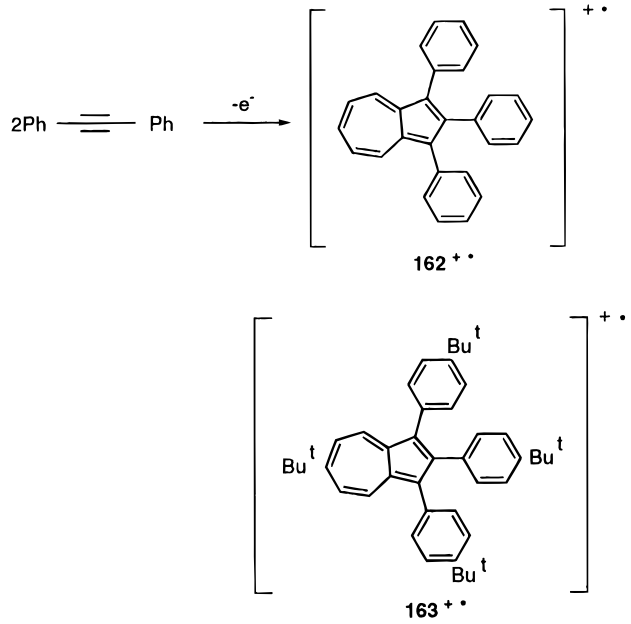

Figure 67. Azulene radical cations from arylalkynes in TFAH.

ening (the EPR signal of the RC was subsequently detected).[27]

For benzo[*e*]pyrene the extent of line broadening appears to be distance dependent: those in the proximity of protonation site were broader. This observation assisted the NMR analysis of the arenium ions.[27]

Eberson and Radner[91] found that the RC formed when bis(pentamethylphenyl)methane is dissolved in TFAH is 1,2,3,4,5,6,7,8-octamethylanthracene $OMA^{\bullet+}$ rather than the π-stabilized RC of the precursor suggested by Kochi et al.[92] A recent EPR study of persistent radical cations of several methylnaphthalenes, 1,1′-binaphthylenes, and perylene has been reported by Eberson et al.[93] For methylnaphthalenes except in cases where a *peri* methyl group interfered with σ coupling at the 1 position, the EPR spectra of the RCs of corresponding 1,1′-binaphthylenes were observed; further oxidation to the perylene RCs was not detected.

1,2,4,5,6,8-Hexamethylanthracene HMA is protonated in TFAH to give its arenium ion. When the sample was exposed to diffuse daylight, $\mathbf{160}^{\bullet+}$ was

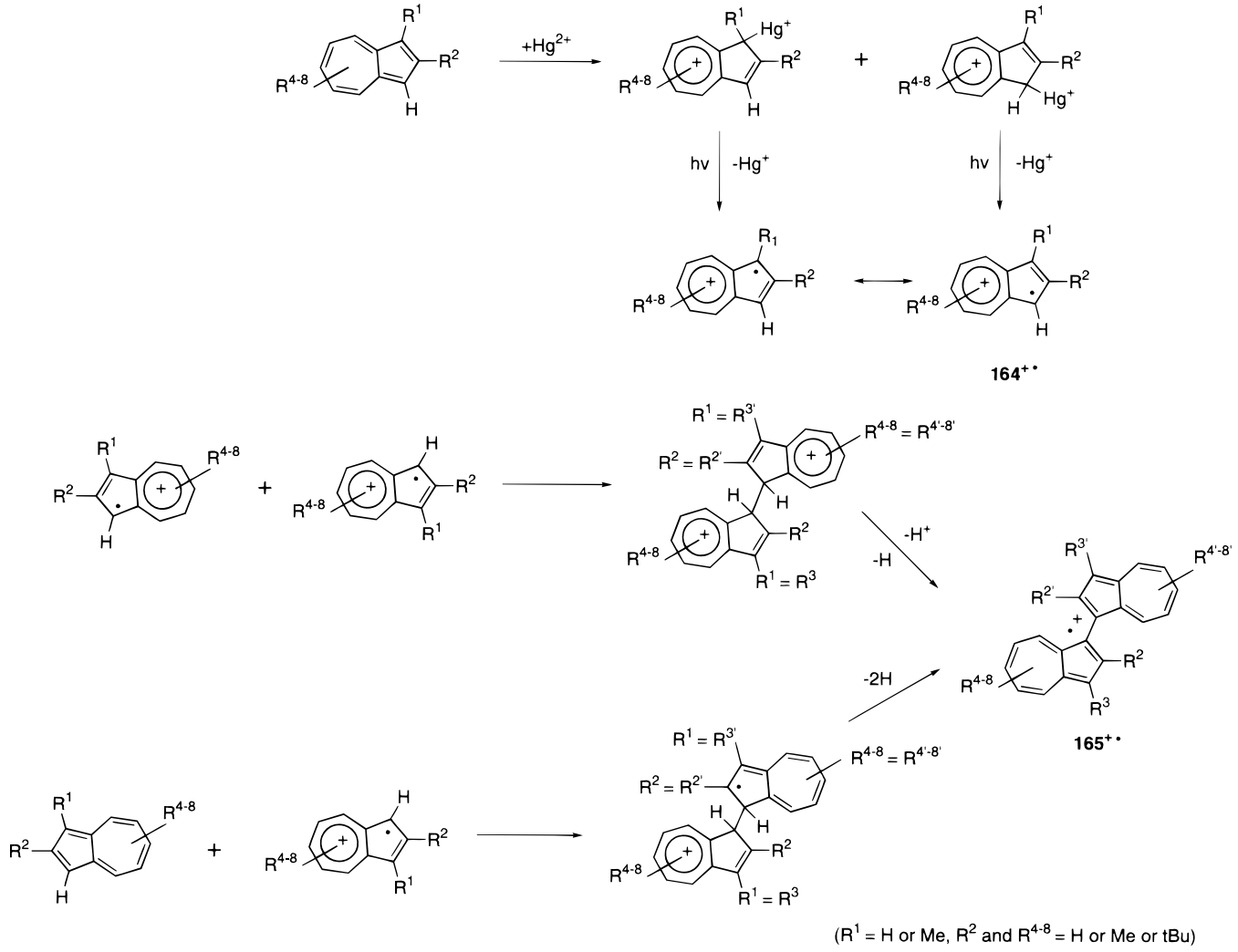

Figure 68. Alkylazulene radical cations and their dimerization.

formed. The EPR spectrum of this sample was identical with that formed via 2,2′,3,4′,5,5,6-heptamethyldiphenylmethane TFAH/light.[94]

The oxidation potential of octamethylbiphenylene **31** is 11.8 kcal/mol lower than biphenylene itself. It is easily oxidized in mild superacids CF_3SO_3H or FSO_3H and direct observation of the arenium ion has not proved possible.[31] Formation of **31**$^{\bullet+}$ in TFAH/$CDCl_3$ was first reported by Hart,[66] and an acid-catalyzed ET process was proposed.

The spin density in the RC is primarily located at the β positions (C-2,3,6,7). Thus the β-methyl resonance disappears in the ^{1}H NMR and the α-methyl signal remains.[66] Persistent **31**$^{\bullet+}$ can be generated also in TFAH-Tl(TFA)$_3$[82] and TFAH−diffuse daylight;[87] its EPR spectrum has been analyzed in detail.[82]

Recently, Friedel−Crafts alkylation and Scholl-type condensation reactions involving benzene-d_6/chloroalkanes with $AlCl_3$ as catalyst (and oxidant) have been used as a protocol for preparation of deuterated RCs of different classes of PAHs in one-pot reactions (Figures 71−73). For example, the RCs of pyrene-d_6 and 9,10-dimethylanthracene-d_8 were generated as outlined (Figure 71).[96]

The *o*-xylene/$CHCl_3$/$AlCl_3$, *o*-xylene/Cl_2CHCH_3/$AlCl_3$, and *o*-xylene/$Cl_2CHCHCl_2$/$AlCl_3$ systems have been used for generation of persistent RCs of tetramethylanthracene, hexamethylanthracene, and tetramethyldibenzo[*a*,*c*]triphenylene.[97] With the system $SbPh_3$/$CHCl_3$/$AlCl_3$ either the anthracene RC or the 9,10-diphenylanthracene RC could be observed depending on the concentration of $SbPh_3$.[98]

These reactions provide facile access to complex PAH radical cations (including the deuterated analogues) from readily available building blocks.

Attempted protonation of coronene **36** in mild superacids led instead to the observation of **36**$^{\bullet+}$.[38]

Gas-Phase Studies: Highlights of Recent Advances

The thermochemical properties of PAH ions and fullerene ions, namely their recombination energies, proton affinities, and hydrogen atom affinities have been discussed in a recent review by Bohme.[99]

Gas-phase ion-equilibrium measurements were used by Meot-Ner (Mautner) to determine proton affinities and ionization energies for a range of PAHs.[100] Comparison of gas-phase PA values with solution basicities in HF shows that the solvent increases the basicity of large PAHs more than it does benzene. A correlation was found between gas-phase PA values and rate constants for protiodetritation and nitration reactions and also with theory.

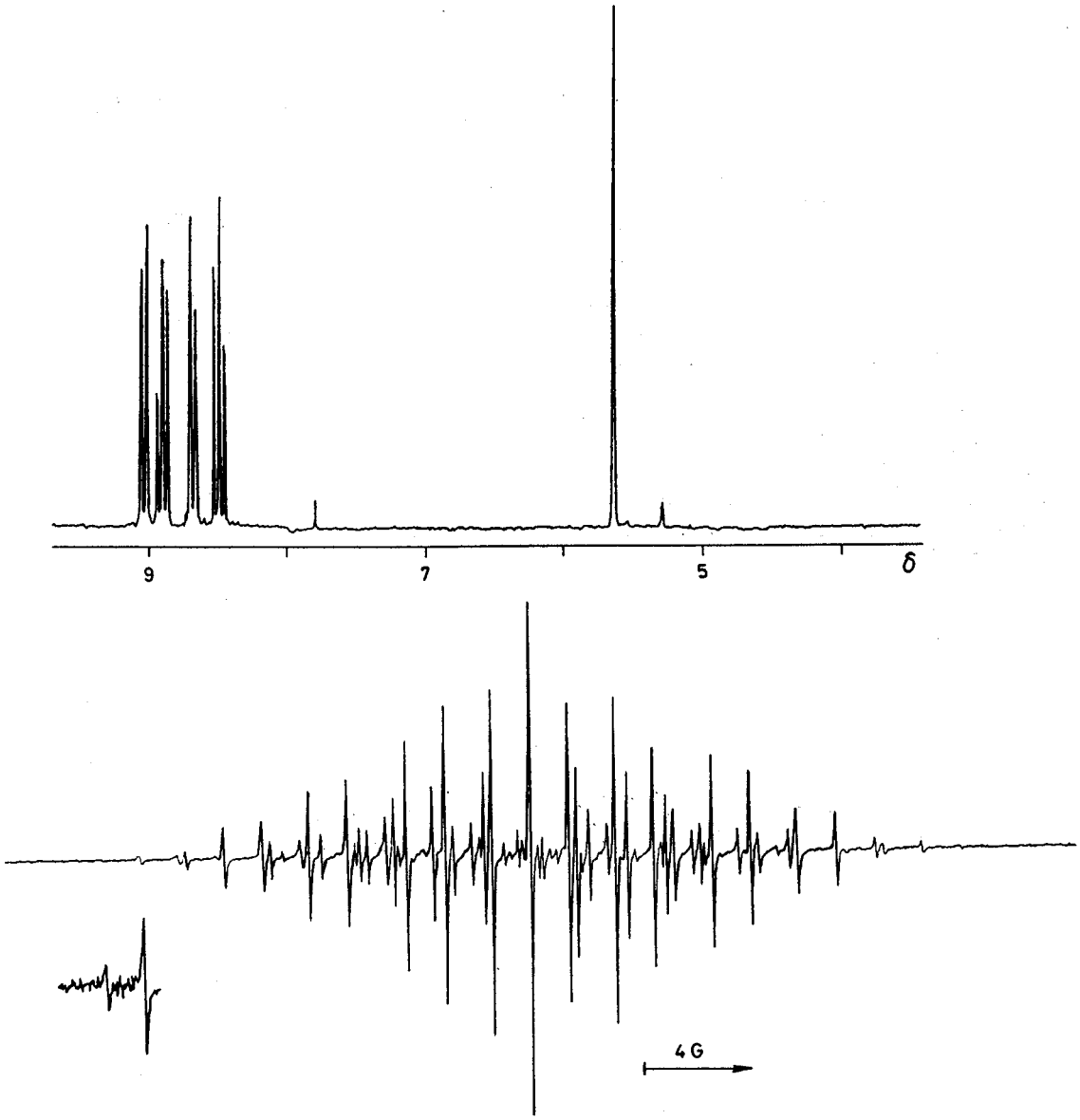

Figure 69. Coexistence of anthracenium cation and its RC in FSO_3H/SO_2. (Reprinted from ref 81. Copyright 1989 Royal Society of Chemistry.)

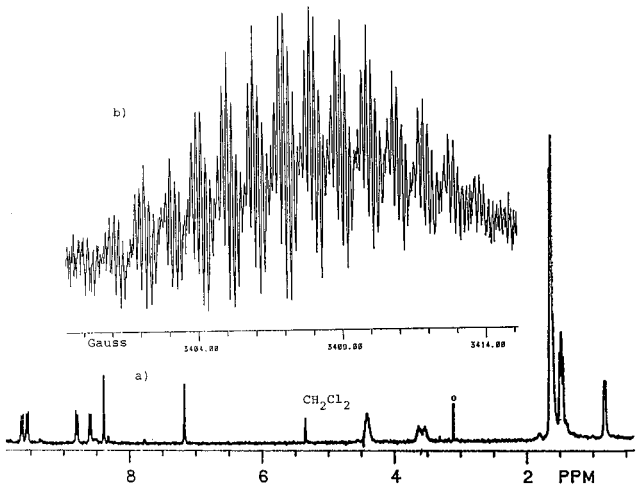

Figure 70. Coexistence of *ipso*-protonated **25H**$^+$ and **25**$^{\bullet+}$ in FSO_3H/SO_2. (o indicates protonated acetone.) (Reprinted from ref 30. Copyright 1993 American Chemical Society.)

As the molecular weight of the PAH increases, hydrogen atom affinity of its RC decreases.[100]

PAH oxidation dications have been generated by double photoionization in a mass spectrometer using filtered HeII radiation. The dications become increasingly stable in larger PAHs. The dications decompose by loss of small fragments, usually as neutral ethene but sometimes as ions.[101]

In the 70 eV EI mass spectra of PAHs the abundance of the multiply charged ions increase with increasing the number of rings. The di- and trications undergo unimolecular decomposition to give mainly $[CH_3]^+$, $[C_2H_2]^+$, and $[C_3H_3]^+$ ions.[102]

The oxidation dications (and trications) are also present in the FAB mass spectra of PAHs using NBA matrix.[103] Indeed the EI and FAB mass spectra are similar for pyrene, coronene: and C_{60}. Their FAB mass spectra are displayed (Figure 74).

When triply charged C_{60} cation and corannulene were allowed to react in a selected-ion flow tube (SIFT) experiment,[104] both single and double electron transfer from corannulene to C_{60} occurred with single ET being the minor process (Figure 75). Similar results were obtained for pyrene and anthracene.

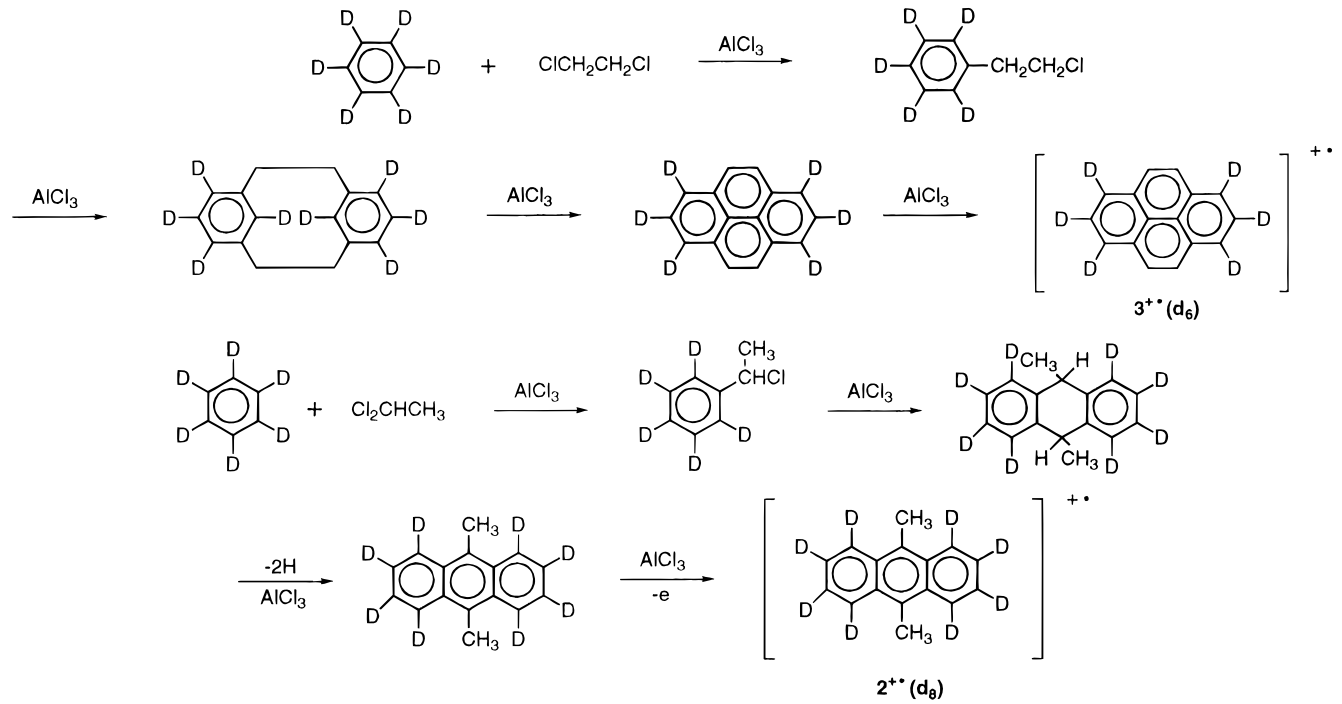

Figure 71. Peristent PAH RCs by Friedel−Crafts chemistry.

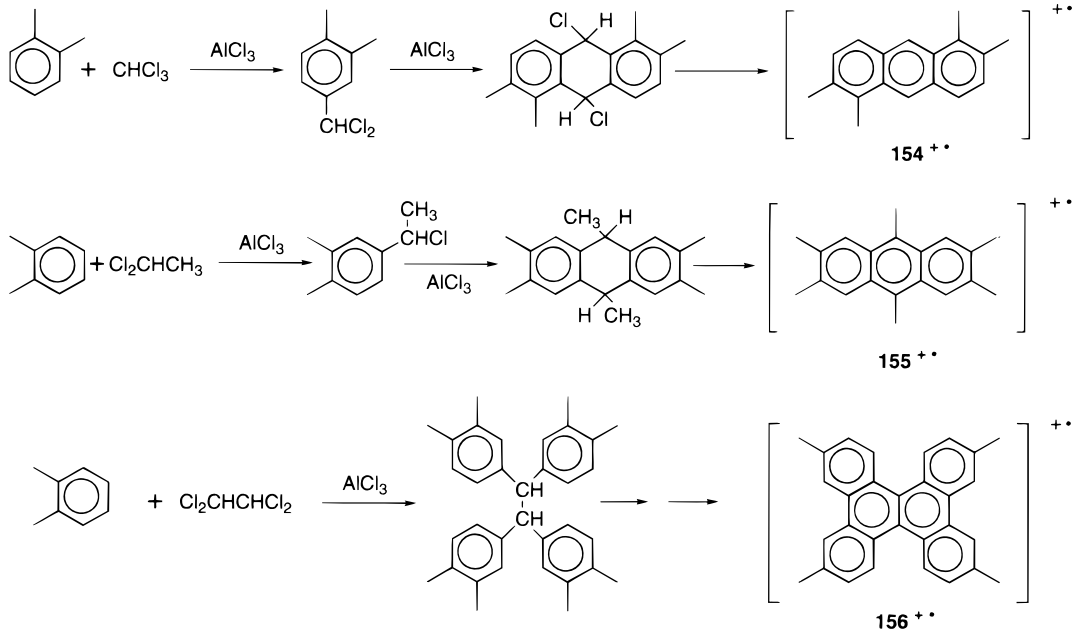

Figure 72. Peristent PAH RCs by Friedel−Crafts chemistry.

With benzo[*rst*]pentaphene double electron transfer was more predominant.

The mechanistic picture involving formation of the PAH radical cations and subsequent nucleophilic attack by DNA bases is gaining increasing support in relation to carcinogenesis (see section below). When the RC of 7,12-dimethylbenzo[*a*]anthracene (a potent carcinogen) was quenched with pyridine, three different isomeric pyridinium salts were formed. Gross and associates[105] utilized the FAB/CAD/MS−MS technique to differentiate these isomers based on the difference in intensities of their daughter ions. Modern mass spectrometry is also being applied to identification of isomeric PAH nucleotides formed by quenching of $PAH^{\bullet+}$.[105]

Whereas previous studies of arene-TMS^+ association complexes led to the conclusion that both σ and π complexes are involved, very recent FT-ICR studies of $[R_3Si\text{-arene}]^+$ adducts are strongly in favor of σ-complex structure.[106]

The oxidative and electrophilic chemistry of **36** has been studied in the gas phase by CI- and EI-MS.[38] Unlike in solution where RC formation hampers NMR the detection of coronenium cation, the protonated cation is present in abundance in the isobutane CI mass spectrum of **36** and is very stable to collisional decomposition (CAD). Its acetylation and trimethylsilylation adducts were generated by reaction with $MeCO^+$ and Me_3Si^+ ions, respectively, in the gas phase. The CAD mass spectra of the adducts

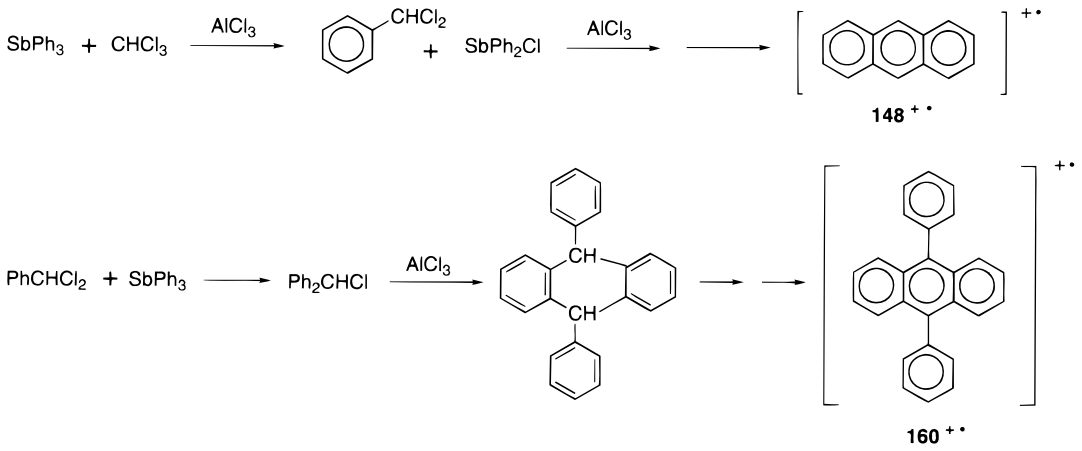

Figure 73. Peristent PAH RCs by Friedel−Crafts chemistry.

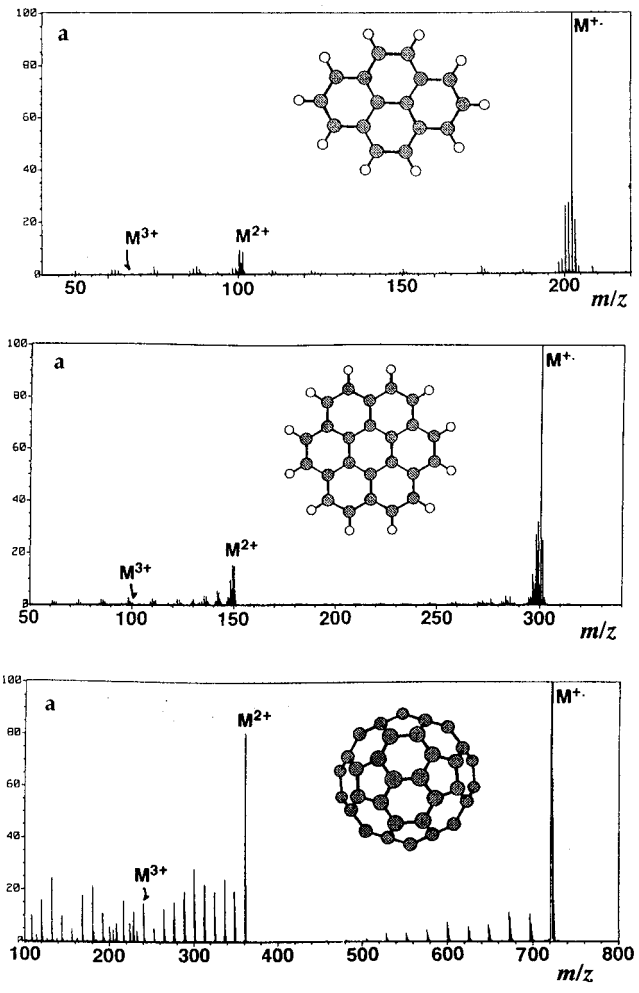

Figure 74. FAB mass spectra of pyrene, coronene, and C_{60}. (Reprinted from ref 103. Copyright 1973 American Chemical Society.)

shows deacetylation and desilylation with significant charge retention on the acyl and silyl moieties.

A gas-phase study of protonation, acetylation, trimethylsilylation, and oxidation of **34** and **35** have also been reported.[38]

In order to extend the available electrophilic and oxidative data on **31** and **130**, a gas-phase protonation, acetylation, and trimethylsilylation (by CI-MS) and an oxidation study (by EI-MS) were undertaken.[67] Collisional decomposition of the acylation and trimethylsilyation monocations are selective toward charge retention at the aromatic moiety. A bissilylated monocation was formed with **130**. Oxidation dications were formed in the EI mass spectra.

Relationship to Carcinogenicity

Metabolic activation of PAHs generates electrophiles which bind covalently to DNA bases and initiate cell damage.[7a,8a,107,109] The electrophilic reactive intermediates are either the carbocations formed by epoxide ring opening, or the radical cations formed by biological oxidation. If the ionization potential of the PAH is < ~7.35 eV it is highly probable that the RC plays a significant role in cancer induction. On the other hand, for the less easily oxidizable PAHs the diol epoxide activation path will predominate in which the carbocations will play a major role. Table 2 provides a summary (based on ref 7a) of PAH structure versus carcinogenic activity. Once formed, the intermediates undergo nucleophilic attack by DNA bases and form PAH−DNA adducts.

The Missing Links and Priority Areas for Future Work

The review has illustrated that substantial progress has been made in the area of generation and NMR studies of arenium ions. Similarly much progress has been achieved in the PAH dication and radical cation areas. Yet, our knowledge concerning the arenium ions and the RCs of large fused PAHs, most of which are carcinogenic, still remains limited. Issues pertaining to the charge distribution mode and its control by remote substituents in such systems must be further evaluated (see also below).

Knowledge concerning the arenium ions of nonalternant PAHs is extremely limited and much needs to be done.

Persistent arenium ions and RCs, derived from cyclopentaannelated and methano-bridged analogues which exhibit increased mutagenic activity and are in many instances environmental pollutants, are yet to be studied.

As for the dications, an area of deficiency is substituent effects on ^{13}C and ^{1}H NMR chemical

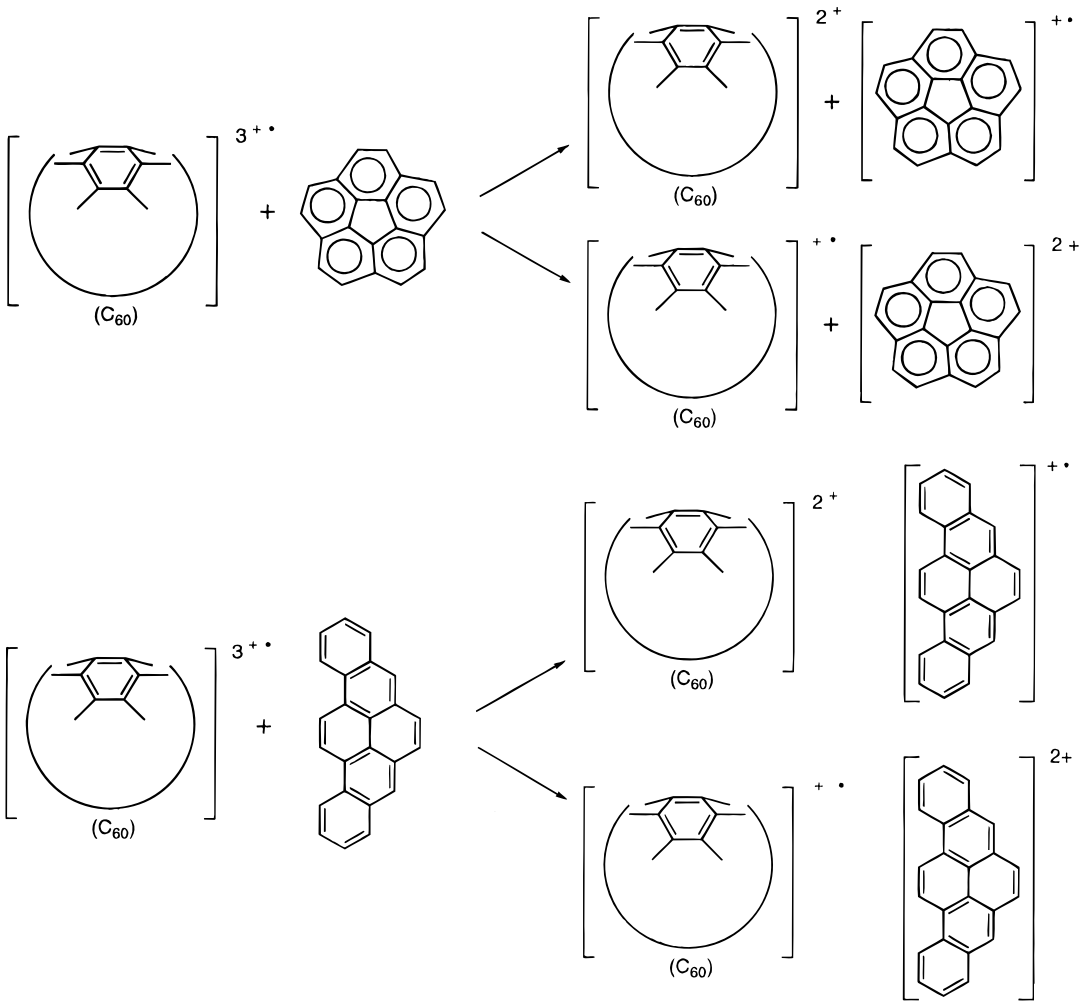

Figure 75. Gas-phase formation of corannulene and benzo[*rst*]pentaphene radical cations and dications by double and single ET from C_{60}^{3+}.

shifts, the latter will shed light on the paramagnetic contributions.

To provide further insight into the reactive intermediates of carcinogenesis of PAHs, it is important to determine if correlations exist between certain modes of charge delocalization (deduced through NMR studies of the PAH arenium ions and EPR studies of $PAH^{\bullet+}$) and the magnitude of carcinogenic activity measured by standard biological tests (such as the Ames test).

Nitro-PAHs are recognized genotoxic environmental pollutants. Although alternate metabolic activation mechanisms have been proposed for nitro-PAHs, recent studies[110] show that for nitrobenzo[*a*]pyrene the diol epoxide pathway is still important, indicative of the significance of carbocations. Protonation studies on the nitro derivatives of benzannelated nitropyrene is, therefore, a priority area.

Selective fluorine introduction into PAHs allows the site where PAH−DNA adduct is formed to be blocked. For example introduction of fluorine at C-2 and C-10 positions of dibenzo[*a*,*i*]pyrene abolishes carcinogenic activity completely.[111] It is significant to determine to what extent the charge delocalization mode is altered in strategically fluorinated arenium ions of benzannelated pyrenes and anthracenes.

An extended experimental and theoretical database when coupled to a database of biological activities will in due course allow more definite conclusions to be drawn in connection to cancer.

Acknowledgments

I thank my associates and co-workers whose names appear in the references for their valuable contributions. Partial support for our work in this area over the years was provided by KSU, NATO(CRG 930113), Danish Research Council, Roskilde University, and more recently by the NCI of NIH (CA63595-01A1). Special thanks go to my NATO partner (P. E. Hansen) for reading the preliminary version of the manuscript, and to Brad Cushnyr (my undergraduate student) for taking on the task of preparing the Chemdraw figures for this endeavor.

References

(1) Olah, G. A. *Friedel-Crafts Chemistry*; Wiley Interscience: New York, 1973. Bethell, D.; Gold, V. *Carbonium Ions*; Academic Press: London, 1967.
(2) Taylor, R. *Electrophilic Aromatic Substitution*; Wiley Interscience: Chichester, 1990.
(3) Olah, G. A.; Malhotra, R.; Narang, S. C. *Nitration; Methods and Mechanisms*; VCH: New York, 1989.
(4) Eberson, L. *Electron Transfer Reactions in Organic Chemistry*; Springer-Verlag: Berlin, 1987.
(5) Jones, P. W.; Leber, P. *Polynuclear Aromatic Hydrocarbons*; 3rd International Symposium on Chemistry and Biology - Carcinogenesis and Mutagenesis; Ann Arbor Science Publishers, Inc.: Ann Arbor, MI, 1979.

(6) Nashed, N. T.; Bax, A.; Loncharich, R. J.; Sayer, J. M.; Jerina, D. M. *J. Am. Chem. Soc.* **1993**, *115*, 1711.
(7) (a) Cavalieri, E. L.; Rogan, E. G. In *Polycyclic Hydrocarbons and Carcinogenesis*; Harvey, R. G., Ed.; ACS Symposium Series 283; American Chemical Society: Washington, DC, 1985; Chapter 11. (b) RamaKrishna, N. V. S.; Cavalieri, E. L.; Rogan, E. G.; Dolnokowski, G.; Cerny, R. L.; Gross, M. L.; Jeong, H.; Jankowiak, R.; Small, G. J. *J. Am. Chem. Soc.* **1992**, *114*, 1863
(8) (a) Cavalieri, E. L.; Devanesan, P. D.; Cremansi, P.; Higginbatham, S.; Rogan, E. G. In *Polynuclear Aromatic Hydrocarbons: Measurements, Means, and Metabolism*; Cook, M., Loening, L., Merritt, J., Eds.; Battelle Press: Columbus, 1991. (b) Rogan, E. L.; Devanesan, P. D.; Cavalieri, E. L. In *Polynuclear Aromatic Hydrocarbons: Measurements, Means, and Metabolism*; Cook, M., Loening, L., Merritt, J., Eds.; Battelle Press: Columbus, 1991; p 767.
(9) Brouwer, D. M.; Mackor, E. L.; MacLean, C. In *Carbonium Ions*; Olah, G. A., Schleyer, P. V. R., Eds.; Wiley Interscience: New York, 1970; Vol. 2, Chapter 20.
(10) Olah G. A.; Mo, Y. K. *Advances Fluorine Chemistry* Tatlow, J. C., Peacock, R. D., Hyman, H. H., Stacey, M., Eds.; CRC Press: Boca Raton, FL, 1973; Vol. 7, p 69.
(11) Prakash, G. K. S.; Rawdah, T. N.; Olah, G. A. *Angew. Chem., Int. Ed. Engl.* **1983**, *22*, 390.
(12) Pagni, R. M. *Tetrahedron* **1984**, *40*, 4161.
(13) Hansen, P. E. *Magn. Reson. Rev.* **1985**, *10*, 1.
(14) Olah, G. A.; Prakash, G. K. S.; Sommer, J. *Superacids*; Wiley Interscience: New York, 1985.
(15) Gold, V.; Tye, F. L. *J. Chem. Soc.* **1952**, 2172.
(16) MacLean, C.; van der Waals, J. H.; Mackor, E. L. *Mol. Phys.* **1958**, *1*, 247.
(17) Dallinga, G.; Mackor, E. L.; Verrijn Stuart, A. A. *Mol. Phys.* **1958**, *1*, 123.
(18) Perkampus, H. H. In *Advances in Physical Organic Chemistry*; Gold, V., Ed.; Academic Press: London, 1966; Vol. 4, pp 195−304.
(19) See for example: (a) Olah, G. A.; Lin, H. C.; Forsyth, D. A. *J. Am. Chem. Soc.* **1974**, *96*, 6908. (b) Olah, G. A.; Spear, R. J.; Messina, G.; Westerman, P. W. *J. Am. Chem. Soc.* **1974**, *97*, 4051. (c) Borodkin, G. I.; Nagy, S. M.; Mamatyuk, V. I.; Shakirov, M. M.; Shubin, V. G. *J. Chem. Soc., Chem. Commun.* **1983**, 1533. (d) Olah, G. A.; Laali, K.; Adler, G.; Spear, R. J.; Schlosberg, R.; Olah, J. A. *J. Org. Chem.* **1985**, *50*, 1306. (e) Borodkin, G. I.; Shakirov, M. M.; Shubin, V. G. *J. Org. Chem. USSR* **1991**, *27*, 391. (f) Laali, K.; Filler, R. *J. Fluorine. Chem.* **1989**, *43*, 415. (g) Laali, K. K.; Gelerinter, E.; Filler, R. *J. Fluorine. Chem.* **1991**, *27*, 391.
(20) Olah, G. A.; Mateescu, G. D.; MO, Y. K. *J. Am. Chem. Soc.* **1973**, *95*, 1865.
(21) Olah, G. A. *Angew. Chem., Int. Ed. Engl.* **1993**, *32*, 767.
(22) Rabinovitz, M. *Top. Curr. Chem.* **1988**, *146*, 99.
(23) Rabinovitz, M.; Cohen, Y. *Tetrahedron* **1988**, *44*, 6957.
(24) Müllen, K. *Angew. Chem., Int. Ed. Engl.* **1987**, *26*, 204.
(25) Lammertsma, K.; Cerfontain, H. *J. Am. Chem. Soc.* **1979**, *101*, 3618.
(26) Lammertsma, K. *J. Am. Chem. Soc.* **1981**, *103*, 2062.
(27) Laali, K. K.; Hansen, P. E.; Houser, J. J.; Zander, M. *J. Chem. Soc., Perkin Trans. 2* **1995**, 1781.
(28) Laali, K. K.; Bolvig, S.; Hansen, P. E. *J. Chem. Soc., Perkin Trans. 2* **1995**, 537.
(29) Forsyth, D. A.; Olah, G. A. *J. Am. Chem. Soc.* **1976**, *98*, 4036.
(30) Laali, K. K.; Hansen, P. E.; Gelerinter, E.; Houser, J. J. *J. Org. Chem.* **1993**, *58*, 4088.
(31) Laali, K. *J. Chem. Res (s)* **1988**, 378.
(32) Olah, G. A.; Singh, B. P. *J. Org. Chem.* **1983**, *48*, 4830.
(33) Eliasson, B.; Johnels, D.; Sethson, I.; Edlund, U. *J. Chem. Soc., Perkin Trans. 2* **1990**, 897.
(34) Müllen, K. *Helv. Chem. Acta* **1978**, *61*, 2307.
(35) Dewar, M. J. S.; Dennington, R. D., II. *J. Am. Chem. Soc.* **1989**, *111*, 3804.
(36) Cohen, Y.; Klein, J.; Rabinovitz, M. *J. Am. Chem. Soc.* **1988**, *110*, 4634.
(37) Mills, N. S. *J. Org. Chem.* **1992**, *57*, 1899.
(38) Laali, K. K.; Houser, J. J. *J. Chem. Soc., Perkin Trans. 2* **1994**, 1303.
(39) Archer, W. J.; Shafig, Y. E.-D.; Taylor, R. *J. Chem. Soc., Perkin Trans. 2* **1981**, 675.
(40) Krusic, P. J.; Wasserman, E. *J. Am. Chem. Soc.* **1991**, *113*, 2322.
(41) Laali, K. K.; Hansen, P. E.; Houser, J. J. To be published.
(42) Archer, W. J.; Taylor, R. Gore, P. H.; Kamounah, F. S. *J. Chem. Soc., Perkin Trans. 2* **1980**, 1828.
(43) Hart, H.; Oku, A. *J. Org. Chem.* **1972**, *37*, 4269.
(44) Bodoev, N. V.; Mamatyuk, V. I.; Krysin, A. P.; Koptyug, V. A. *J. Org. Chem. USSR* **1978**, *14*, 1789.
(45) Warner, P.; Winstein, S. *J. Am. Chem. Soc.* **1969**, *91*, 7785.
(46) (a) Lammertsma. K.; Cerfontain, H. *J. Am. Chem. Soc.* **1980**, *102*, 3257. (b) Lammertsma, K.; Cerfontain, H. *J. Am. Chem. Soc.* **1980**, *102*, 4528.
(47) Wallraff, G. M.; Vogel, E.; Michl, J. *J. Org. Chem.* **1988**, *53*, 5807.
(48) van der Lugt, W. TH. A. M.; Buck, H. M.; Oosterhoff, L. J. *Tetrahedron* **1968**, *24*, 4941.
(49) van de Griendt, F.; Cerfontain, H. *Tetrahedron* **1979**, *34*, 2563.
(50) (a) Harvey, R. G. In *Polycyclic Hydrocarbons and Carcinogenesis*; Harvey, R. G., Ed.; American Chemical Society: Washington DC, 1985; Chapter 3.
(51) Laali, K. K. Work in progress.
(52) Borodkin, G. I.; Shakirov, M. M.; Shubin V. G. *J. Org. Chem. USSR* **1990**, *26*, 2254 and references to previous related work cited therein.
(53) Laali, K.; Cerfontain, H. *J. Org. Chem.* **1983**, *48*, 1092.
(54) Laali, K. K.; Gano, J. E.; Gundlach IV, C. W.; Lenoir, D. *J. Chem. Soc., Perkin Trans. 2* **1994**, 2169.
(55) Laali, K. K.; Hansen, P. E. *Res. Chem. Intermed.* **1996**, in press.
(56) Laali, K. K.; Hansen, P. E. *J. Org. Chem.* **1991**, *56*, 6795.
(57) Laali, K. K.; Hansen, P. E. *J. Chem. Soc., Perkin Trans. 2* **1994**, 2249.
(58) Laali, K. K.; Hansen, P. E. *J. Org. Chem.* **1993**, *58*, 4096.
(59) Ohta, T.; Shudo, K.; Okamoto, T. *Tetrahedron Lett.* **1984**, *25*, 325.
(60) Laali, K. K.; Liang, T.-M.; Hansen, P. E. *J. Org. Chem.* **1992**, *57*, 2658.
(61) Laarhoven, W. H.; Prinsen, W. J. C. *Top. Curr. Chem.* **1984**, *122*, 63.
(62) Morozov, S. V.; Shakirov, M. M.; Shubin, V. G. *J. Org. Chem. USSR* **1981**, *17*, 139.
(63) Morozov, S. V.; Shakirov, M. M.; Shubin, V. G. *J. Org. Chem. USSR* **1983**, *19*, 899.
(64) Morozov, S. V.; Shakirov, M. M.; Shubin, V. G. *J. Org. Chem. USSR* **1988**, *24*, 700.
(65) Hart, H.; Tuerstein, A. *Synthesis* **1979**, 693.
(66) Hart, H.; Tuerstein, A.; Babin, M. A. *J. Am. Chem. Soc.* **1981**, *103*, 903.
(67) Laali, K. K. *J. Chem. Soc., Perkin Trans. 2* **1993**, 1873.
(68) de Wit, P.; Cerfontain, H. *Rec. Trav. Chim. Pay. Bas* **1985**, *104*, 25.
(69) (a) Masamune, S.; Brooks, D. W.; Morio, K.; Sobczak, R. L. *J. Am. Chem. Soc.* **1976**, *98*, 8277. (b) Scott, L. T.; Brunsvold, W. R.; Kirms, M. A.; Erden, I. *J. Am. Chem. Soc.* **1981**, *103*, 5216. (c) Scott, L. T.; Haddon, R. C. *Pure. Appl. Chem.* **1986**, *58*, 127.
(70) Scott, L. T.; Sumpter, C. A.; Oda, M.; Erden, I. *Tetrahedron Lett.* **1989**.
(71) Brouwer, D. M.; Van Doorn, J. A. *Rec. Trav. Chim. Pays. Bas* **1972**, *91*, 1110.
(72) Lammertsma, K.; Olah, G. A.; Berke, C. M.; Streitwieser, Jr., A. *J. Am. Chem. Soc.* **1979**, *101*, 6658.
(73) Olah, G. A.; Liang, G. *J. Am. Chem. Soc.* **1977**, *99*, 6045.
(74) Bausch, J. W.; Gregory, P. S.; Olah, G. A.; Prakash, G. K. S.; Schleyer, P. v. R.; Segal, G. A. *J. Am. Chem. Soc.* **1989**, *111*, 3633.
(75) Chiang, L. Y.; Thomann, H. *J. Chem. Soc., Chem. Commun.* **1989**, 172.
(76) Müllen, K.; Meul, T.; Schade, P.; Schmickler, H.; Vogel, E. *J. Am. Chem. Soc.* **1987**, *109*, 4992.
(77) Lewis, I. C.; Singer, L. S. *J. Chem. Phys.* **1965**, *43*, 2712.
(78) Bolton, J. R.; Carrington, A.; McLachlan, A. D. *Mol. Phys.* **1962**, *5*, 31.
(79) de Boer, E.; Mackor, E. L. *Rec. Trav. Chim. Pays. Bas* **1962**, 493.
(80) Buchanan, A. C., Livingston, R.; Dworkin, A. S.; Smith, G. P. *J. Phys. Chem.* **1980**, *84*, 423.
(81) Davies, A. G.; Shields, C. J. *J. Chem. Soc., Perkin Trans. 2* **1989**, 1001.
(82) Avila, D. V.; Davies, A. G.; Girbal, M. L.; McGuchan, D. C. *J. Chem. Res (s)* **1989**, 256.
(83) Courtneidge, J. L.; Davies, A. G.; McGuchan, D. C.; Yazdi, S. N. *J. Organomet. Chem.* **1988**, *341*, 63.
(84) Cooksey, C. J.; Courtneidge, J. L.; Davies, A. G.; Evans, J. C.; Gregory, P. S.; Rowlands, C. C. *J. Chem. Soc., Chem. Commun.* **1986**, 549.
(85) Courtneidge, J. L.; Davies, A. G.; McGuchan, D. C. *Rec. Trav. Chim. Pays. Bas* **1988**, *107*, 190.
(86) Avila, D. V.; Davies, A. G.; Girbal, M. L.; Ng, K. M. *J. Chem. Soc., Perkin Trans. 2* **1990**, 1693.
(87) Davies, A. G.; Gescheidt, G.; Ng, K. M.; Shepherd, M. K. *J. Chem. Soc. Perkin Trans. 2* **1994**, 2423.
(88) Kochi, J. K.; Lau, W. *J. Am. Chem. Soc.* **1986**, *108*, 6720.
(89) Krohnke, C.; Enkelmann, V.; Wegner, G. *Angew. Chem., Int. Ed. Engl.* **1989**, *19*, 918.
(90) Gerson, F.; Scholz, M.; Hansen, H.-J.; Vebelhart, P. *J. Chem. Soc., Perkin Trans. 2* **1995**, 215.
(91) Eberson, L.; Radner, F. *J. Chem. Soc., Chem. Commun.* **1991**, 1233.
(92) Sankararaman, S.; Lau, W.; Kochi, J. K. *J. Chem. Soc., Perkin Trans.* **1991**, 396.
(93) Eberson, L.; Hartshorn, M. P.; Persson, D. *J. Chem. Soc., Perkin Trans. 2* **1995**, 409.
(94) Eberson, L.; Radner, F.; Lindgren, M. *Acta Chem. Scand.* **1993**, *47*, 835.

(95) Eberson, L. Private communication.
(96) Sang, H.; Wang, H. *Magn. Reson. Chem.* **1992**, *30*, 143.
(97) Wang, H.; Kispert, L. D.; Sang, H. *J. Chem. Soc., Perkin Trans. 2* **1989**, 1463.
(98) Wang, H.; Kispert, L. D.; Sang, H. *J. Org. Chem.* **1988**, *53*, 5967.
(99) Bohme, D. K. *Chem. Rev.* **1992**, *92*, 1487.
(100) Meot-Ner (Mautner), M. *J. Phys. Chem.* **1980**, *84*, 2716.
(101) Hagan, D. A.; Eland, H. D. *Rapid Commun. Mass. Spectrom.* **1991**, *5*, 512.
(102) Kingston, R. G.; Guihaus, M.; Brenton, A. G.; Beynan, J. H. *Org. Mass. Spectrom.* **1985**, *20*, 406.
(103) Takayama, M. *J. Am. Soc. Mass. Spectrom.* **1995**, *6*, 114.
(104) Jahavary, G.; Becker, H.; Petrie, S.; Cheng, P.-C.; Schwarz, H.; Scott, L. T.; Bohme, D. K. *Org. Mass. Spectrom*, **1993**, *28*, 10005.
(105) Geaye, M.; Wellemans, J. M. Y.; Gross, M. L.; Li, K.; Cavalieri, E. L. *J. Am. Soc. Mass. Sepctrom.* **1994**, *5*, 1021.
(106) Cacace, F.; Attina, M.; Fornarini, S. *Angew. Chem., Int. Ed. Engl.* **1995**, *34*, 654. Cacace, F. In *Organic Reactivity: Physical and Biological Aspects*; Golding, B. T., Griffin, R. J., Maskill, H., Ed.; The Royal Society of Chemistry: London, 1995.
(107) Cremonesi, P.; Stack, D. E.; Rogan, E. G.; Cavalieri, E. L. *J. Org. Chem.* **1994**, *59*, 7683.
(108) Cavalieri, E. L.; Rogan, E. G.; Cremonesi, P.; Devanesan, P. *Biochem. Pharmacol.* **1988**, *37*, 2173.
(109) Cavalieri, E.; Roth, R. *J. Org. Chem.* **1976**, *41*, 2679.
(110) Wu, Y.-S.; Lai; J.-S.; Fu, P. *J. Org. Chem.* **1993**, *58*, 7283. Fu, P. P.; Ni, Y.-C.; Zhang, Y.-M.; Heflich, R. H.; Wang, Y.-K.; Lai, J.-S. *Mut. Res.* **1989**, *225*, 121.
(111) Sardella, D. J.; Mahathalang, P.; Mariani, H. A.; Boger, E. *J. Org. Chem.* **1980**, *45*, 2064.

CR941175S